Neural Precursor Cell Galvanotaxis is Conserved Across Age and is Modulated by Resting Membrane Potential

by

Nancy XiaoNan Liu

A thesis submitted in conformity with the requirements
for the degree of Master of Science

Institute of Medical Sciences
University of Toronto

Neural Precursor Cell Galvanotaxis is Conserved Across Age and is Modulated by Resting Membrane Potential

Nancy XiaoNan Liu

Master of Science

Institute of Medical Sciences
University of Toronto

2018

Abstract

Neural stem and progenitors cells, together termed “neural precursor cells” (NPCs), line the subependyma of the mammalian brain. NPCs are multipotent and undergo a proliferative and migratory response in development as well as in response to injury, making them an attractive target for cell replacement therapeutics. NPCs respond to electric fields with increased migratory directedness and speed. This thesis focuses on characterizing the differences in galvanotactic migration over age. We have discovered that NPC galvanotaxis showed conserved migratory patterns in the presence or absence of niche factors over age. We demonstrate that resting membrane potential modulations, using the hyperpolarizing drug Diazoxide, induced increased migration. Moreover, NPC niche derived factors found within conditioned media is able to modify the NPC galvanotactic response. Our preliminary studies have identified IGF-1 as a potential modulator of membrane potential and NPC galvanotaxis. This work will inform the efficacy of neural repair strategies across age.

Acknowledgments

This thesis is the culmination of two years of research. I am grateful to the many mentors, colleagues, and family that have encouraged and supported my academic journey.

To my mentors, I thank Dr. Cindi Morshead and Dr. Milos Popovic for your committed support and insightful deliberations. With your guidance, I have developed and grown as a scientist and individual. Your confidence and excitement in my potential has motivated me to overcome many setbacks and strengthened my own confidence in myself. Thank you both for your thoughtful and enduring counsel.

To my colleagues and collaborators, I thank you all in sharing with me experiences of discovery, frustration, elation, failure, and success. We have worked hard together from early mornings to late into night (who hasn't had a fun story of startling the 3am staff?). It has been a wonderful two years learning and teaching in turn with you all. Thank you Ashkan Azimi, Daniel Derkach, Elana Sefton, Emily Gilbert, Homeira Moradi, Ilan Vonderwalde, Jessica Livingston-Thomas, Kelsey Adams, Nishanth Lakshman, Petri Takkala, Rebecca Ruddy, Rehnuma Islam, Rob Babona-Pilipos, Stasja Drecun, Stephanie Iwasa, and Umalkhair Ahmed for all your advice, patient training, fun conversations, creative discussions, informative experiments, and shared learning experiences. Thank you to my undergraduate students Iflah Shahid, James Anupol, and Prashanth Surjeet for your studious and curious minds. I hope you have learned much in your time with me. To everyone, I thank you all for your integrity and friendship that have supported us all in broadening the body of human knowledge and building a more enlightened tomorrow. I wish you all the best in your future pursuits.

Finally, to my family, who have unconditionally supported me. Thank you for your dedication, sacrifices, and strength. You have dedicated your lives to guiding me in becoming a principled citizen of the world and being the best I can be. I will always aim to honour your teachings and strive to make you proud.

Table of Contents

List of Abbreviations

Aldh1l1 – Aldehyde Dehydrogenase 1

BBB – Blood Brain Barrier

bFBS – Basic Fetal Bovine Serum

BLBP – Brain Lipid Binding Protein

BMP – Bone Morphogenic Protein

BrdU – Bromodeoxyuridine

CM – Conditioned Media

CRAN – Comprehensive R Archive Network

CSF – Cerebrospinal Fluid

CSPG – Chondroitin Sulphate Proteoglycan

CTGF – Connective Tissue Growth Factor

DAG – Diacylglycerol

DBS – Deep Brain Stimulation

dcEF – Direct Current Electric Field

Dcx – Doublecortin

DG – Dentate Gyrus

ECM – Extracellular Matrix

EF – Electric Field

EGF – Epidermal Growth Factor

EGFR – Epidermal Growth Factor Receptor

ELISA – Enzyme-Linked ImmunoSorbent Assay

ENaC – Epithelial Sodium Channel

F-actin – Filamentous Actin

FAK – Focal Adhesion Kinase

FBS – Fetal Bovine Serum

FES – Functional Electrical Stimulation

FGF – Fibroblast Growth Factor

GABA – γ-aminobutyric acid

GDNF – Glial Cell-Derived Neurotrophic Factor

GFAP – Glial Fibrillary Acidic Protein

GLAST – Glutamate Aspartate Transporter

HGF – Hepatocyte Growth Factor

HSPG – Heparin Sulphate Proteoglycan

IGF – Insulin-like Growth Factor

IGFBP – Insulin-like Growth Factor Binding Protein

KCC2 – Potassium/Chloride Ion Exchanger

KEGG – Kyoto Encyclopedia of Genes and Genomes

MAPK – Mitogen-Activated Protein Kinase

MCAO – Middle Cerebral Artery Occlusion

MMP – Matrix Metalloproteinase

NHE – Sodium-Hydrogen Antiporter OR Sodium-Hydrogen Exchanger

NHEJ – Nonhomologous End Joining

NO – Nitric Oxide

NPC – Neural Precursor Cell

NSC – Neural Stem Cell

NSE – Neuron-Specific Enolase

P0 – Primary

P1, -2, -3, -4 – Passaged

PANTHER – Protein ANalysis THrough Evolutionary Relationships

PIP_2 – Phosphatidylinositol 4,5-Bisphosphate

PIP_3 – Phosphatidylinositol 3,4,5-Trisphosphate

PLL – Poly-L-Lysine

PSA – Polysialic Acid

PSA-NCAM – Polysialylated Neural Cell Adhesion Molecule

PVC – Polyvinyl Chloride

RMP – Resting Membrane Potential

ROS – Reactive Oxygen Species

SDF – Stromal Cell-Derived Factor

SEZ – Subependymal Zone

SGZ – Subgranular Zone

SFM – Serum Free Media

SVZ – Subventricular Zone

TAP – Transit Amplifying Progenitor

tDCS - Transcranial Direct Current Stimulation

TEP – Transepithelial Potential

TGFβ – Transforming Growth Factor β

TTF – Tumour Treating Fields

VCAM – Vascular Cell Adhesion Molecule

VEGF – Vascular Endothelial Growth Factor

V_{mem} – Membrane Voltage

YFP – Yellow Fluorescent Protein

List of Tables

List of Figures

1 Chapter 1
Literature Review

The aim of this review is to describe the known characteristics, behaviours, and functions of neural stem cells (NSCs) and progenitors, collectively termed neural precursor cells (NPCs), in relation to changes in age and niche. Specifically, to build a background to interpret how changes in the niche through aging can affect the migration of NPCs in response to electric field (EF) stimulation. This chapter highlights four main ideas. The first detailing NPC changes over time. The second detailing temporal changes in their niche throughout age. The third detailing known NPC migratory mechanisms. The fourth detailing resting membrane potentials (RMPs) and electric fields plus their applications.

1.1 Brief History and Context of Adult Neural Stem Cells

Since the late 1800's, it was widely believed adult neurogenesis did not occur in mammals. Based on the neuronal characterization work of Wilheml His, Gustaf Retzius, and Santiago Ramón y Cajal (Breunig et al. 2011), the dogma of no new neurons in the mature brain persisted for nearly a century. Even in the early 2000's, Rakic maintained that cortical neurons lost due to injury or disease could not be replaced (Rakic 2006). This dogma was challenged by seminal work in the 1960's that showed that mammalian post-natal neurogenesis did occur (Altman & Das 1966; Altman & Das 1965; Altman 1969; Altman 1962; Hinds 1968) and that the cells giving rise to these new neurons were located in the subependymal zone (SEZ; also referred to in literature as the subventricular zone – SVZ; Smart 1961) and the hippocampus (Altman 1963). Limitations in the studies, in terms of the techniques available, to establish ongoing neurogenesis as a feature of the uninjured adult brain kept the dogma intact but in the early 1990's, adult neurogenesis was proven possible *in vitro* as well as *in vivo* and widely perceived as a reality.

In 1992, Reynolds and Weiss showed that cells isolated from the adult mouse brain could proliferate to form free-floating, clonal colonies in response to epidermal growth factor (EGF; Reynolds & Weiss 1992). These colonies were termed neurospheres and were shown to express nestin, an intermediate filament found in neuroepithelial stem cells. Neurospheres were also shown to display the two cardinal properties of stem cells: self-renewal and multipotency: (1)

individual neurospheres could be dissociated and replated to produce more neurospheres (passaging) and (2) neurosphere cells could be differentiated into neuron-specific enolase (NSE) expressing neurons, glial fibrillary acidic protein (GFAP) expressing astrocytes and oligodendrocytes (Reynolds and Weiss, 1992). Subsequent research then identified these nestin positive, neurosphere forming cells as NSCs located in the adult subependyma lining the lateral ventricles (Morshead et al, 1994).

The precise locations of stem cell populations within the central nervous system as well as the biomolecular markers specific to these multipotent cells was then investigated by many groups. There are currently 3 regions of the CNS where NSCs reside. Firstly, the subependyma of the SEZ. This regions contains a NSC population that expresses the mature astrocyte marker GFAP (Morshead et al, 1994; Chiasson et al, 1999; Doestch et al, 1999; Tramontin et al, 2003). Secondly, the subgranular zone (SGZ) of the dentate gyrus (DG) within the hippocampus (Altman and Das, 1965; Bayer, 1982; Kaplan and Bell, 1984; Kuhn et al., 1996; Johansson et al, 1999). These DG NSCs are also GFAP-positive (Garcia et al, 2004) and typically give rise to granule cell layer neurons but can be stimulated to give rise to astrocytes and oligodendrocytes (Bayer et al. 1982; Palmer et al. 1997). Thirdly, the spinal cord (Sabourin et al. 2009; Weiss et al. 1996; Yamamoto et al. 2001; Martens et al. 2002). These ependymal layer cells (Smart 1972; Horner & Gage 2000; Meletis et al. 2008) respond to injury by undergoing predominantly gliogenesis (Oumesmar et al. 1995) and are only neurogenic in vitro (Shihabuddin et al. 1997). This thesis will focus only on the NSCs present in the SEZ of the mammalian brain.

The discovery of adult NSCs raises questions of how these cells are maintained throughout life and what physiological role they fulfill through aging. Differences between young and aged NSCs and their progeny were first investigated in the late 1990's (Kuhn et al. 1996; Tropepe et al. 1997), raising a number of questions regarding NPC behaviour and its regenerative capacity. Such as: Why does functional repair between the neonate and adult differ? Why are there limits to adult neural repair? Is endogenous functional repair even possible in the aged animals? Why do adult NSCs behave differently than embryonic/neonatal NSCs? Is it due to intrinsic differences that occur within the stem cell over time, or is it due to differences in the niche/organismal environment? These questions are still yet to be fully explored.

To answer these questions by investigating age related differences, we may better optimize transplantational and endogenous regenerative therapies. Perhaps certain transplantational therapies are only effective in a set developmental time-period. We may begin to understand how ages of donors and recipients might affect functional outcomes. We may begin to stimulate endogenous quiescent stem cell populations to a more activated, “young” phenotype.

Discoveries of age-related changes will continue to broaden our fundamental understanding of stem cell biology and translate into better optimization of clinical stem cell therapies. The following two sections will detail current knowledge of NSC and niche changes (respectively) over time

1.2 Neural Stem Cell Roles during Development and Adulthood

Embryonic development begins with fertilization and then follows the well-characterized steps of programmed proliferation and polarization through the stages of development (reviewed in Schoenwolf & Larsen 2015, Chapter 4). This review will focus primarily on the role of SEZ NPCs during early developmental and adult stages of the brain.

1.2.1 Development

The mammalian central nervous system begins developing via a process known as neurulation. After gastrulation, three primary germ layers are formed; ectoderm, mesoderm, and endoderm. The ectoderm will give rise to cells of neural and non-neural (epidermal) lineages. Neural induction is dictated by secretion of noggin, chordin, and follisatin by axial mesoderm. These factors act as inhibitors of bone morphogenic protein-4 (BMP4), a member of the transforming growth factor β (TGFβ) family, which acts as a ventralizing signal (reviewed in Sasai & De Robertis 1997). Primary neurulation begins with ectodermal neuroepithelial cells thickening and flattening to form the neural plate. The ends of the plate are named the neural folds. Simultaneously, the neural plate begins to invaginate to form the neural groove just as the neural folds on either side fold up and join together, creating the neural tube. (reviewed in Greene & Copp 2009; Schoenwolf & Larsen 2015, Chapter 9).

The neural tube develops along the notochord, becoming the basis of the brain and spinal cord. The lumen of the neural tube will go on to form the contiguous ventricles and central canal. In the developing brain, the layer of cells surrounding the lumen are described as belonging to the ventricular zone. Neuroepithelial cells then proliferate and begin to undergo asymmetric divisions, thus beginning to form layers in the brain. The SVZ lies just adjacent to the ventricular zone, basally (pial). Neurogenesis begins around embryonic day 10 in mice. At this point, neuroepithelial cells become radial glial cells, or embryonic neural precursors (reviewed in Kriegstein & Alvarez-Buylla 2009). Neuroepithelial cells continue to proliferate and give rise to the neurons, astrocytes, and oligodendrocytes comprising the brain and spinal cord (reviewed in Stiles & Jernigan 2010; Schoenwolf & Larsen 2015, Chapter 9). To form the brain, new cells migrate and differentiate with an “inside-out” pattern; where the inner layers are populated first, followed by the outer. In early development, the distances cells travel are small. Cells traverse via somal translocation; where a cell extends a long basal process to the pial surface and moves its nucleus along the process out of the ventricular zone and into the embryonic cortex (reviewed in Nadarajah & Parnavelas 2002). As brain sizes increase, radial glial cells fill the role of guides to laminar development. Radial glial cells extend both an apical and basal (pial) process that acts as a scaffold for cell migration. In brief, cells migrate along the radial extensions until they encounter a stop signal of reelin from Cajal-Retzius cells, forming laminar layers of the cortex (reviewed in Rice & Curran 2001).

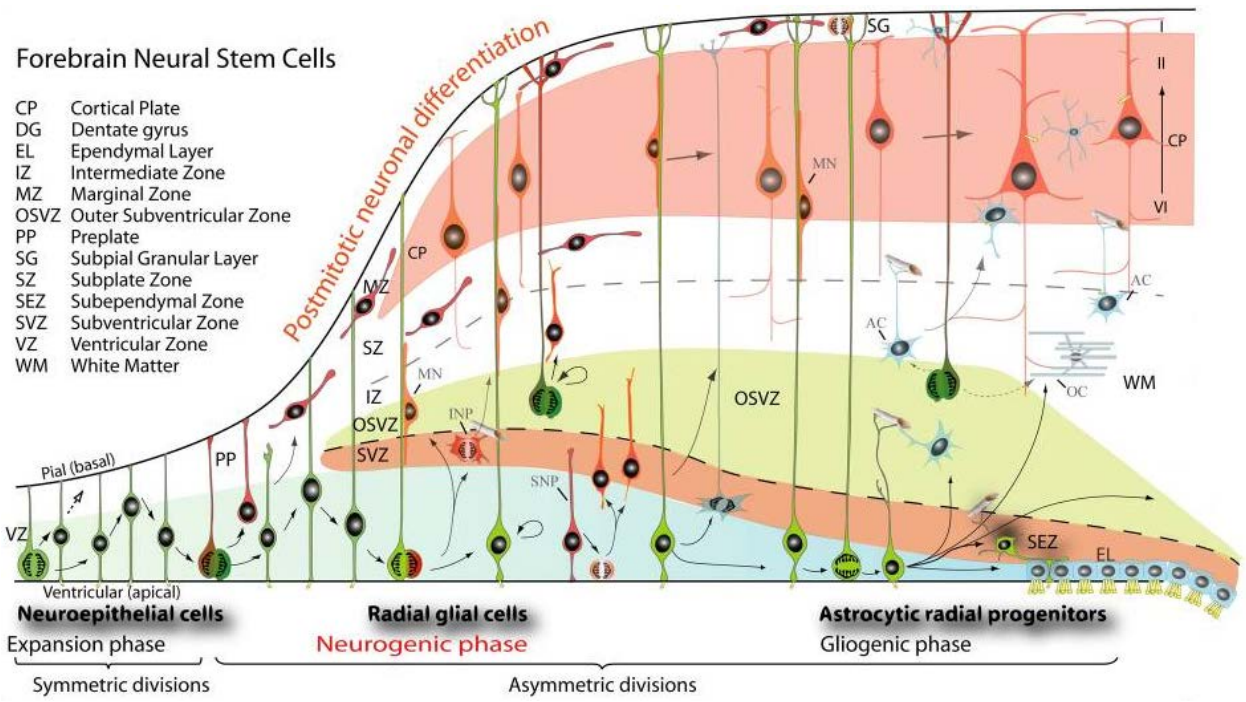

Figure 1: Adapted from Breunig et al. 2011. Shows neural stem cell and brain layer development from neuroepithelial cells to radial glial cells to adult NSCs.

Previously, radial glial cells have been shown to be defined by embryonic day 11 and identifiable by their expression of GFAP and glutamate aspartate transporter (GLAST; Haubensak et al. 2004; Taverna et al. 2014; Malatesta & Gotz 2013). By embryonic day 12.5, radial glial cells can be characterized by their expression of nestin, brain lipid binding protein (BLBP), GLAST (Anthony et al. 2004), Tenascin-C (Kriegstein & Alvarez-Buylla 2009), vascular cell adhesion molecule 1 (VCAM-1; Hu et al. 2017), Emx1, Sox2, and Pax6 (Yuzwa et al. 2017). As development concludes, radial glial cells lose their pial attachments and change their morphology (Pollen et al. 2015; Yuzwa et al. 2017). By embryonic day 17.5 radial glial cells exit the cell cycle, with greater than 90% of these cells out of the G2/M or S phases, and increase expression of markers expressed on adult NSCs such as nestin, VCAM-1, Sox2, Tenascin-C, and aldehyde dehydrogenase 1 (Aldh1l1; Yuzwa et al. 2017). As development continues, the ventricular zone shrinks down to the ependymal cell layer, a single cell layer lining the ventricles. A subpopulation of radial glial cells maintain their apical connections with the lateral ventricle, interposing with ependymal cells, and extend processes to blood vessels within the SEZ. These cells are the NSCs of the adult brain (Pinto et al. 2008; Malatesta et al. 2008; Merkle et al. 2004; Spassky et al. 2005).

1.2.2 Adulthood

Postnatally, the ventricular zone layer shrinks down to a layer of ciliated ependymal cells (derived from radial glial cells) surrounding the ventricles (Spassky et al. 2005) and the SVZ becomes a thin layer termed the SEZ (Morshead et al. 1994).

The region adjacent to the ventricular zone during development (the subventricular zone) shrinks down to form a 4-5 cell layer thick region known as the subependymal zone (SEZ; Luo et al. 2006). Adult NSCs are relatively quiescent (Codega et al. 2014; Kokovay et al. 2012) within the SEZ and are arranged in pin-wheel like structures on the ventricular face of the stem cell niche.

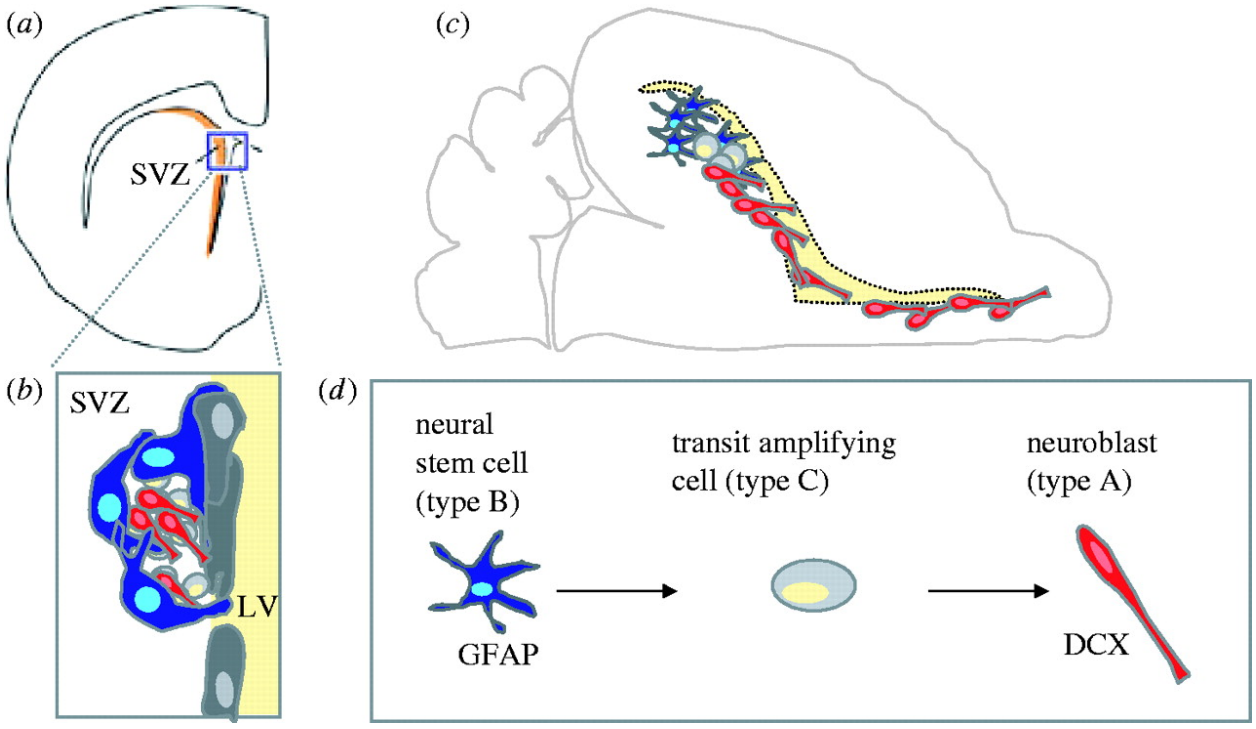

Figure 2: Structural location of neural stem cells and progeny. a) Half a coronal section through the lateral ventricle of the mouse brain showing the physiological location of the SVZ. b) Arrangement of NSC and progeny in SVZ, shown in grey are ependymal cells. c) Sagittal section through the lateral ventricle of the mouse brain showing the arrangements of NSCs and downstream progeny along the rostral migratory stream. d) Lineage of NSC (type B cells) to progenitor/transit amplifying cell (type C cell or TAP) to neuroblast (type A cell). Image taken from Okano & Sawamoto 2008.

In adulthood, NSCs give rise to interneurons of the olfactory bulb. As shown in Figure 2, NSCs give rise to rapidly proliferative progenitors which become neutrally committed neuroblasts that migrate along a well-defined pathway termed the rostral migratory stream (RMS) to give rise to

inhibitory GABAergic granule neurons (Lledo et al. 2008; Fuentealba et al. 2012). In literature, NSCs are term B cells, their progenitors are termed C cells (or transit amplifying progenitors [TAPs]), and neuroblasts are termed A cells.

Adult NSCs are characterized by their expression of GFAP and CD133 (Codega et al. 2014; Fischer et al. 2011). NSCs exist in two states: a quiescent and activated state. Activated NSCs are characterized by their expression of EGF receptor (EGFR) whereas quiescent NSCs do not express EGFR. Under homeostatic conditions, activated NSCs have a cell-cycle time of 2-3 weeks (Morshead et al., 1998; Reeve et al., 2017).

It is commonly thought that quiescence allows NPCs to withstand metabolic stress and maintain genomic integrity. However, quiescent NPCs may be activated by changes in their environment, whether by neuronal inputs and neurotransmitter release or more systemic factor releases. Song et al. have shown inhibition of tonic γ-aminobutyric acid (GABA) release from hippocampal neurons (Song et al. 2012) increased NSC proliferation. As well, Piccin et al. have shown that Wnt signaling increases NSC proliferation (Piccin et al. 2014). Quiescent NSCs give rise to activated NSCs, characterized by their expression of GFAP and EGFR (Codega et al. 2014). Quiescent NSCs may also be activated by more systemic processes such as aerobic exercise, seizures, and brain injury (Wang et al. 2011).

The progeny of NSCs give rise to migrating neuroblasts. Neuroblasts are characterized by their expression of doublecortin (Dcx) (Nacher et al. 2002), polysialylated neural cell adhesion molecule (PSA-NCAM), and βIIItubulin (Doetsch et al. 1997) and migrate along each other via chain migration. Chain-migration of neuroblasts is PSA dependent (Hu et al. 1996). Neuroblasts migrate in a closely apposed fashion within a glial tube formed of astocytes and astrocytic projections (Peretto et al. 1996) and has been shown to be guided by vasculature (Bovetti, Hsieh, et al. 2007). Neuroblasts migrate in a saltatory fashion by first extending a microtubule-rich leading process, then pushing a microtubule organizing centre into the leading process, creating a swelling within the leading process. The leading process forms focal adhesions with the extracellular matrix (ECM). The cell body then is translocated towards leading process via actomyosin contractions (reviewed in Kaneko et al. 2017). Neuroblasts continue to proliferate as they migrate. Once at the olfactory bulb, they become interneurons between the granular and periglomerular layers and play a role in olfaction (Belvindrah et al. 2009).

There is also evidence to suggest that NSCs may also give rise to glial lineages in vivo (Kriegstein & Alvarez-Buylla 2009; Llorens-Bobadilla et al. 2015). NSCs have also been shown to generate oligodendrocytes within the corpus callosum of the adult brain (Neri et al. 2010; Brousse et al. 2015; Akkermann et al. 2017).

1.3 Stem Cell Niche

Stem cells reside within specialized, defined microenvironments termed “niches”. Across the body, multiple tissue stem cell niches exist and regulate stem cell behaviour (reviewed in Morrison & Spradling 2008). In the adult neurogenic regions lining the lateral ventricles, the NSC niche is composed of multiple physical components: ventricular choroid plexus/cerebrospinal fluid (CSF), ependymal cells, extracellular matrix, blood vessels, microglia, and astrocytes (Quiñones-Hinojosa et al. 2006; Doetsch 2003; Conover & Notti 2008). The physical and secreted factors within the niche can influence NSC behaviour including stem cell kinetics such as multipotency, quiescence versus activation, proliferation, cell cycle time, mode of division, and lineage commitment (Chaker et al. 2016).

1.3.1 Cytoarchitecture

The SEZ is approximately five cell layers thick and separated from the ventricular CSF by a contiguous layer of ciliated ependymal cells (Morshead & van der Kooy 1992; Morshead et al. 1994). The NSC, or B cell in literature, extends an apical primary cilium that directly contacts the lumen of the lateral ventricle (Mirzadeh et al. 2008; Shen et al. 2008). NSCs also extend a long basal process that contacts blood vessels. On the apical side, ependymal cells surround the primary cilium, forming a pinwheel structure (Mirzadeh et al. 2008). Ependymal cells are multiciliated and direct CSF flow with a beating motion (Sawamoto et al. 2006; Mirzadeh et al. 2010). Basally, NSC progenitors (or TAPs, or C cells in some literature) lie adjacent to NSCs, along the ependymal layer. TAPs then proliferate rapidly to give rise to neuroblasts (or A cells) (Riquelme et al. 2008). Neuroblasts are organized in chains ensheathed by astrocytic processes, and will migrate to the olfactory bulb (Lois & Alvarez-Buylla 1994; Malatesta & Gotz 2013; Luskin 1993; Doetsch & Alvarez-Buylla 1996).

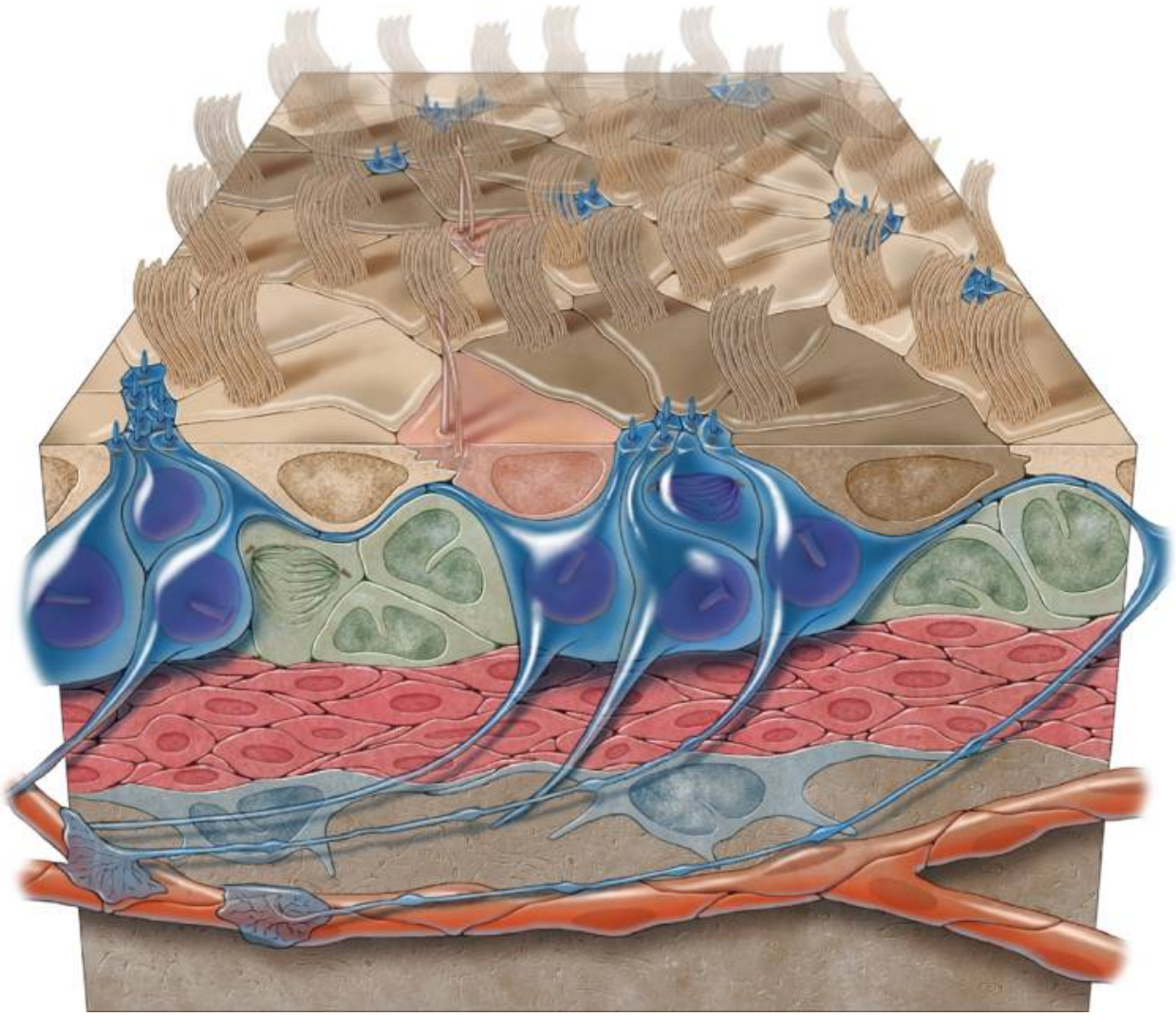

Figure 3: Image from Mirzadeh et al. 2008. Dark blue cell are NSCs, green cells are TAPs, red cells are neuroblasts, light blue cells are astrocytes, orange cells are blood vessels, light and dark brown cells are ependymal cells in pinwheel shape, and light pink cells are a subset of ependymal cells.

Figure 3 focuses on the arrangement of NSCs, their progeny and ependymal cells. However, there are many other factors at play within the NSC niche. Further detailed in subsections below, the SEZ is also innervated by serotonergic and dopaminergic axons from the raphe nuclei (Tong et al. 2014) and substantia nigra (Höglinger et al. 2004; Baker et al. 2004), respectively. As well, cell-cell connections within the niche affect NSC proliferation kinetics (Jiao et al. 2017). All of these cells and their interactions are enveloped by extracellular matrix (ECM)-rich basal laminae (Doetsch 2003; Tavazoie et al. 2008; Shen et al. 2008) and blood vessels (Shen et al. 2008; Kazanis et al. 2010). This organization provides niche cells with a myriad of growth factors,

cytokines, and signaling mechanisms that all serve to regulate proliferation, differentiation, and migration.

1.3.2 Axonal/Neurotransmitter Influences

Using a modified whole mount preparation to better visualize the apical surface of the lateral ventricle, Tong et al. used immunohistochemistry, staining for acetylated tubulin, and transmission electron microscopy to visualize a network of 0.25-0.95 uM overlapping processes closely associated with ependymal cilia. These processes expressed microtubules, mitochondria, dark-core vesicles containing serotonin, and serotonin transporter along membranes; suggesting a monoaminergic cell origin. Using a retrograde tracer, injected into the lumen of the ventricle, Tong et al. identified the origin of these axons as caudal neurons of the dorsal raphe nucleus.

Following up with an anterograde tracer and transmission electron microscopy, Tong et al. showed the axons made direct, non-synaptic contact with neural stem cells and ependymal cells. Neural stem cells extend microvilli enwrapping these axons. Through serotonin infusion and polymerase chain reaction experiments testing for expression of serotonin receptors by NSCs, Tong et al. suggest serotonin induces increased proliferation and neurogenesis. Interestingly, they also show an electrophysiological change in neural stem cells of an inward current, or depolarization, of the cell after serotonin exposure (Tong et al. 2014).

In addition to serotonergic innervation, the SEZ is also innervated by dopaminergic axons originating from the substantia nigra (Baker et al. 2004). Dopamine release increased NPC proliferation in vitro at 10μM (O'Keeffe et al. 2009; Höglinger et al. 2004). However, other studies have reported that dopaminergic input has no effect on NPC proliferation (Van Den Berge et al. 2011) and may even be inhibitory (Tod E. Kippin et al. 2005; Hedlund et al. 2016). These contradicting results have been proposed to differentially affect stem versus progenitor cells.

Closer to the SEZ, neurons of the adult niche express nitric oxide (NO) synthase. Romero-Grimaldi et al. have shown that high doses of NO decreased proliferation. Whereas, low doses of NO increased proliferation. Interestingly, these neurons are only found within the adult brain,

suggesting that with age, further regulatory mechanisms or different regulatory mechanisms play a role in regulating the complex and changing neurogenic niche (Romero-Grimaldi et al. 2008).

Furthermore, drugs modulating neurotransmitter release have been correlated with behavioural changes in NPCs. Hitoshi et al. have shown that imipramine, a tricyclic antidepressant, and fluoxetine, a selective serotonin reuptake inhibitor, increased NPC proliferation (Hitoshi et al. 2007). As well, other addictive substances (ie. opioids, cannabis, cocaine, and methamphetamines) have been shown to decrease NPC proliferation (Xu et al. 2016).

1.3.3 Cerebrospinal Fluid and Flow

The choroid plexus is a thin convoluted structure composed of an elaborate vascular network encased by a single cell layer of epithelium within the lateral ventricles. The choroid secretes and controls the passage of molecules in the cerebrospinal fluid (CSF) (reviewed in Liddelow 2011). The choroid is a source of bone morphogenic protein 7 (BMP7), critical in radial glial cell attachment to the pial surface of the brain and progenitor proliferation during development. It also secretes fibroblast growth factor (FGF) and well as Wnt and Shh pathway components, all of which have been shown to increase NPC proliferation (Lee et al. 2012; Piccin & Morshead 2011). Interestingly, the choroid plexus secretes Slit2, a repulsive chemotactic factor guiding neuronal migration (Hu 1999; Sawamoto et al. 2006). Lastly, the choroid epithelium releases insulin-like growth factor 2 (IGF-2) throughout life and has been shown to increase NSC proliferation. Interestingly, levels of IGF-2 decrease over age and is correlated to a decrease in proliferation (Lehtinen et al. 2011). Embryonic CSF has been shown to contain factors that rescue the neurogenic decline in older mice (Carnicero et al. 2013). The complete identities of those factors and the mechanisms of their action have still yet to be fully elucidated.

Recently, human CSF has also been shown to be beneficial in increasing NSC proliferation. Interestingly, proliferation promoting factors are upregulated in pathologic stroke conditions (Chen et al. 2018). CSF contains many signaling factors as well as mechanical signals that play a role in direct regulation of NSC behaviour. Petrik et al. have recently shown that sodium in the CSF increase NSC proliferation by entering the cells through epithelial sodium channels (ENaCs) on their apical surfaces. These channels are sensitive to shear stresses, allowing them to

sense CSF flow. As shown by Petrik et al., higher flow speeds enhance NSC proliferation. However, that proliferation is abrogated in the presence of an ENaC inhibitor. Petrik et al. further correlate ENaC signaling with intracellular calcium waves and activation of the mitogen-activated protein kinase (MAPK) pathway to enhance proliferation at higher flow speeds (Petrik et al. 2018).

1.3.4 Ependymal Cells

Ependymal cells line the apical surface of the lateral ventricles. Ependymal cells form a contiguous, single-cell layer connected by gap junctions and tight apical-lateral adherens junctions, with each cell sending out beating cilia that help direct the flow of CSF (Sawamoto et al. 2006; Mirzadeh et al. 2010; Del Bigio 2010). These cells act as a barrier between CSF and the brain and maintain the NSC niche in two major ways.

Firstly, through expression of trophic factors such as: basic fibroblast growth factor (bFGF; Fuxe et al. 1996), hepatocyte growth factor (Hayashi et al. 1998), connective tissue growth factor (CTGF), insulin-like growth factor binding protein-2 (IGFBP-2), and noggin (a BMP antagonist; Lim et al. 2000). All these factors are hypothesized to help maintain NPCs and aid in proliferation.

Secondly, ependymal cells are thought to play a role in metabolic regulation of NSCs. Ependymal cell uptake glucose and store it as glycogen (Prothmann et al. 2001), thus controlling energy availability in the NSC niche. Glycogen breakdown is then triggered by serotonin (Verleysdonk et al. 2005), which may link to serotonergic inputs from axons of the raphe nucleus aiding in neurogenesis (Tong et al. 2014).

1.3.5 Extracellular Matrix

The extracellular matrix (ECM) of the SEZ is a complex network composed of laminins (Timpl et al. 1979), fibronectin, heparin sulphate proteoglycans (HSPGs), chondroitin sulphate proteoglycan (CSPG; Steindler et al. 1996), Tenascin-C (Gates et al. 1995; Faissner et al. 2017) and collagen type I (Mercier et al. 2002). These elements interact with cognate receptors

expressed by niche cells. The extracellular matrix forms an extensive basal lamina through the SEZ. The basal lamina of the SEZ takes on a specific structural morphology, known as “fractones” due to their fractal organization.

Fractones are branched, extravascular organizations of basal laminae. They are regularly arranged along the SEZ and consist of stems originating from basal SEZ blood vessels and terminating in bulbs at the ependymal cell layer. They are extensively folded networks near blood vessels and overlie a large area. A single fractone can enfold numerous astrocytic processes, ependymal cells, microglia, and NPCs. They are composed of laminin, HSPGs, perlecan, nidogen, and collagen (Mercier et al. 2002).

Fractone heparan sulphates have been shown to bind BMP-4 (Mercier & Douet 2014) and BMP-7 (Douet et al. 2012), both of which inhibit neurogenesis. They have also been shown to bind bFGF which stimulates neurogenesis (Douet et al. 2013). Kerever et al. have shown that NSCs proliferation in response to bFGF by activating the Akt and Erk1/2 pathways. However, this activation does not occur in the absence of perlecan, an HSPG (Kerever et al. 2014). As fractones are a key modulator of signaling, it is hypothesized fractones could deliver spatially specific signals of quiescence versus activation.

In addition to delivery of signaling molecules, the ECM also plays a role in structural signaling, or mechanosignaling. Leipzig and Shoichet have shown that stiffness affects the differentiation profile of NSCs. Using a polymer with a range of stiffness states, they showed that softer material (lower Young’s modulus) favoured neuronal differentiation, whereas a stiffer material favoured oligodendrocyte differentiation (Leipzig & Shoichet 2009). Furthermore, Keung et al. have shown that ECM stiffness is a Rho GTPase dependent signal. Increasing stiffness increased RhoA and Cdc42 (known regulators of cell contractility and motility) expression within NSCs, leading to a suppression of neuronal lineage commitment (Keung et al. 2011).

The ECM acts to structurally support the SEZ niche architecture. Thus, matrix remodeling by matrix metalloproteinases (MMPs or matrixins) also plays a role in regulating NSC behaviour (Shan et al. 2018). Ependymal cells were found to maintain intracellular stores of MMP-12, which promotes ciliogenesis through the upregulation of FOXJ1. As well, extracellular MMP12 was found to promote NSC quiescence (Shan et al. 2018).

The ECM, with its many components and changing composition thus regulates the proliferation, differentiation, and migration of NSCs and their progeny by modulating mechanical stresses/matrix stiffness (Arulmoli et al. 2015) as well as delivers signaling molecules.

1.3.6 Microglia

Microglia are mononuclear phagocytes of the central nervous system arising from yolk sac erythromyeloid precursors (Kierdorf et al. 2013). Microglial cells survey the brain parenchyma (Nimmerjahn et al. 2005), acting as phagocytic “cleaners”, removing apoptotic waste or foreign bodies (Sierra et al. 2013). Microglia have been shown to secrete BDNF, neurotrophin-3, bFGF, HGF, and insulin-like growth factor; all of which serve to increase proliferation of NSCs. Under the M1 activation state (Ransohoff 2016), microglia have also been shown to express TNF-α, an inhibitor of NPC differentiation (Monje et al. 2003; Carpentier & Palmer 2009).

Microglia exist either in a resting (M0) state or a classically activated (M1) or alternative activation (M2) state. Classical activation occurs in response to proinflammatory lipopolysaccharides or interferon gamma. M1 microglia produce proinflammatory cytokines and are thought to mediate inflammatory tissue damage. M2 microglia are further subdivided into 3 categories: M2a, M2b, and M2c. M2a microglia activate in response to IL-4 or IL-13. M2a microglia produce IGF-1 and anti-inflammatory IL-10 and are thought to aid in the removal of cellular debris and promote tissue repair. Lastly, M2b and M2c are similar classes of microglia activated by other microglia and is characterized by expression of CD32 and CD64. M2b/c microglia display an increased phagocytic phenotype (reviewed in Walker & Lue 2015).

Microglia have been shown to engulf NPCs to modulate neurogenesis in the adult hippocampus (Sierra et al. 2010). Fourgeaud et al. have shown that this process is by microglial expression of AXL, a receptor tyrosine kinase (TAM), and its ligand growth-arrest-specific protein 6 (Gas6). In AXL deficient mice, increased neurogenesis was observed as greater numbers of NPCs were spared from phagocytosis (Fourgeaud et al. 2016). The full extent of downstream effects of microglia signaling and whole cell NPC phagocytosis have still yet to be wholly elucidated (reviewed in Li & Barres 2018).

1.3.7 Vasculature

Angiogenesis begins around embryonic day 8-10 (Marin-Padilla 1985). Angioblasts form a meshwork around the neural tube and proliferate to create a perineural vascular plexus (Strong 1964). Vascular sprouts then begin to emerge from this meshwork and anastomose to form the subventricular plexus of the ventricular zone (Tata et al. 2015). In the developing embryo, radial glial cells stabilize newly formed blood vessels by activating the Wnt pathway in endothelial cells (Tata et al. 2015).

The developing vessels express vascular endothelial growth factor (VEGF) and are critical in forming correctly patterned cytoarchitectures of the cortex (Li et al. 2013). VEGF has been shown to enhance NPC proliferation (Jin et al. 2002; Wada et al. 2006). In adulthood, endothelial cells no longer express VEGF, and instead express stromal-cell derived factor 1 (SDF-1), a potent chemotaxin for neuroblast migration in response to injury (Arvidsson et al. 2002; Yamashita et al. 2006). Along with SDF-1, blood vessels also express brain-derived neurotrophic factor (Snapyan et al. 2009). Adult blood vessels are hypothesized to act as scaffolding guides for neuroblasts to migrate along towards the olfactory bulb and as enhancers of NPC proliferation (Bovetti et al. 2007; Whitman et al. 2009).

Endothelial cells of the SEZ express pigment epithelium-derived factor (Ramírez-Castillejo et al. 2006), betacellulin (Gomez-Gaviro et al. 2012), and neurotrophin-3 (Delgado et al. 2014), which have all been shown to regulate the proliferation of NPCs. The entry of blood borne factors including cytokines, glucose, gases, hormones, and metabolic byproducts into the CNS is regulated by endothelial cells. Tavazoie et al. suggest that the blood brain barrier (BBB) at the SEZ may be “looser” than in other vessels, thus allowing circulating molecules to modulate NPC behaviours such as neurogenesis. Furthermore, NPCs directly contact endothelial vessel walls in regions lacking pericytes in the SEZ (Tavazoie et al. 2008). While the effects of systemic signals are still being investigated, a number of studies have demonstrated that circulating hormones can regulate neurogenesis. In pregnant mice, Shingo et al. have shown that prolactin can increase neurogenesis (Shingo et al. 2003). Under stress, glucocorticoids have been shown to suppress neurogenesis (Snyder et al. 2011). In a parabiosis model, Katsimpardi et al. showed neurogenesis in aged animals may be rescued by circulating systemic factors from a young animal.

Specifically, Katsimpardi et al. postulate that a circulating member of the TGFβ family, growth differentiation factor 11, is responsible for the increase in proliferation (Katsimpardi et al. 2014).

In summary, brain vasculature plays an important structural role in guiding neuroblast migration as well as act as gatekeepers for niche access to nutrients and other systemic signals that in turn regulate NPC behaviour.

1.3.8 Other Interactions

Beyond the interactions affecting NPCs detailed in the subsections above, NPCs have also been shown to undergo autocrine signaling activity in development (Yuzwa et al. 2016), cell-cell contact mediated signaling (Jiao et al. 2017), and exosome signaling (Bátiz et al. 2016). More broadly, NPC proliferation has been shown to be induced by running/aerobic exercise (Van Praag et al. 1999), and in pathological states of seizure (Lugert et al. 2010), and stroke (Zhang et al. 2014).

Questions remain as the field attempts to understand the reciprocal interplay between external influence and cell behaviour (Seleit et al. 2017). Dumont et al. recently showed that mechanical stress produced by blood flow affects NPC proliferation, adhesion, and differentiation. Under dynamic flow conditions, ECM composition increased in heparin sulphate glycosaminoglycans and promoted neuronal differentiation. However, static conditions promoted adherent growth and oligodendrocyte differentiation (Dumont et al. 2017). Aging and some pathologies reduce vascularization and blood flow in the brain and may have broad effects on niche composition and NPC behaviour. Understanding differences between young versus old and healthy versus disease states of the niche can offer novel, therapeutic insights into how the neural stem cell population is maintained and how its regenerative capacity is regulated.

1.4 Age-Related NPC Changes

Adult NSCs are typically quiescent with a cell cycle time of around 28 days (Morshead et al. 1994). Their proliferative progeny have a cell cycle time of around 12.5 hours (Morshead & van

der Kooy 1992). Typically, the average lifespan of a laboratory mouse is 28 months (Ruddy & Morshead 2018). As age progresses, NSC proliferation and neurogenesis decreases (Tropepe et al. 1997; Enwere et al. 2004; Luo et al. 2006; Conover & Shook 2011) as shown by studies reporting decreased bromodeoxyuridine (BrdU) staining at later ages. BrdU is a thymidine analog incorporated into the DNA during DNA replication, or S-phase, thus indicating what cells will most likely be dividing over time. This reduction in NPC number and regenerative potential has been correlated to cognitive impairment in old age (Ben Abdallah et al. 2010; Bondolfi et al. 2004; Kempermann et al. 2018; Kuhn et al. 1996). This functional decrease may be due to changes within the niche affecting the cells, systemic changes, or due to intrinsic cell changes over time. Evolutionarily, there is decreased selection for the maintenance of organismal function past reproductive age. According to this theory, pathways controlling development up until optimal evolutionary fitness may be dysegulated at later ages and promote the aging process (Ermolaeva et al. 2018). The pathways may be extrinsic factors dictating cell behaviour or intrinsic factors modifying niche controls leading to organismal decline. The causality of these relationships still remains unclear.

1.4.1 Niche Related Changes

Throughout age, gross changes of the lateral ventricle shape begin to take place. Stenosis of the SVZ occurs along with a concomitant loss of ependymal cells and subsequent reduction in the size of the SEZ niche, shrinking from 5 cell layers thick to approximately 3 cell layers thick (Luo et al. 2006). As well, the SEZ niche thins from 5 cell layers thick to 1-3 cells thick. Ependymal cells lose cilia density (Capilla-Gonzalez et al. 2014) and the production of neuroblasts becomes restricted to the dorsolateral corner of the lateral ventricle subependyma (Luo et al. 2006).

Luo et al. also showed vascular reorganization during aging (Luo et al. 2006) with changes in the orientation of the vasculature and increased tortuosity of vessels. The microglial population also changes with age, increasing in number and taking on a pro-inflammatory phenotype. Microglia can be classified as M0 in their resting state, typified by ramified morphology, and M1 refers to activated microglia with more amoeboid morphology. With age, M0 microglia where shown to increase neurogenesis and proliferation, whereas M1 microglia reduced neurogenesis (Solano Fonseca et al. 2016). Microglia have been shown to release factors affecting neural development

(Shigemoto-Mogami et al. 2014) and under different activation states, may interact with vascular (Checchin et al. 2006) and ependymal elements (Solano Fonseca et al. 2016) of the niche to mediate an inflammatory response leading to decreased NSC activation.

Recent studies using single-cell transcriptomics have identified differential inflammatory responses in the aging brain. Shi et al. have identified a host of activated proinflammatory factors affecting microglia activation as well as metabolic processes. Interestingly, they have also identified differential gene expression profiles in quiescent NPCs that suggest the overall quiescent phenotype in aging may be due to different and separate processes acting on individual NPCs (Shi et al. 2017).

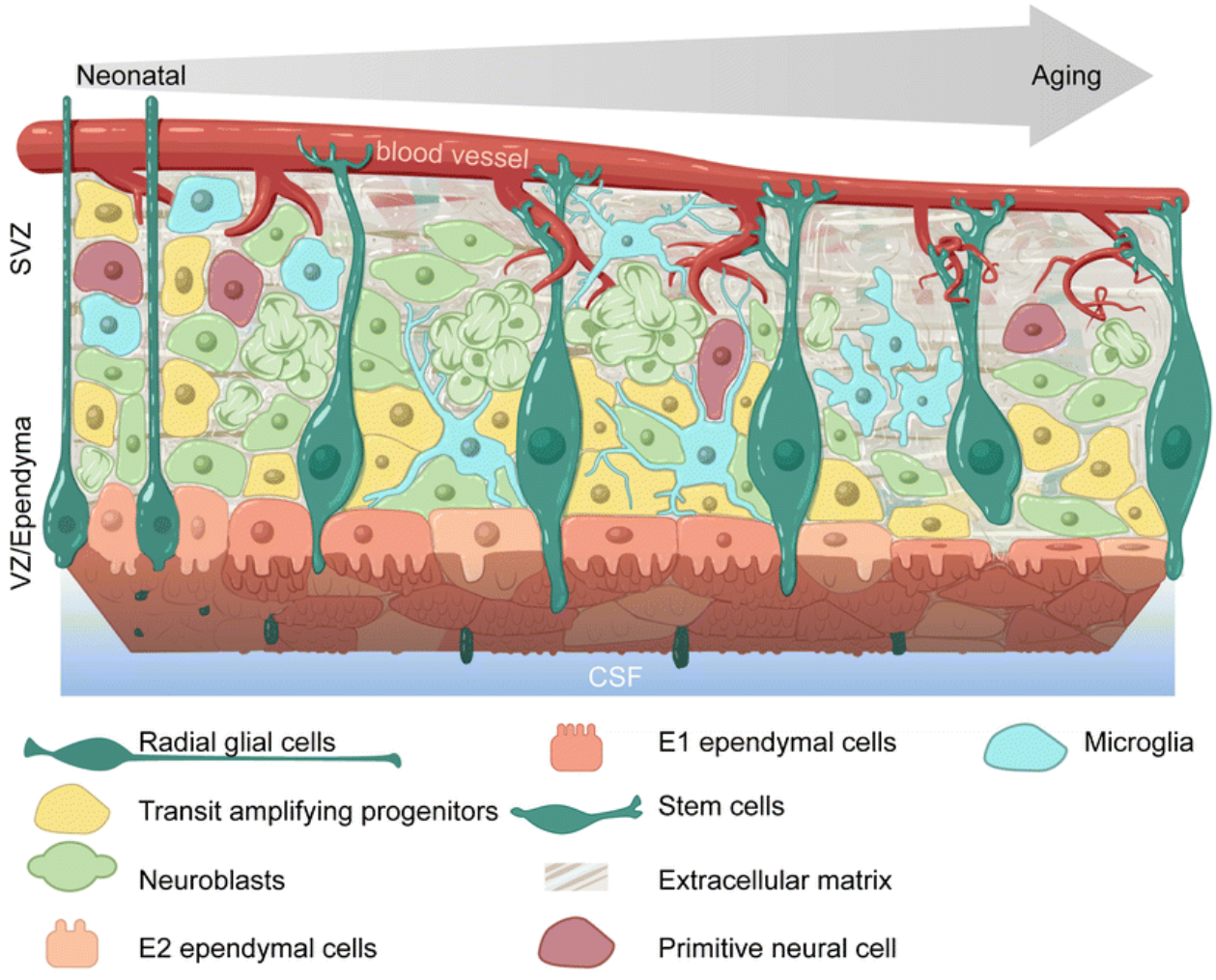

Figure 4: Adapted from Ruddy & Morshead 2018. Changes in extracellular matrix, cell composition, as well as ependymal and stem cell morphology in young versus aged neural stem cell niche.

1.4.2 Cell Related changes

On a cellular scale, age can be categorized into two forms of measurement: chronological time and replicative age. In a single cell organism, chronological and replicative age are nearly equivalent. However, in the multicellular organism, chronological time is the age of the cell itself, or the cell's constituents, whereas replicative age is determined by the number of cell cycles/divisions a cell has undergone. Factors at play in affecting replicative age is a cell's telomere length/modulators and cell cycle time. Chronological time is affected by exposure to reactive oxygen species (ROS), mitochondrial changes, cell metabolism, and protein aggregation (reviewed in Maskell et al. 2003).

As a cell divides, it must maintain the fidelity of its genetic material. ROS-induced DNA damage is an unavoidable obstacle all cells must overcome. Past a threshold of DNA damage, cells will no longer be able to undergo mitosis and will eventually be directed to undergo apoptosis (reviewed in Gonfloni 2013). Guards against DNA damage include base excision repair, nucleotide excision repair, nonhomologous end joining (NHEJ), homologous recombination, and telomere elongation. Due to a stem cell's quiescent nature, NHEJ is the dominant repair mechanism used to repair double stranded DNA breaks. However, NHEJ is an error prone mechanism as the cell does not have another copy of DNA to use as a template (reviewed in (Iyama & Wilson 2013). Over time, the probabilities of acquiring DNA damage accumulate and could potentially impact stem cell function.

When a cell undergoes mitosis, DNA replication needs to occur with high fidelity. However, DNA replication machinery is incapable of fully copying the ends of a chromosome. To protect against gene loss over multiple replications, each chromosome contains long nucleotide repeats termed "telomeres". Telomeres cap the ends of chromosomes and shorten with every replication. Once telomeres shorten below a certain threshold, cell checkpoint responses are activated and the cell will be directed to undergo apoptosis or become permanently quiescent (otherwise known as entering senescence). The number of cell divisions a cell may undergo before reaching this threshold is termed the "Hayflick limit" (reviewed in O'Sullivan & Karlseder 2010). To extend a cell's replicative lifespan, cells may elongate their telomere length with the enzyme telomerase. Telomeric integrity, or length, is often associated with replicative longevity, with quiescent stem cells often having very long telomeric repeats. However, it has been shown that telomere length

decreases with age (Flores et al. 2008). As well, telomerase mutations show a premature aging phenotype (Lee et al. 1998).

If a cell cannot correct a major mutation, cell cycle inhibitors are activated. Cell cycle inhibitors $p16^{lnk4a}$, $p19^{Arf}$, and p53 become activated and directs the cell towards cell cycle arrest, senescence, or apoptosis (Signer & Morrison 2013; Sperka et al. 2012). Interestingly, $p16^{lnk4a}$, $p19^{Arf}$, and p53 are increased with age (Sperka et al. 2012) potentially mediating age related quiescence. As well, p57 is a cyclin-dependent kinase inhibitor required to maintain NSC quiescence. Deletion of p57 inhibits NSC quiescence, leading to increased neurogenesis. However, this increased activation depletes the NSC pool leading to impaired neurogenesis in aged mice (Furutachi et al. 2013). Similarly, p21 is another cyclin-dependent kinase inhibitor that has been implicated in maintaining NSC quiescence. In p21-null mice, deficiencies in NSC proliferation only occurred after ischemic injury (Kippin et al. 2005; Qiu et al. 2004). Both of these kinase inhibitors help to arrest cells at the G1 phase and prevent entry into S phase of the cell cycle. NSC activation exhausts the stem cell pool, suggesting quiescence may be necessary for long-term maintenance of NSC proliferation (Kippin et al. 2005). Yet these different proliferative responses suggest NSCs may be differentially activated in response to injury or another form of external stimulus.

Interestingly, recent work has shown that the aging phenotype of decreased proliferation is not fully correlated with age. In an in vivo murine model, using RNA-sequencing, Apostolopoulou et al. have shown that up until 18 months of age, this aging phenotype holds true. However from 18 to 22+ months of age, proliferation increased in the brain following the initial decline through adulthood. Above 18 months of age, $Mash1^{+}$ progenitor cells increased in number compared to adult (2-18 months of age) numbers. However, 18-22+ month progenitor cell numbers were still less than half of progenitor numbers found in young (less than 2 months of age) animals. Apostolopoulou et al. identified 292 genes most highly expressed at the 18 month period relative to earlier ages (less than 18 months of age). These genes were found to be involved in calcium, mTOR, and insulin signaling, as well as chromatin modification, helicase activity, and senescence. Apostolopoulou et al. also identified 226 genes with minimal expression at 18 months compared to younger aged groups. These genes were found to be involved in modulating cell cycle, cell adhesion, metabolism, and chaperone-mediated protein folding. As well, there exists considerable crosstalk between the mechanisms affected by maximally and minimally

expressed genes. These interactions have yet to be fully elucidated, however their phenotype is conserved between in vivo and in vitro analyses (Apostolopoulou et al. 2017).

Interestingly, not all stem cells change the same way throughout aging. Muscle progenitor cells (Alsharidah et al. 2013) and epidermal stem cells (Racila & Bickenbach 2009) do not change in proliferation kinetics or show altered signs of cellular senescence through age. It is yet unknown if the constancy of these stem cells are due to intrinsic or extrinsic factors. As described above, cell intrinsic factors do not always operate in isolation from cell extrinsic factors. Teasing apart niche vs. cell intrinsic phenomena, particularly through aging, requires a sound knowledge of the complex relationships between cell intrinsic and extrinsic controls.

Although there is still much to learn regarding the factors affecting stem cell behaviour, studies have shown that aged NPCs are capable of responding to neonatal cues. Using cell-cell and conditioned media (CM) mixing experiments, Piccin et al. have shown that neonatal NPCs can activate quiescent, aged NPCs and increase their proliferation and conversely, aged NPCs could suppress neonatal NPC proliferation. (Piccin et al. 2014). Similarly in parasymbiosis experiments, neonatal blood borne factors have been shown to increase neurogenesis in aged animals (Katsimpardi et al. 2014) and conversely, aged blood borne factors have been shown to decrease neurogenesis in young animals (Villeda et al. 2011). Many questions still remain regarding the identities and mechanisms of action of the specific factors involved in the differing young and aged environments that can affect NPC behaviour.

1.5 Cell Migration

Cell migration is a fundamental interaction of a cell with its environment. In unicellular organisms, cell migration allows the organism to navigate their environment in search of nutrients and to evade potential predators. In multicellular organisms, cell migration allows the organism to form complex architectural arrangements, maintain and repair damage, as well as seek out foreign invaders. Cell migration can be divided into two broad categories: passive or active. Passive migration is described as cell mobility, where a cell is simply capable of movement, regardless of its ability to generate its own movement or counteract external forces.

Active migration is described as cell motility, where a cell is capable of generating and/or directing its own movement (reviewed in Allen 1981). Herein, we will focus on cell motility.

There are many forms of cell motility. Some cells generate protein motors to power beating cilia and flagella. These structures propel cells through their environment through non-adherent physical force, in addition to moving a cell's environment around the cell. Other cells move through attachment mediated processes, where a cell will attach to its surroundings then push and/or pull itself along (reviewed in Allen 1981). Adherence dependent migration may be divided into three major categories: single cell/amoeboid migration, collective migration, and scaffold cell dependent migration (reviewed in Kawauchi 2012). Single cell migration is characterized by extension of filamentous actin (f-actin) rich membrane sheets termed lamellipodia, or round protrusions termed membrane blebs. The directional, quick movement requires rapid cytoskeletal reorganization. Collective migration, which can occur in sheets, strands, tubes, or clusters, is characterized by cell-cell junctions between cells during movement. Lastly, scaffold cell dependent migration, as its name suggests, uses another cell as a migratory scaffold to guide the cell from its origin to its destination (reviewed in Kawauchi 2012). Herein, I will focus on adherence dependent migration mechanisms as NPCs have been shown to exhibit substrate adherent single-cell migration in vitro (Babona-Pilipos et al. 2011) and in vivo, neuroblasts migrate via chain migration, a scaffold dependent form of migration (Malatesta & Gotz 2013; Doetsch & Alvarez-Buylla 1996; Bovetti, Hsieh, et al. 2007).

Orchestrated cell migration depends on external signals to coordinate their motion. These signals include chemical, mechanical, and electrical signals. To initiate cell migration, the cell must first adhere to matrix elements through adhesion proteins expressed in the plasma membrane. Other sensors on the membrane detect the external signal resulting in a cascade of motility machinery remodeling internally. As a cell begins to move, the side of the cell in the direction of motion is termed the "leading edge". The side opposite to the direction of migration is termed the "trailing edge" (reviewed in Kaneko et al. 2017). The motion of cell migration may be described in two main phases.

1. ***Leading Edge Protrusion***

   The cell becomes polarized, forming a leading and trailing edge with concentrations of actin focused towards the leading edge. The cell uses f-actin bundles to push the plasma

membrane outwards, extending the area it covers. Flat, fan-like protrusions of f-actin are termed lamellipodia (Ponti et al. 2004; Verkhovsky et al. 2003). Punctate, parallel bundles of f-actin are termed filopodia. It is hypothesized that filopodia fulfill an exploratory and mechanosensory role, whereas lamellipodia provide a large surface area to generate traction for forward movement. In the generation of the leading edge, focal adhesions at the front of the cell are formed. Adhesions to the substratum occur through integrin receptors that link ECM components to the cytoskeleton. As the cell sends out protrusions, new adhesions are formed along the base of these protrusions. As the cell continues to push outwards, these adhesions anchor the cell to a new location (reviewed in Trepat et al. 2012; Zamir et al. 2000).

2. ***Trailing Edge Retraction***

   The trailing edge, as well as the majority of the cell body is translocated forwards. This translocation is mediated by the release of adhesions near the trailing edge, as well as actomyosin and microtubule dependent intracellular contractions (Svitkina et al. 1997; reviewed in Trepat et al. 2012). These contraction forces, coupled with an adhesion disassembly process, promote the movement of the cell body towards the leading edge. In some cell types, this motion is enough to tear integrins from the plasma membrane and leave a trail bound to the substratum (Schmidt et al. 1993). Focal adhesions are formed at the leading edge and released at the trailing edge. Over 150 different molecules may be present in a focal adhesion. Paxillin and focal adhesion kinase (FAK) are two main regulators of the Rho family GTPases that in turn regulate actin polymerization/organization and microtubules dynamics. As well, talin, vinculin, and α-actinin are all involved in attaching integrins to actin filaments (Webb et al. 2004; reviewed in Trepat et al. 2012).

The following subsections will discuss the mechanisms of migration in embryonic and adult neurogenesis.

1.5.1 Developmental Migration

In development, radial glial cells have their cell bodies in the ventricular zone and extend a pial process that acts as a scaffold, or ladder, for cells to migrate along. This scaffold dependent migration of new neurons along these extended processes is termed “radial migration” (Noctor et al. 2004). This form of migration follows paradigms of scaffold dependent migration. Migrating neurons interact with radial glial processes via cell-surface integrin receptors, specifically α3β1 integrins (Anton et al. 1999). Integrins are heterodimeric membrane proteins that connect the ECM (predominantly fibronectin and laminin during development) with intracellular cytoskeletal elements. β1 integrins have also been shown to aid in basement membrane maintenance, helping radial glial processes attach to the pial surface (Graus-Porta et al. 2001). Disrupting integrin receptor binding leads to abnormal cortical lamination. Studies have also shown gap junctions are present between migrating neurons and radial glial processes, allowing electrical and chemical coupling of these cells. These gap junctions provide dynamic adhesive contacts that stabilize the leading edge (Elias et al. 2007).

Other signaling factors such as reelin (Hirota & Nakajima 2017), ApoER2 (Hirota et al. 2018), Vldlr (Hack et al. 2007), and Dab1 (Franco et al. 2011) also play a role in guiding neuronal migration, specifically playing a role in cortical lamination and mediating cell detachment from radial glial processes. Migrating neurons also express GABA and AMPA/NMDA receptors, allowing them to respond to detachment signals of GABA and glutamate (Miyoshi & Fishell 2011). These neurotransmitters are thought to depolarize newborn neurons, resulting in calcium ion transients that promote cell motility (Bortone & Polleux 2009). Interestingly, upon arrival to the cortex, newborn neurons begin upregulating the potassium/chloride ion exchanger (KCC2) which modifies the cells response to GABA from depolarizing to hyperpolarizing. The current hypothesis is that this leads to a reduction in calcium influx and slowing/halting of neuronal migration (Bortone & Polleux 2009).The underlying mechanisms governing these interactions are still an active area of investigation.

1.5.2 Chain Migration

As described previously, neuroblasts migrate through the rostral migratory stream to the olfactory bulb where they become interneurons. This specific form of migration is termed chain migration. Migrating neuroblasts have been shown to possess a bipolar morphology with a long leading process and short trailing process. These cells migrate in a non-synchronized saltatory fashion involving process extension and somal translocation, as well as an additional intermediate step of swelling formation and centrosomal migration. This additional phase is characterized by a cytosolic dilation in the proximal portion of the leading process where a centrosome will migrate to and act as a microtubule-organizing centre to regulate the microtubule networks supporting the leading process and/or cell nucleus which form a perinuclear cage (reviewed in Kaneko et al. 2017). Studies have shown that both actin and microtubules (Schaar & McConnell 2005) are necessary in extending and supporting the leading process. To alter directions, neuroblasts form a new leading process by first reorienting the centrosome in response to signals from the repulsive guidance molecule Slit (Higginbotham et al. 2006). There is still much to learn about the intracellular mechanisms that integrate and coordinate the cytoskeletal machinery of migration. However, many extracellular cues have been found.

The olfactory bulb produces Prokineticin-2 (Ng et al. 2005), Netrin1 (Murase & Horwitz 2002), and glial cell-derived neurotrophic factor (GDNF; Paratcha et al. 2006) which act as chemoattractants for neuroblasts. As well, HGF is distributed along the RMS, keeping cells within their defined path (Wang et al. 2011). As discussed previously, CSF flow and Slit secretion guides the rostral migration of neuroblasts (Sawamoto et al. 2006). As neuroblasts migrate, they form discontinuous adherens junctions with each other, suggestive of a scaffolding migration paradigm as opposed to a true collective cell migration paradigm. Interestingly, dissociated neuroblasts are capable of individual migration in vitro. However, in vivo, chain disruption has been reported to show decreased directional migration (reviewed in Kaneko et al. 2017). Neuroblasts express β integrins (Belvindrah et al. 2007), PSA-NCAM (Peretto et al. 2005), and N-cadherin (Fujikake et al. 2018), all of which are adhesion molecules implicated in chain formation.

In the RMS, migrating neuroblasts are surrounded by glial tubes, essentially a tunnel surrounded by astrocytes (Malatesta & Gotz 2013). Neuroblasts maintain this tunnel architecture via Slit-Robo signaling (Kaneko et al. 2010). Neuroblasts secrete Slit1 and surrounding astrocytes express Robo, a transmembrane receptor. Slit regulation of Robo in turn affects astrocyte distribution and morphology. As well, blood vessel basal laminae can be bound by the integrins expressed by neuroblasts. Neuroblasts also express MMP-3 and MMP-9 (Bovetti et al. 2007; Barkho et al. 2008), modifiers of matrix density.

When neuroblasts leave the RMS, they begin using the olfactory bulb vasculature as a scaffold for migration (Snapyan et al. 2009). Endothelial cells secrete SDF-1, a powerful chemoattractant for NPCs to recruit cells (Kokovay et al. 2010). β1 integrins expressed by neuroblasts are also necessary for migration along vasculature (Fujioka et al. 2017).

1.6 Membrane Potential

All living, animal cells possess an electrical potential difference across their plasma membranes ranging from -10 to -90mV (negative intracellularly) under baseline resting conditions (Sundelacruz et al. 2009). The membrane potential is a gradient of electrical energy that influences nutrient transport, coordinating cellular and organismal motility, and ultimately, cognition. Membrane potentials are influenced by two major parameters: the transmembrane gradient of charged ions (predominantly Na+, K+, but also Ca2+ and Cl-) and the relative permeability of the membrane to these ions. Transmembrane Na+ and K+ gradients are predominantly established by the Na+/K+ ATPase, an active ion pump on most animal cells that maintains outwardly directed K+ and inwardly directed Na+ gradients. A membrane's relative permeability to a particular ion is fluid and depends on passive diffusion as well as selective ion channels that may be open or closed. The sum of the impact each ion contributes to the overall "strength" of the potential membrane is the resulting resting membrane potential (RMP; reviewed in (Wright 2004; Cardozo 2016).

The impact of an ion, in isolation, may be calculated using the Nernst equation, an equation representing how much energy in volts must be applied across a cell membrane to prevent the movement of a particular ion across the membrane. In other words, what a particular ion's

contribution to the cell membrane potential would be if allowed to equilibrate according to its concentration gradient. The Nernst equation only gives the contribution of a single ion to the membrane potential. The Goldman-Hodgkin-Katz equation combines the potential for all ions (combines Nernest equations) to calculate the final membrane potential.

$$V_k = \frac{RT}{zF} \ln \frac{[K^+]_o}{[K^+]_i}$$

$$V_m = \frac{RT}{F} \ln\left(\frac{p_K[K^+]_o + p_{Na}[Na^+]_o + p_{Cl}[Cl^-]_i}{p_K[K^+]_i + p_{Na}[Na^+]_i + p_{Cl}[Cl^-]_o} \right)$$

Figure 5: The Nernst equation (top) for calculating solely potassium's contribution to the membrane potential and the Goldman-Hodgkin-Katz equation (bottom) for calculating overall membrane potential taking into account 3 ions; Na^+, K^+, and Cl^-. Where R = the universal gas constant (8.314472J/(K·mol)); T = temperature in Kelvin; z = valence of ion (+1 for potassium); F = Faraday's constant (96485C/mol); $[ION^{+/-}]_o$ = extracellular concssssentration of an ion (eg. 150mM for K^+); $[ION^{+/-}]_i$ = intracellular concentration of an ion (eg. 4mM for K^+); p_{ION} = membrane permeability for an ion (Typically, relative permeabilites are used with p_K having a reference value of 1. This is done because permeability changes depending on the cell state as the resting membrane permeabilities are different from action potential membrane permeabilities.) To give an example, using typical values for intra- vs extracellular ion concentrations ($[K^+]_o$ = 4mM; $[K^+]_i$ = 150mM; $[Na^+]_o$ = 145mM; $[Na^+]_i$ = 15mM; $[Cl^-]_o$ = 110mM; $[Cl^-]_i$ = 10mM; and resting membrane relative permeabilities of p_K = 1; p_{Na} = 0.05; p_{Cl} = 0.45; the Nernst equation gives the individual equilibrium potentials of V_K = -96.81mV; V_{Na} = +60.6mV; V_{Cl} = -64.05mV leading to a total V_m = -67.92mV according to the Goldman-Hodgkin-Katz equation.

The importance of RMPs are often discussed with respect to neuronal or cardiac action potentials (APs). However, membrane potentials also play a role in many other AP-independent cellular processes. In the early 1970's Clarence Cone first reported a link between depolarized RMP and an increased proliferative potential (Cone 1971; Stillwell et al. 1973; Cone & Cone 1976) and has been corroborated by other recent studies (Sundelacruz et al. 2009; reviewed in Blackiston et al. 2009; Urrego et al. 2014).

Conversely, a hyperpolarized membrane has been shown to be linked to cell quiescence. Hyperpolarized cells proliferate less (Sundelacruz, Levin, and Kaplan, 2009) and polarization of membranes may also be related to cell extrinsic and/or intrinsic age-related factors (Cervera et al. 2016). Co-culture experiments have demonstrated that a young niche can modify the quiescence of older cells, (Piccin, Tufford, and Morshead, 2014). It is yet unknown what non-ion channel, protein factors play in role in modulating membrane potential.

RMP magnitudes have been reported to be ranging from -40 to -90 mV in differentiated cells, -8.5 mV in fertilized frog eggs and -23 to -25 mV in subsequent divisions before the morula stage

(Binggeli & Weinstein 1986; Levin 2007). Tumour cell membrane potentials have also been reported to be in similar ranges as embryonic cells (Chernet & Levin 2013; Funk 2013).The association between depolarized membrane and increased proliferative potential and its effectors are still being discovered.

Recently, Zhou et al. have reported a potential mechanism of RMP mediated proliferation. Zhou et al. showed that membrane depolarization induced a specific nanoscale inner-leaflet membrane phospholipid reorganization (phosphatidylserine [PS] and phosphatidylinositol 4,5-bisphosphate [PIP_2]) using baby hamster kidney cells. Zhou et al. found that the Ras family isoform, K-Ras, a membrane bound signaling protein, was targeted to PS via electrostatic interactions to form Ras-GTP nanoclusters essential to the activation of MAPK signaling. Nanocluster formations involve complex interactions between charged membrane lipids, Ras lipid anchors, and Ras basic residues and is enhanced with membrane depolarization. Enhanced PS nanoclustering is a rapid process, showing 80% completion within 30 seconds. PS depletion also rendered K-Ras nanoclustering insensitive to RMP changes (Zhou et al. 2015). Downstream of Ras activation, the MAPK signaling pathway has been well-characterized in its effects on cell proliferation kinetics, differentiation, neuronal plasticity (Kelleher et al. 2004), gene expression, metabolism, motility, survival, and apoptosis (reviewed in Cargnello & Roux 2011).

Dysregulation of membrane potential has been linked to cancer (reviewed in Yang & Brackenbury 2013; Pardo & Stühmer 2014; Litan & Langhans 2015) as well as cell migration (discussed in subsequent sections; reviewed in Schwab et al. 2012). Interestingly, Labeed et al. suggest that differentiation of human NPCs may be predicted by their membrane potentials and may be clustered into sub-populations of neurogenic or gliogenic progenitors (Labeed et al. 2011). Nourse et al. have also reported that NPCs may be identified as neurogenic or astrogenic progenitors by differing membrane capacitance (Nourse et al. 2014).

While the roles and mechanisms of membrane potential action are still being actively investigated for many cell types, to date, there are still many unknowns linking applied EFs to conserved RMP changes and downstream effects. This thesis provides support for RMP serving as a potential mechanism by which NPCs can sense external electric fields that regulate NPC behaviour.

1.7 Electric Fields

An electric field (EF) is commonly described as a vector field due to an electrically charged object or apparatus that can exert a force on other charged objects. Depending on the polarity of the object, the force exerted may be an attractive or a repulsive force. The strength of an EF can be measured as newtons per coulomb of charge, or rearranged to represent potential difference (or voltage) per unit distance. For ease of measurement in a biological system, the most common measurement is milliVolts per millimeter (mV/mm). EFs can be generated by partitioning electric charges or varying magnetic fields. In an organism, the EFs generated will seldom be uniform. Field strengths experienced in one portion of the organism may be dramatically different from field strengths in other parts of the organism. Even fields within a particular region may fluctuate over time (Pokorný et al. 2005; Pokorný et al. 2013; Messerli & Graham 2011). However, in vitro, uniform EFs may be created by placing two uniform, conductive charge sources (electrodes or plates) parallel to each other and maintaining a potential difference (or voltage) between them (Zhao et al. 1999; Zhao et al. 2002). Bioelectricity and a cell's response to an EF are nascent fields and much about the regional electric fields present in the brain is still yet to be discovered.

1.7.1 Endogenous Electric Fields

To generate an EF, charges must be physically separated. In biology, EFs are often found when charged particles are separated across an epithelium or membrane. The most common EFs are the action potentials used by neurons and muscles to transmit electrical impulses. However, there are also bioelectric currents that play a critical role in embryogenesis as well as modulating normal, homeostatic adult tissue repair (Nuccitelli 2003). EFs exist both cytoplasmically and extracellularly. Although, baseline endogenous EF strengths have not yet been reported for all tissues of the body, they have been shown to range from strengths of a few mV/mm to hundreds of mV/mm and have been found in the central nervous system (Weiss & Faber 2010), skin (Nuccitelli et al. 2008), bone (Marino & Becker 1970), eyes (Chiang et al. 1992), blood vessels (Zhao et al. 2004), adult stem cells (reviewed in Maziarz et al. 2016), and even whole limbs (McGinnis & Vanable 1986). Although the mechanisms of EF sensing and transduction into cell behaviours are still not well understood, the effects of EF stimulation have been shown to be

positive, provided that EF strength and duration are within a tolerable limit. Below, I will briefly discuss some of the major effects of EFs on endogenous tissue with specific focus on galvanotaxis.

1.7.1.1 Transepithelial Potential

Epithelial cells act as a barrier between internal and external aspects of the body. Epithelial cells are polarized to apical and basolateral domains with each side performing specific tasks. The apical side features selective protein pumps, channels, transporters, and receptors, allowing transport of nutrients and interactions with the external environment. The basolateral side also features selective channels but importantly, also expresses tight junctions that form an electrically resistive barrier. Each epithelial cells carries a potential difference across the apical versus basolateral membranes (Foulds & Barker 1983). The sum of these potentials across the whole epithelium make up the transepithelial potential (TEP). In the early embryo, TEPs are generated by passive Na^+ uptake from the environment. Differences in TEPs between distinct regions of the embryo forms intra-embryonic voltage gradients (Hotary & Robinson 1990). These gradients carry a potential of 100-500mV/mm and are capable of affecting cell morphology and migration (reviewed in Funk 2015).

The TEP with the largest area is generated by the skin (Nuccitelli et al. 2008). TEPs have also been reported in the cornea (Reid et al. 2011), gastrointestical tract (Orlando et al. 1989), kidney (Clausell et al. 2014), respiratory tract (Knowles et al. 1981), prostate epithelium (Szatkowski et al. 2000), and urinary tracts (Schafer et al. 1974). TEPs act as embryonic morphogenic signals and in the adult, disruptions of TEPs by physical damage (ie. cut in the skin) can serve as a homing cue for regenerative machinery and tissue repair (Nuccitelli et al. 2008).

1.7.1.2 Developmental Electric Fields

To measure the EF strength of an organism, at least one electrode must make direct contact with the target area. However, for an embryo, this tactile disturbance disrupts the very potential being measured. To overcome this limitation, indirect measures of current densities are taken. Current

density is the electric current per cross sectional area (A/m^2) and is proportional to EF strength (mV/mm) for a given systemic resistance. In 1974, Jaffe and Nuccitelli invented a vibrating microelectrode capable of measuring current density and thus could indirectly measure the EF of an intact embryo (Jaffe & Nuccitelli 1974).

Other studies have capitalized on this observational limitation by purposefully disrupting embryonic EFs and observing the resulting changes. In this way, TEPs have been reported in the neural tube and limb buds. Applied EFs used to disrupt endogenous TEPs during neurulation resulted in incomplete neural tube folding and formation. However, exogenous EF application before or after neurulation, when local endogenous EFs decrease in magnitude, had no effect on development (Metcalf & Borgens 1994). More recently, these membrane potential disruptions have been linked to misexpression of Notch signaling. During neurulation, the cells of the neural tube are hyperpolarized. In the Xenopus embryo neuroepithelial cells had a membrane potential of -51mV, approximately 40mV more hyperpolarized than neighbouring non-neuroepithelial cells. Depolarizing these hyperpolarized neuroepithelial cells led to decreased expression of early brain markers (Otx2, Emx, and Bf1) and brain malformations. Moreover, hyperpolarizing non-neural tissue caused ectopic formation of neural tissue (Pai et al. 2015). During limb development, epithelial tight junctions break down leading to punctate TEP loss at specific locations days prior to limb bud emergence (Levin 2014; Altizer et al. 2001; Borgens et al. 1987).

Intriguingly, these membrane potential modulations are temporally and spatially specific and seem to dictate these large structural developmental paradigms. This form of instructional patterning has been termed the “bioelectric code” and has been shown to regulate a number of developmental processes (Levin & Martyniuk 2018). However, much of this code remains to be deciphered and the mechanisms tranducing this code into downstream effects are yet to be clarified.

These cell morphology directing potentials have been observed to form in specific domains in single fertilized eggs (Adams & Levin 2013). Outward currents have also been found at the lateral edges of the neural ridges and the blastopore, and inward currents have been found at the centre of the neural groove (Shi & Borgens 1995). These EFs are some of the first informational cues determining anterior-posterior or left-right polarity in the embryo (Oviedo et al. 2010;

Beane et al. 2013). Cells then transduce this electrical signal into a chemical cascade of signaling factors that eventually give rise to large morphological patterns.

1.7.1.3 Subcellular Component Modulation

Electric fields exert forces on charged objects, but may also interact with dipoles and neutral objects through the dielectrophoretic effect. To carry out the many functions of life, cells utilize charged proteins. For example, in motility, actin and tubulin are polar molecules that form long polymers with a positive and negative pole. Actin filament nucleation and elongation has been shown to be an electrostatically governed process, dependent on pH (Crevenna et al. 2013) as are microtubule dependent molecular transport, and electron transport (reviewed in Pokorný et al. 2005). Coherent physical fields have been shown to be long acting but may also be very short-acting (Petri et al. 2017), potentially influencing polarization of intracellular elements.

1.7.1.4 Neural Activity

Neurons are known to classically communicate via neurotransmitter release or gap junctions. Neurons have been described as giving rise to oscillatory waves of electrical activity with varying field strengths. These oscillatory waves have been shown to affect neuronal activity (Fröhlich & McCormick 2010).

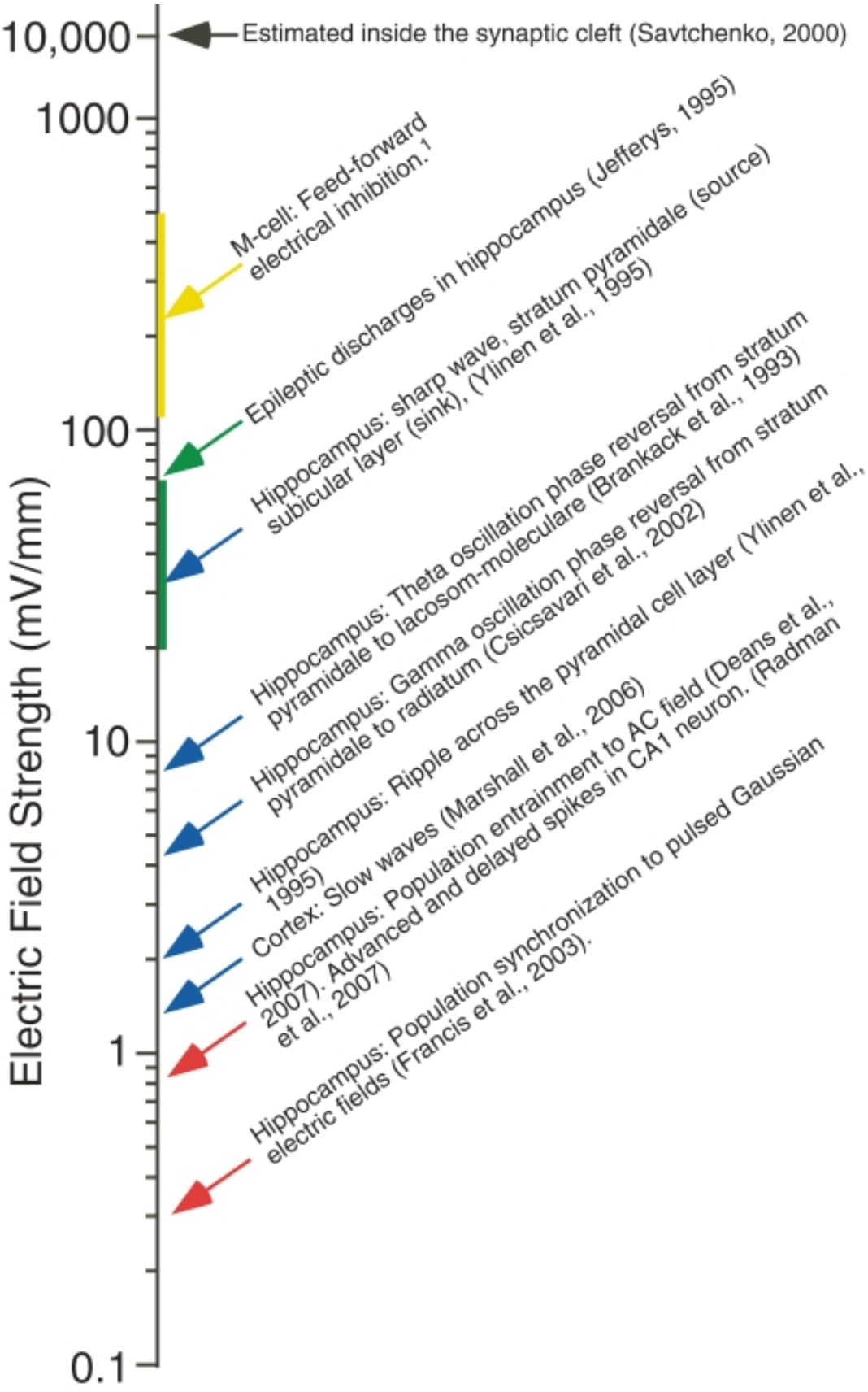

Figure 6: Field strengths generated by neurons of the brain. From Weiss & Faber 2010.

Nerve fibres have also been observed to share similar firing speeds and patterns due to axonally generated electric fields. This form of neuronal communication is term “ephaptic coupling”. Qiu et al. have shown that murine hippocampal EFs of 2.5 – 5mV/mm was sufficient to propagate APs across layers of neurons at speeds of 0.10m/s (Qiu et al. 2015). Ephaptic connections have also been implicated in propagating seizures (Dudek et al. 1998). Although the origin of these EFs are not yet clear, electrophysiological correlations of neurons and astrocytes activity have been observed and astroglial currents has been shown to regulate Ca^{2+} in the extracellular space and could play a role in regulating these EFs (Martinez-Banaclocha 2018). By understanding ephaptic coupling, we can also better design and utilize novel therapeutic techniques such as transcranial electric field stimulations which have been shown to improve cognition (Datta et al. 2009).

1.7.2 Galvanotaxis

Named for Italian physicist-physician, Luigi Galvani, the reaction of cells to electricity was coined as Galvanism. His forays into electrophysiology showed muscle activation resulting from electrical stimulation of a frog’s leg (Verkhratsky et al. 2006). Almost 200 years after this discovery, the mechanisms by which a cell translates this external signal into a physical movement is still unknown. It has been hypothesized to be due to membrane potential differences that allow a differential passive calcium ion entry into either the cathodal or anodal side of the cell. EF sensing may be due to the polarization and change in configurations of voltage-gated ion channels, cell internal polarization, and membrane potential changes (Robinson 1985). While the mechanism is not well-delineated, it is well established that cell migration in the presence of an EF occurs in a variety of cell types (Nuccitelli 2003). This directional locomotion of a cell in response to an external electric field is termed “galvanotaxis”.

EFs have been recognized as important and well-conserved migration cues. Found in cells of mammalian, amphibian, and fish phylogenies (Nuccitelli 2003; Robinson 1985), galvanotaxis is a necessary process in directing the proper growth and maintenance of body tissues. Cells reported to be EF responsive include neural crest cells (Cooper & Keller 1984); lens (Wang et al. 2003), retinal (Sulik et al. 1992), and corneal (Farboud et al. 2000; Zhao et al. 1996) epithelial cells; vascular endothelial cells (Li & Kolega 2002); Schwann cells (McKasson et al. 2008);

leukocytes (Lin et al. 2008); macrophages (Orida & Feldman 1982); keratinocytes (Nishimura et al. 1996); osteoblasts and osteoclasts (Ferrier et al. 1986); chondrocytes (Chao et al. 2000); fibroblasts (Chao et al. 2007); mesenchymal stem cells (Jezierska-Wozniak et al. 2017); skin derived precursors (Iwasa et al. 2018); and NPCs (Babona-Pilipos et al. 2011). EF strengths sufficient to induce galvanotaxis have been reported to range between tissues and cells from 3mV/mm to over 1000mV/mm (reviewed in Iwasa et al. 2017), which is comparable to developmental and endogenous EFs.

Although the phenomenon of galvanotaxis is ubiquitous across many organisms and cell types, the phenotypes are not all equivalent. Galvanotactic movement can be measured using seven metrics: distance, displacement, speed, velocity, x-axis displacement, tortuosity and directedness. Different cell types display heterogeneity in response to EF intensity, migration speeds, directedness, and robustness. In vitro experiments have shown that NPCs, neural crest cells, fibroblasts, keratinocytes, chondrocytes, rat prostate cancer cells, and corneal epithelial cells (Nishimura et al. 1996; Djamgoz MBA et al. 2001; Zhao et al. 1997; Babona-Pilipos et al. 2011) migrate cathodally at EF strengths of 10-1000mV/mm (Robinson 1985; McCaig & Zhao 1997) (Robinson, 1985; McCaig and Zhao, 1997). Other cells, although fewer in number, have been reported to migrate anodally: corneal endothelial cell, bovine lens epithelium, human granulocytes, vascular endothelial cells (reviewed in Funk et al. 2009), and skin derived precursors (Iwasa et al. 2018). Remarkably, cells of the same tissues are capable of opposite migratory directedness when experiencing the same EF stimulation. Osteoblasts and osteoclasts migrate in opposite directions from each other (Ferrier et al. 1986), as does corneal epithelial cells and corneal stromal fibroblasts (Soong et al. 1990). Both speed and direction of migration are voltage dependent. Single-cell galvanotactic migration speeds have been shown to range from 0.2 to 8 μm/min (Sun et al. 2016; Guo et al. 2015; Babona-Pilipos et al. 2011). Interestingly, directedness has been shown to be EF strength dependent in some cell populations. Bovine lens epithelial cells exhibit anodal migration at 50mV/mm but migrate cathodally between 150-250mV/mm (Wang et al. 2003). The phenomena of galvanotaxis has been vigourously observed, however the mechanisms underlying it are not completely understood.

Specific to NPCs, it has been shown that they are not capable of producing action potentials, due to a lack of voltage-gated sodium channels on their cell membrane (Mirsadeghi et al. 2017) however NPCs are still responsive to external EFs (Babona-Pilipos et al. 2011). Cao et al. have

reported EF strength values of -2±5.6 mV/mm in the olfactory bulb and +7.9±5.6 mV/mm in the SEZ, leading to a potential difference of 9.9±1.8 mV/mm between the two structures. Measurements along the RMS showed consistent changes in voltage potential, with an average field gradient of approximately 3mV/mm. Interestingly, in this biological system, the olfactory bulb acts as a cathodal terminus, and the SEZ acts as an anodal terminus. Cao et al show that neuroblasts follow this endogenous gradient in vitro and that purinergic receptors P2Y1 was necessary to mediate the directedness of neuroblast migration (Cao et al. 2015). Similar findings have been reported in human neural stem and progenitor cells (Feng et al. 2012) at field strengths of 16mV/mm.

How NPCs sense electric fields has not yet been fully established. However, in order to facilitate motility, there needs to be a connection between an external EF and cytoskeletal elements or reorientation of a cell (Saltukoglu et al. 2015). In chemotactic migration, receptors on the cell surface initiate signaling cascades to reorganize the cytoskeleton. Interestingly, there is a growing body of evidence suggesting that electrotactic signals differ from those chemotactic signals initially (Gao et al. 2011), and then converge on shared motility machinery (Artemenko et al. 2016; Bear & Haugh 2014). Moreover, electric stimuli have been shown to override chemical signals (Feng et al, 2012). It is hypothesized that EFs induce intracellular and membrane protein polarization which in turn affect baseline ion flow. Polarization and altered ion flow then trigger cytoskeletal changes.

Polarization of a galvanotaxis-responsive cell involves sodium-hydrogen antiporter (NHE) 1 dependent pH differences, where NHE1 accumulates at the leading edge to export H^+ from the cell and creating a more basic environment at the leading edge (Martin et al. 2011). Due to NHE1 activity, “proton pockets” outside the leading edge form and actin begins to accumulate inside the leading edge (Özkucur et al. 2011). NHE3 was found to colocalize with actin and vinculin. In osteoblasts, Özkucur et al. show that membrane potential, due to Na^+/K^+ ATPase activity, maintains directionality of migrating cells. Using a V_{mem} reporting dye (DiBAC), increased membrane hyperpolarization at the leading edge was observed and when Na^+/K^+ ATPases were inhibited, cells lost directedness of migration. Özkucur et al. propose that this hyperpolarization is dependent on PIP_2 translation to downstream intracellular effects (Özkucur et al. 2011).

As cytoskeletal reorganization is Ca^{2+} dependent, a number of studies have investigated the role of calcium in galvanotaxis (Özkucur et al. 2009; Trollinger et al. 2002; Babona-Pilipos et al. 2018). In osteoblasts, EF stimulation was shown to increase calcium influx in the trailing edge of the cell. This increase in Ca^{2+} was theorized to activate the protein kinase C pathway through activation of membrane lipids components phosphatidylinositol 4,5-bisphosphate (PIP_2) and diacylglycerol (DAG; Özkucur et al. 2009). Notably, when calcium channels were blocked, migration velocity significantly decreased in keratinocytes (Trollinger et al. 2002) and NPCs (Babona-Pilipos et al. 2018).

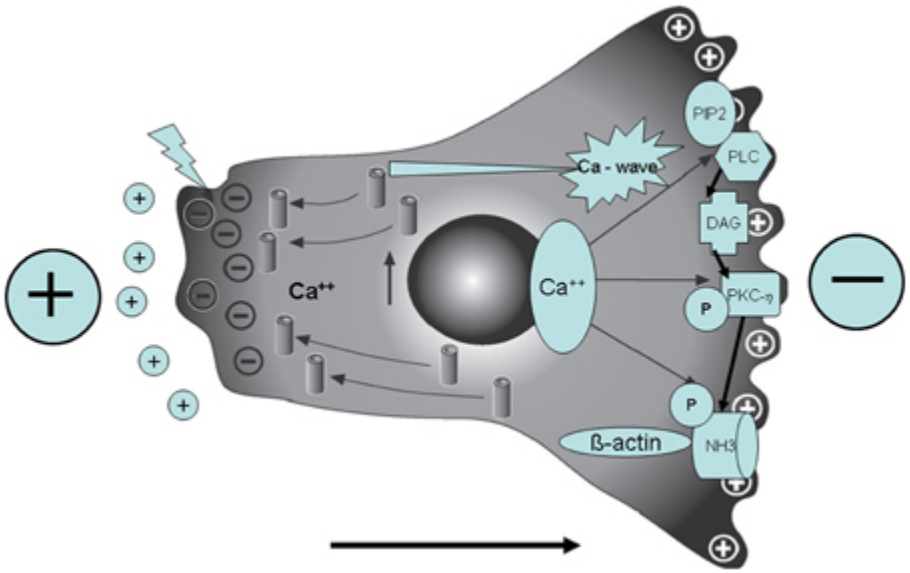

Figure 7: Figure describing the proteins and membrane elements involved in cell polarization and galvanotaxis. Hypothesized mechanisms for galvanotactic motility. Image from Funk 2015.

Ion channels have also been investigated as potential mediators of galvanotaxis. EGF addition has been shown to increase migration velocity. When the EGF receptor blocker erlotinib was used, migration velocity decreased in NPCs (Babona-Pilipos et al. 2011). ENaC was shown to play a role in keratinocyte directedness. ENaC was shown to be polarized to the leading edge and knockdown led to undirected migration and lack of stable lamellipodia. Interestingly, ENaC overexpression induced galvanotactic migration of human lung epithelial cells, which are normally non-galvanotactic cells (Yang et al. 2013). Polyamines binding to inward rectifying potassium channels have been shown to polarize to the cathodal side the cell (regardless of migration direction). Polyamines are hypothesized to alter local membrane voltage (V_{mem}) and ionic environments that directs phosphatidylinositol 3,4,5-trisphosphate (PIP_3) to the leading

edge of the cell during galvanotaxis (Nakajima et al. 2015). PIP_3 is also a downstream effector of EGFR-PI3K activation (Meng et al. 2011), leading to potential activation of Akt pathways (Xue & Hemmings 2013; Wang & Basson 2011).

There exist multiple hypotheses of how a cell translates an EF signal into a mechanical response. Our knowledge of EF sensing mechanisms is still limited, and it is perhaps one of the greatest questions in bioelectricity.

1.8 Applied Electric Fields and Clinical Applications

As previously described, EFs affect cellular components and complex cell behaviours. Applied EFs have been designed to either recapitulate endogenous fields or non-physiologically stimulate existing, EF-sensitive cell machinery. The technology of bioelectrics may be broadly divided into four categories: electroporation, pulsed electric fields, cold plasmas, and direct current electric fields.

Electroporation is a high intensity technique that permeabilizes the cell membrane, allowing delivery of normally membrane-impermeable products such as viral particles, genes, plasmids, and drugs. Pulsed electric fields deliver powerful bursts of electric energy over the span of nanoseconds and even picoseconds. These bursts create intracellular conditions of high power and low, non-thermal energy. It can be used in ablation of external skin tumours in addition to internal tumours. Pulsed electric fields also play in a role in platelet activation during wound healing. Cold plasma is an ionized gas of positive and negative ions. Non-thermal atmospheric-pressure plasma is utilized therapeutically in the growing field of plasma medicine. Most applications of cold plasma involve sterilization of tools and devices, however the use of cold plasmas are being developed in areas of pain management and fat ablation (reviewed in J. Beebe 2013).

Direct current electric fields (dcEFs) typically confer a direct charge to the tissue and current therapies vary greatly in intensity and duration. In vivo therapies employ a charge-balanced biphasic stimulation paradigm to avoid the corollaries of charge accumulation. Therapies include deep brain stimulation in treating Alzheimer's (Xu & Ponce 2017) and Parkinson's (Groiss et al.

2009), low-intensity transcranial direct current stimulation (tDCS) in modulating cognitive performance (Ruf et al. 2017), and functional electrical stimulation (FES) in maintaining muscle tone in paralyzed patients (Handa et al. 1998).

The potential role of dcEFs in activating NPCs with the ultimate goal of promoting neural repair still has many questions yet to be explored.

1.8.1 Endogenous NPC Response to Injury

Resident NSCs and their progeny have been shown to respond to injury with increased proliferation and migration to an injury site (Saha et al. 2013; Capilla-Gonzalez et al. 2015). NPC based therapies have shown promise in traumatic injuries including physical injuries (reviewed in Rolfe & Sun 2015), stroke (Dai et al. 2013; Arvidsson et al. 2002), and acute tumours (Bagó et al. 2016). NSC therapies have also shown benefits in degenerative diseases that are more chronic in nature and are often genetic, including multiple sclerosis, Alzheimer's disease, Parkinson's disease, Huntington's disease, and amyotrophic lateral sclerosis (reviewed in Gincberg et al. 2012).

1.8.1.1 Neonatal

Normally, radial glia disappear shortly after neurogenesis by transforming into different types of astrocytes and adult NSCs (Mori et al. 2005). Recently, Jinnou et al. have shown that radial glial cells may be maintained postnatally within a brief window in the presence of a cortical injury (Jinnou et al. 2018). They observed $Nestin^{+}$ fibres present up until postnatal day 4, but absent after postnatal day 14. Using a cryogenic injury to produce a localized cortical lesion at postnatal day 2, they showed an increased number and length of radial glial fibres (Pax6, Nestin, and ErbB4 positive) in injured versus uninjured brains. Looking at new doublecortin positive neuroblasts a week later in the lesion site, they showed that 96% migrated along radial glial fibres directed towards the lesion via N-cadherin mediated cell-cell adhesions. This finding suggests that radial glial fibres act as migratory scaffolds in injury as well as normal development (Jinnou et al. 2018).

Jinnou et al. then further assessed the potential of their findings towards a clinical application by developing a polyethylene terephthalate fibre and gelatin sponge conjugated to N-cadherin which they transplanted into the lesion site. They showed that transplantation across ages still showed the most robust response at postnatal day 2, when radial glial cells were still present. However, the rescue for older brains (postnatal day 21 and 56) following injury was more pronounced with the addition of the N-cadherin sponge. In older cohorts, greater numbers of migrating neuroblasts were found at the lesion site with sponge implantation versus controls. As well, behavioural responses in catwalk and foot fault tests were improved with implantation (Jinnou et al. 2018). Similar to previous studies showing benefits of scaffolding transplantation (Fujioka et al. 2017; Song & George 2017; N. Li et al. 2013; Shrestha et al. 2014; Tate et al. 2009), optimizing the parameters of NPC therapies offers a promising future for regenerative medicine.

1.8.1.2 Adulthood

In adulthood, NPCs are also responsive to injury through proliferation and migration to distant sites of injury. In a middle cerebral artery occlusion (MCAO) model of stroke, Arvidsson et al. showed that NPCs increased neurogenesis within the ipsilateral hemisphere. Within the SEZ, they showed increased numbers of $BrdU^+/Dcx^+$ cells (indicating newly formed neuroblasts) followed by an increase of $BrdU^+/NeuN^+$ cells (indicating newly formed mature neurons) in the injured striatum. Arvidsson et al. concluded stroke insults had activated SEZ dependent neurogenesis. However, they also showed that the endogenous response did not rescue functional recoveries. Arvidsson et al. estimated that only 0.2% of lost neurons were replaced by six weeks after injury (Arvidsson et al. 2002).

The NSC response of proliferation, migration, and integration have been recapitulated in many different forms of injury, such as traumatic cortical injuries (Wang, Seekaew, et al. 2016; Wang, Gao, et al. 2016) and epilepsy (Lugert et al. 2010). Migrating cells use vasculature as a scaffolding (Kojima et al. 2010) and cells undergo chain-like migration, guided by SDF-1 and other factors (Imitola et al. 2004). Injury has been shown to greatly increase endogenous EFs 50-100 fold in non-mammalian vertebrates and 10 fold in mammals (Baer et al. 2015). The response of NPCs to this increased injury potential has yet to be investigated.

1.8.2 Clinical Applications

The regenerative potential of applied EFs have been seen in axon guidance, wound healing, eye regeneration, deep brain stimulation, cancer ablation, functional electrical stimulation, transcranial direct current stimulation, and bone healing. This section will briefly outline the different effects of medical EFs and will not be a comprehensive analysis of clinical reports.

Axon and neurite growth are a normal part of development characterized by the presence of a microtubule and lamellipodia rich growth cone. In an applied EF greater than 50mV/mm, cells showed a significant preference for cathodal development of neurites and increased neurite length (Marsh & Beams 1946; Purdy et al. 2015).

Wound healing is mediated by disruption of the TEP. Injury damages the epithelial tight junctions that an electrically resistive barrier between the negative apical and positive basolateral sides. As described earlier, the TEP is dependent on the sum of individual, contiguous membrane potentials. This absence of cells causes a local “short-circuiting” effect where a lateral EF orthogonal to the TEP is generated, termed the “injury potential” (Zhao 2009). In humans, TEPs range from 15-50mV/mm. In injury, this potential ranges from 40-150mV/mm. As the injury begins to heal, field strengths decreases in intensity, making the injury potential a potent guide for modulated activation of wound healing processes (Nuccitelli et al. 2011). Interestingly, in humans, it has been reported that younger patients (18-25 year olds) exhibit a 2x more intense injury field strength than aged patients (65-80 year olds; Nuccitelli et al. 2011). This difference over age suggests there may be cell intrinsic or environment architectural changes that disrupt injury potential formation.

Eye regeneration is directed by TEPs of the corneal epithelial cells. As described previously, lens, retinal, and corneal epithelial cells have all been shown to be electrosensitive cells. When wounded, prostaglandin E2 stimulates ion transport across the corneal epithelium and increases the strength of injury EFs to promote wound healing (Song et al. 2004). Transorbital alternating current stimulation has shown potential in treating vision loss due to glaucoma and optic nerve damage (Gall et al. 2016).

Deep brain stimulation (DBS) utilized surgically implanted neural pacemakers into deep structures of the brain to deliver electrical impulses that modulate neuronal activity. Clinical successes have been seen in treatment of Parkinson's disease (Williams et al. 2010; Castrioto et al. 2011), tremors (Zhang et al. 2010), dystonia (Hu & Stead 2014), chronic pain (Lempka et al. 2017), and depression (Dandekar et al. 2018).

Functional electrical stimulation (FES) stimulates peripheral nerves to activate paralyzed muscles. Typically used in spinal cord injury treatments to promote motor function restoration and peripheral nerve growth (Hodkin et al. 2018), it has also recently found applications in erectile dysfunction (Carboni et al. 2018).

Transcranial direct current stimulation (tDCS) is a low-intensity direct current delivered via extracranial electrodes. Originally developed to treat psychiatric conditions (Brunoni et al. 2016; Agarwal et al. 2013), it is also being researched for its potential in enhancing cognition and memory deficits, though preliminary studies do not suggest an appreciable effect (Wang et al. 2018). tDCS is also being studied as a novel tool to improve post-stroke motor recovery (Kang et al. 2018).

Overall, the clinical applications of EFs are extensive and manifold. Current research shows promise of treating CNS and PNS injury in animal models (reviewed in Haan & Song 2014). Further research into EF mechanisms and effects on NPCs may provide additional treatments to target endogenous stem cells to lesion sites and promote proliferation and differentiation. In the future, this regenerative therapy could be developed to treat a host of neurodegenerative and traumatic brain injuries (Rolfe & Sun 2015).

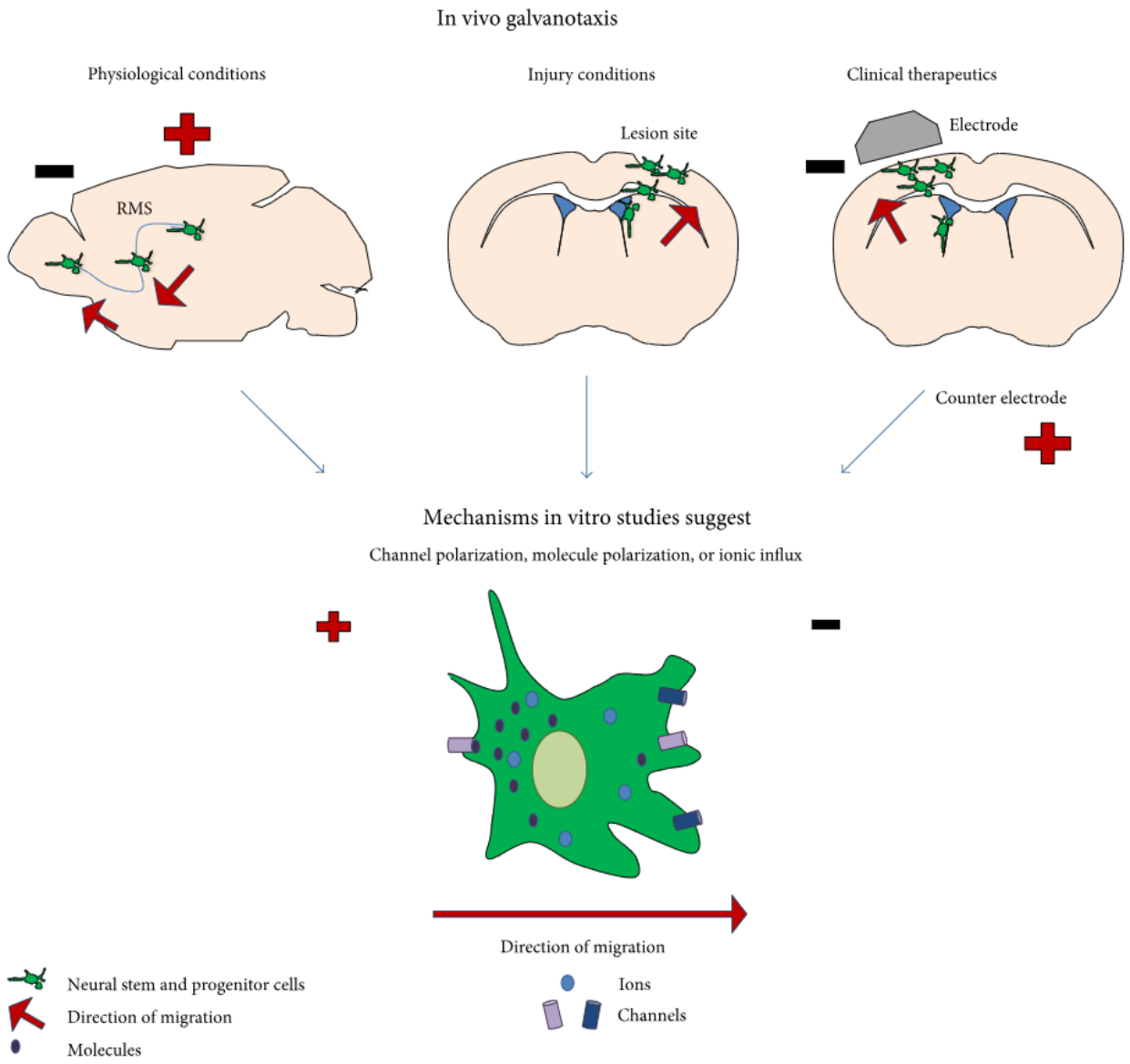

Figure 8: Potential for therapeutic endogenous stem cell activation. Image from Iwasa et al. 2017.

2 Chapter 2
Research Aims

The overall goal of this thesis is to characterize neural precursor cell galvanotactic migratory behaviour through age. Through the analysis of their differences and similarities to each age group (described below) and with other forms of directed migration, this thesis also seeks to investigate the mechanisms behind how a cell senses an electric field and how it transduces that signal into motility. The potential of EF application to stimulate NPC migration to sites of injury and enhance neural repair is an exciting prospect. In clinical applications, endogenous NPCs are a promising target for repair, as the strategy avoids issues of immunogenicity, cell sourcing, and ethics which surround transplantation studies. Given the significant changes in the brain, including the stem cell niche, during aging and in response to injury, responses of different ages of NPCs to EF application will likely vary. This work may inform the efficacy of NPC activation strategies, using EFs, in parsing out the effects of a changing extracellular environment versus what may be intrinsic properties inherent to a stem cell (should they exist).

2.1 Hypothesis

I hypothesize that the NPC galvanotactic response is conserved across age and it is the stem cell niche that modulates the NPC galvanotactic response. I will test my hypothesis with the following objectives.

2.2 Objectives

Objective 1: Characterize baseline galvanotactic response across age groups using 7 migration metrics.

Age groups are divided into:

a) Post-natal day 8 (Neonate)

b) 6 months (Adult)

I will use the neurosphere assay to isolate NPCs and examine the galvanotactic response of neurospheres derived from primary cultures (P0) up until passage 4 (P4). These studies will permit an understanding of the galvanotactic behavior of cells across age, in the presence or absence of niche cells. Should we see differences in galvanotactic parameters, the neurosphere assay will permit mixing of NPCs and niche factors in conditioned media (CM) experiments (mixing neonatal and adult cells with opposite niches) in Objective 3.

Objective 2: Investigate role of resting membrane potential on NPC

I will first determine the baseline membrane potentials of cells of temporally distinct NPCs using patch clamping (in collaboration with Dr. Taufik Valiante's group, University Health Network, University of Toronto). Given the link between membrane potential and cell proliferation (Sundelacruz et al. 2009), I propose that NPCs from aged brains will be in a more hyperpolarized than NPCs from younger brains. In this objective I will hyperpolarize NPC cell membranes using a membrane potential modifying drug, Diazoxide, and assess changes in NPC galvanotactic migration as well as proliferation.

Objective 3: Investigate niche effects on galvanotactic migration across ages

By mixing purified NPC population across ages with conditioned media from differing niches across age, I will determine whether niche derived factors in conditioned media play a role in galvanotaxis across ages.

The galvanotactic response of neonatal and adult derived NPCs will be examined in co-cultures where the conditioned media (CM) from neonatal and adult niche cells will be applied to pure populations of passaged NPCs of adult and neonatal ages and their galvanotactic response will be examined. These experiments will determine whether niche cells or secreted niche factors can influence the migratory behaviour of NPCs across age. As well, CM will be analyzed using a sandwich-based enzyme-linked immunosorbent assay for the identity of its constituents to help isolate any potential factors playing a role in mediating galvanotactic changes.

3 Chapter 3
Methods

3.1 Ethics Statement

All animal work was approved by the University of Toronto Animal Care Committee in accordance with the institutional guidelines (protocol no's 20011279 and 20011515).

3.2 Galvanotaxis

The galvanotaxis assay is powerful tool in analyzing cell behaviour. In assessing different migration metrics between different cell populations, we can analyze the phenomenology between different populations and gain clues regarding mechanisms of galvanotaxis by assessing differences and similarities between metrics of different populations. Galvanotaxis of singular NPCs utilizes the neurosphere assay to isolate pure population of NPCs. Then chambers coated with matrigel (Corning, USA) substrate are constructed to allow neurospheres to adhere and dissociate into single-cell layers. Single NPCs are then imaged under EF stimulation for 3 hours.

3.2.1 Neurosphere Assay

The neurosphere assay is a colony forming assay that assesses the two cardinal properties of stem cells: self-renewal and multipotency. Since individual neurospheres are clonally derived from a single stem cell, the number of free-floating neurospheres is reflective of the number of neural stem cells (Piccin et al. 2014). Individual neurospheres can be plated in growth factor supplemented serum free media (SFM) to promote neurosphere growth, or on a substrate in differentiation medium to demonstrate multipotency (generation of neurons, astrocytes, and oligodendrocytes).

3.2.1.1 Gross Dissection

C57BL/6 mice were organized into neonatal, post-natal day 8 (PN8), and adult (6 months) age groups. In cell-cell co-culture experiments, all adult groups were of YFP background. All groups were anesthetized with isofluorane, and then adults were sacrificed via cervical dislocation followed by decapitation with sharp dissection scissors. Neonate groups were sacrificed via surgical decapitation following anesthetization.

Following removal of heads, all age groups were treated the same.

Heads were doused in 70% ethanol. Then, holding the head using surgical forceps, skin on the dorsal surface was cut away to expose the skull. Using a scalpel and no. 11 blade, the skull was scored at the frontal sinus along the mediolateral axis and along the sagittal suture in the rostrocaudal direction. The parietal bones were then peeled away from the head with no. 7 curved forceps, taking precautions not to pierce brain tissue. A thin spatula is then inserted underneath the brain (from cerebellum advancing towards olfactory bulbs) and pulled to remove the brain from the skull. The brain is then immediately placed in ice-cold hi/lo artificial cerebrospinal fluid (hi/lo aCSF).

Under a dissection scope, using sterile dissection scissors and forceps, the brains were cut in half along the midline. Each hemisphere was rotated so that the medial (cut) surface faced upwards. Using dissection scissors, an incision was made from the surface of the cortex to the splenium of the corpus callosum along the dorsoventral axis. The incised cortex was peeled away towards the olfactory bulb and removed, exposing the medial and lateral walls of the lateral ventricle. Rotating the hemisphere again, so that the dorsal surface faced upwards, curved microscissors were used to cut out and collect the exposed medial and lateral walls (the periventricular region where NPCs reside). Isolated tissue samples were immediately placed into a 15mL falcon tube (BD Falcon, Canada) containing 12mL ice-cold aCSF. SEZ dissection was repeated on the other hemisphere.

3.2.1.2 Cell Culture

After SVZ tissue was isolated, excess aCSF was aspirated to less than 0.5mLs per sample. 7mLs Trypsin Enzyme Solution (1.33 mg/mL Bovine Pancreas Trypsin; Sigma-Aldrich, Germany + 0.623 mg/mL Sheep Testes Hyaluronidase; Sigma-Aldrich, Germany + 0.1 mg/mL Kynurenic Acid; Sigma-Aldrich, Germany + hi/lo aCSF) was then added to each sample. The falcon tube was then placed on a rocker in and incubated at 37°C for 25 minutes. After trypsinization, the sample tube was centrifuged for 5 minutes at 1500 RPM. The supernatant was aspirated and the pellet resuspended in 2mLs of Trypsin Inhibitor Solution (0.66 mg/mL Ovomucoid Trypsin Inhibitor; Worthington-Biochem, USA + SFM). Using a small borehole Pasteur pipette, the sample was gently triturated 30 times, avoiding air bubbles. The sample was then centrifuged again for 5 minutes at 1500 RPM. The supernatant was aspirated and the pellet resuspended in 2mLs of SFM supplemented with Epidermal Growth Factor (EGF; 20ng/mL; Sigma-Aldrich, Germany), basic Fibroblast Growth Factor (bFGF; 10ng/mL; Sigma-Aldrich, Germany), and Heparin (2μg/mL; Sigma-Aldrich, Germany) (collectively termed SFM + EFH) by triturating with a fire-polished Pasteur pipette 10 times. The sample was then centrifuged again for 3 minutes at 1500 RPM. The supernatant was aspirated and the pellet resuspended in 1mL of SFM + EFH by triturating 5 times with a P1000 micropipette. Live cell density was then counted with a haemocytometer. Cells were then either plated in a 24-well plate (ThermoFisher Scientific, Canada) or a T75 culture flask (BD Falcon, Canada) at a density of 10 cells/μL in SFM + EFH. The culture was allowed to grow for 7 days undisturbed to yield free-floating primary neurospheres comprised of NPCs (Coles-Takabe et al. 2008).

Plating in a T75 culture flask (BD Falcon, Canada) does not allow for accurate quantification of neurosphere number counts. To count and quantify neurosphere numbers, cells must be plated in a 24-well plate (ThermoFisher Scientific, Canada) at a clonal density of no more than 10 cells/μL. A maximum of 5000 cells (or 500μL) may be plated in each well. After undisturbed growth for 7 days, neurospheres may be counted.

3.2.1.2.1 Passaging

After 7 days, primary neurospheres may be collected and passaged to create secondary neurospheres. Passaged cultures contain a more purified population of NPCs as non-stem cells will not have experienced the NPC expansion in number and some may have died off in stem-promoting conditions lacking endogenous cytoarchitectural cues.

After 7 days of growth in 24-well plates (ThermoFisher Scientific, Canada) or a T75 flask (BD Falcon, Canada), the isolated individual cells have grown into non-adherent clonal spheres. These spheres are termed primary (P0) neurospheres. P0 neurospheres are grown in SFM + EFH, but also components of the niche from the gross dissection. These neurospheres consist of approximately 1% neural stem cells and 99% neural progenitor cells. Together, neural stem and progenitor cells are termed neural precursor cells (NPCs). These primary neurospheres may then be passaged into passaged (P1, -2, -3, -4) neurospheres.

To passage, P0 neurospheres are collected into a 15mL Falcon tube (BD Falcon, Canada) and centrifuged for 5 minutes at 1500 RPM. The spheres pellet at the bottom and the supernatant is discarded. The pellet is reconstituted in 1mL of SFM + EFH by 5x trituration with a small borehole Pasteur pipette. Cells were counted via haemocytometer and plated at a concentration of 10 cells/μL and allowed to grow for 7 days to form passaged neurospheres.

Passaged neurospheres represent a pure population of NPCs as only neurosphere derived cells are replated upon passaging. All passaged neurosphere populations were taken from passage 1 to passage 4 (P1-4). Data from P1-4 were combined in passaged results.

3.2.2 Chamber Construction

Per chamber, one square glass no. 1 cover slip (22mm x 22mm x 0.17mm; VWR, USA) was placed in a bottle of 12N hydrochloric acid (EMD, Canada) overnight. Using a diamond-tip glass cutter, 2 rectangular strips (22mm x 5mm x 0.17mm) of glass were cut from non-acid treated no. 1 glass coverslips (VWR, USA). The next day, acid-treated square slips and rectangular slips were transferred to a laminar flow hood. All glass strips were then washed with 70% ethanol, then with tissue-culture grade autoclaved water and allowed to dry on a KimWipe (Kimberly-

Clark Professional, USA). Vacuum grease (Dow Corning, USA) was then applied to the perimeter of one surface of the square slip. Using a P20 pipette tip, the square slip was sealed to the centre of the base of a 60mm plastic Petri dish (Fisher Scientific, Canada). Vacuum grease (Dow Corning, USA) was then along the long axes of the rectangular slips. Using a P20 pipette tip, the rectangular slips were sealed along opposite edges of the square slip (such that they are parallel to each other), creating a central trough. The chambers were then UV-sterilized for 15 minutes in the laminar flow hood.

Once sterile, 300µL of Poly-L-Lysine (PLL; Sigma-Aldrich, Germany) was pipetted into the central trough of the chamber and incubated at room temperature for 2 hours. PLL was then aspirated and the troughs gently washed with 3mLs tissue-culture grade autoclaved water and aspirated. 300µL of Matrigel (Corning, USA) solution was then pipetted into the central trough and incubated for 1 hour at 37°C. After incubation, the Matrigel (Corning, USA) solution was aspirated and the chambers washed with 1mL of SFM three times and aspirated. Lastly, 300µL of SFM + EFH was pipetted onto the central trough, taking care not to touch the surface of the glass slides. Under a 5x objective of a counting microscope, a P10 pipette is used to transfer 8 neurospheres (4 along top, 4 along bottom) into the central trough without disrupting the thin layer of Matrigel (Corning, USA) substrate. The galvanotaxis chambers are then left at room temperature without movement for 5 minutes, allowing the neurospheres to settle onto the Matrigel (Corning, USA) substrate, then moved into a 37°C/5% CO2; 100% humidified incubator for 17-21 hours. This incubation period allows the neurospheres to adhere to and radially dissociate into a single cell layer on the Matrigel (Corning, USA) substrate.

3.2.3 Time-Lapse Imaging and Galvanotaxis Setup

Before time-lapse imaging, the live cell imaging system is allowed to equilibrate at 37°C/5% CO2 for a minimum of 30 minutes. Electrodes were created from 12cm pieces of 1mm diameter silver wire (Alfa Aesar; USA) coiled at one end into a tightly bound, flat spiral of three revolutions. The electrodes were then placed in 4.25% bleach (Lavo, Canada) for 20 minutes to form Ag/AgCl electrodes. Gel bridges were created using 2 pieces of 10cm 3/32 inch internal diameter PolyVinyl Chloride (PVC; Tygon, USA) tubing filled with agarose gel (300 mg agarose + 10 mL H_2O + 8 mLs SFM + 2 mLs heat inactivated FBS). The agarose gel is carefully piped

into the PVC tubes (Tygon, USA) using a 10cc syringe with an 18 gauge needle, so that no bubbles form within the tube, and allowed to set for a minimum of 5 minutes and a maximum of 30 minutes.

To prepare the galvanotaxis chamber for imaging, a chamber is first selected and imaged under 5x objective on a counting scope to assess neurosphere dissociation. Chambers with well-dissociated cells (i.e. single cells with at least one cell body distance between adjacent cells) were transferred to a laminar flow hood along with a non-acid (EMD, Canada) treated square no.1 glass coverslip (VWR, USA) and vacuum grease (Dow Corning, USA). The coverslip is then washed with 70% ethanol and then tissue-culture grade autoclaved water and allowed to airdry on a KimWipe (Kimberly-Clark Professional, Canada). Vacuum grease (Dow Corning, USA) was then applied to two opposing, parallel edges of the coverslip. Quickly, the culture media in the well was aspirated from the central trough and the new coverslip (VWR, USA) placed on top the chamber (with the vacuum greased sides contacting the rectangular slips), effectively creating a roof to the chamber. 150μL of SFM + EFH was then pipetted, using a P200, into the central trough gently via capillary action. Vacuum grease was then applied on top of the edges of the roof that houses the openings to the central trough so that it forms two chords across the petri dish. This creates the border for two pools of culture media conjoined only by the central trough.

The completed galvanotaxis chamber was then transferred to the live cell imaging system, along with agarose gel bridges, Ag/AgCl electrodes, 37°C SFM + EFH, cold SFM, and an empty pair of 60mm petri dishes (Fisher Scientific, Canada) that will serve as culture media reservoirs and contain the Ag/AgCl electrodes. Before imaging, the galvanotaxis chamber is allowed to rest within the 37°C/5% CO2 environment for 30 minutes. During this time, 20mL of cold SFM is placed in each empty reservoir petri dish and placed on the receptacles on either side of the imaging stage. Electrodes were placed in the reservoir dish through the designated covers (a 60mm Petri dish cover with 2 holes drilled into either side of the cover) and connected to leads of an external power supply, with an ammeter in series to measure electrical current. The power supply was then turned on and set to low voltage before connecting the galvanotaxis chamber to prevent any power spikes.

Once 30 minutes have passed, 1.5mL of 37°C SFM + EFH is added to each side of the galvanotaxis chamber and the central lid, a 60mm petri dish (Fisher Scientific, Canada) cover with 4 holes drilled along the diameter, is placed on and taped down in place to the stage. The gel bridges are then inserted through the outermost holes of the central covers and the remaining holes on the reservoir covers, connecting the galvanotaxis chambers with the electrode reservoirs. The system was then taped down to prevent any movement during imaging. Lastly, the leads of a voltmeter were inserted through the middle holes of the central cover to measure the direct current electric field (dcEF) strength directly across the central trough. The power supply is then adjusted so that the dcEF strength is 250mV/mm with electrical current between 1 and 1.5mA, as previously described (Babona-Pilipos et al. 2012).

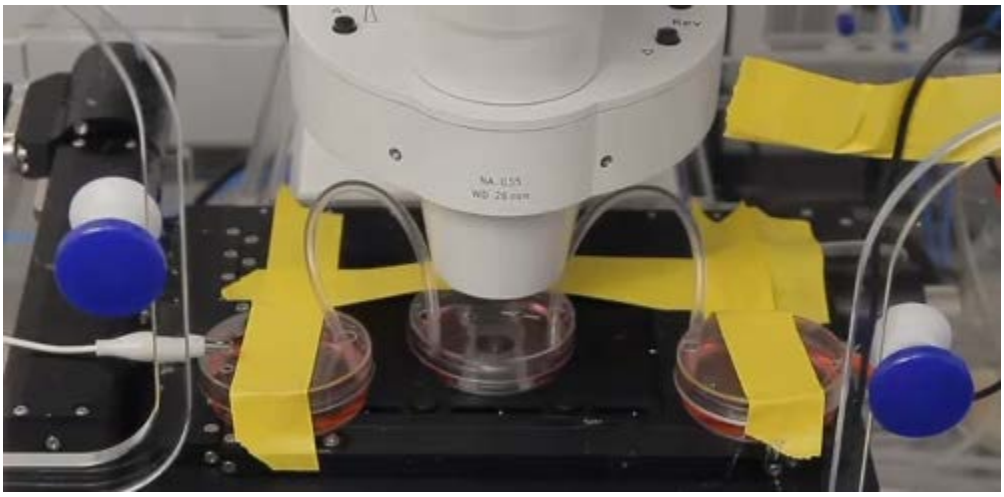

Figure 9: The setup of a galvanotaxis experiment as described above. Method of setup described in Babona-Pilipos et al. 2012.

The live cell imaging system used in our experiments is a Carl Zeiss Axiovert 200M microscope (Zeiss, Germany) situated within a temperature and CO_2 controlled, 100% humidity casing. Using Zeiss Axiovision 4.8.2 software, cells were imaged at 10X objective with phase contrast illumination. Images were stabilized with DefiniteFocus (Zeiss, Germany) and imaged every minute for 3 hours. In experiments involved fluorescent cell line galvanotaxis, images were stabilized with DefiniteFocus (Zeiss, Germany) and imaged every 10 minutes for 3 hours.

3.2.4 Quantification of Cell Migration

Cell migration was tracked using Zeiss Axiovision 4.8.2 software's automated tracking module. Selection criteria of cells for kinematic analysis was restricted to cells that were at least one cell body's length away from the nearest cell. This decreases the likelihood of cells overlapping each other during migration and improves tracking accuracy. In experiments involving fluorescent cell lines, images were tracked using Zeiss Axiovision 4.8.2 software's manual tracking module. Cell position was determined by cell centroid locations. 15 cells were tracked and averaged for each trial.

Seven kinematic metrics may be quantified to describe galvanotaxis. In all analyses, the positive values represent cathodally directed migration and the negative values represent anodally directed migration. This convention allows analysis of movement parallel to the direction of the applied dcEF.

1. Total distance: the complete path length the cell travelled for the duration of the total experiment time (3 hours).

2. Straight-line displacement: the shortest distance between a cell's starting point and end point.

3. Speed: the total distance a cell travels divided by total experiment time. Given in μm/min.

4. Velocity: the total displacement divided by total experimental time. Given in μm/min.

5. X-axis displacement: the projection of a cell's straight-line displacement onto the x-axis; this metric shows the component of a cell's migration due to the effect of the dcEF.

6. Tortuosity: the total distance travelled by the cell over the straight-line displacement; this shows how much a cell's path deviates from a straight line.

7. Directedness: the x-axis displacement divided by the displacement of the cell; this metric is a measure of how much a cell's migration is in the direction of the dcEF.

The different metrics can be dissociated from one another (ie. total path distance can be affected without affecting directedness).

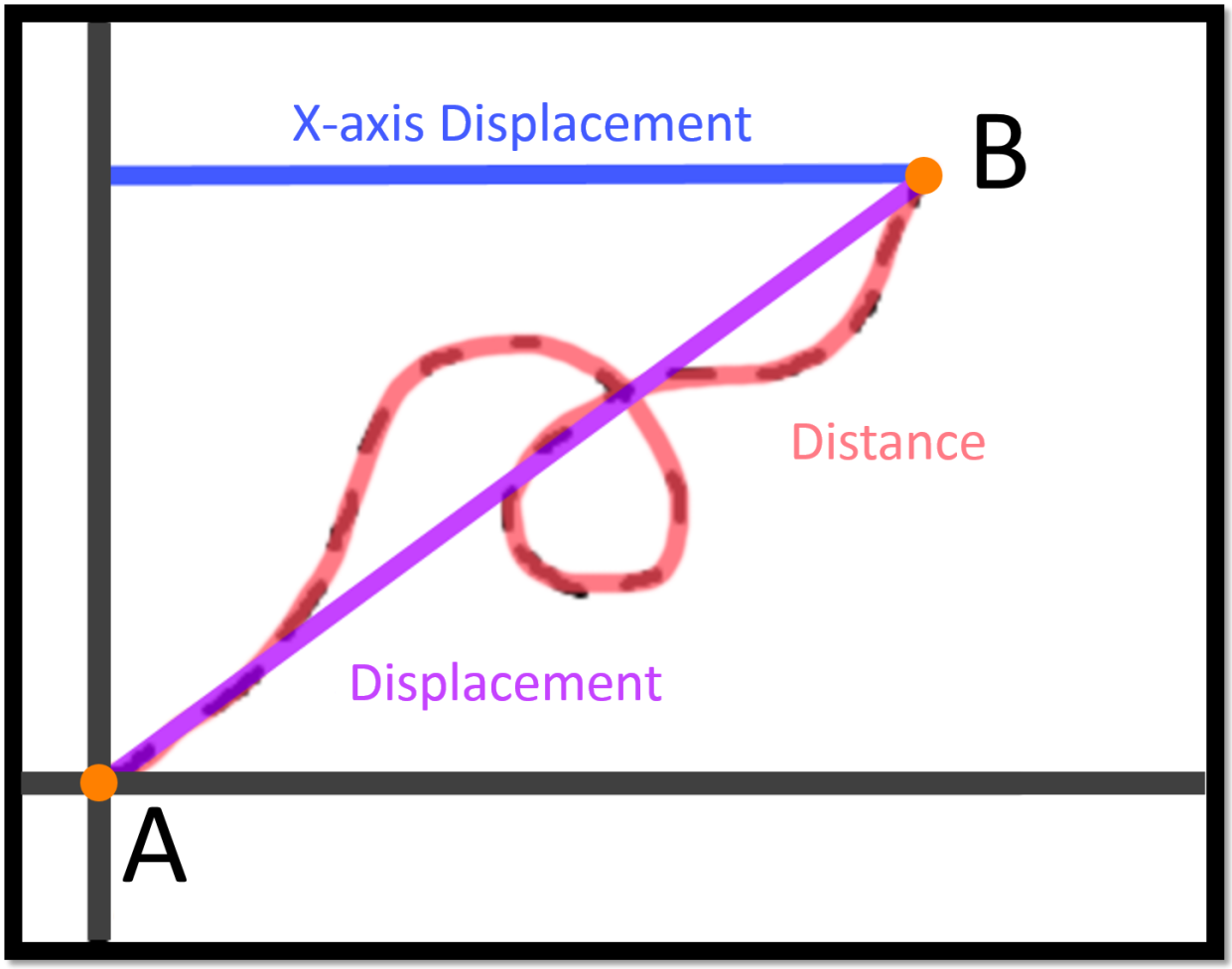

Figure 10: Basic migration metrics.

3.3 Conditioned Media Mixing Experiments

To generate primary neonate and adult conditioned media (CM), primary cultures from the neurosphere assay were plated at a density of 40 cells/µL in a T75 culture flask (BD Falcon, Canada). Cells were grown in standard SFM + EFH conditions for 24 hours. After the 24 hour incubation period, cells were centrifuged for 5 minutes at 1500 RPM. The supernatant was collected and filtered through a 40µm cell strainer (Fisher Scientific, Canada). A separate flask of passaged adult or passaged neonate cells (opposite to the CM age group; ie. adult CM is used with passaged neonate cells and neonate CM is used with passaged adult cells) are then counted via a haemocytometer and plated into the filtered supernatant at a cell density less than 10 cells/µL for 7 days.

After 7 days of incubation, neurospheres are collected and their galvanotactic migration was assessed as described.

3.4 Conditioned Media Factor Analysis

Conditioned Media from neonate and adult age groups was collected and analyzed by RayBiotech using their Quantibody Testing Service: Quantibody Mouse Cytokine Array 4000 (Norcross, GA). 200 cytokines were tested for expression within our conditioned media.

Table 1: Table showing complete list of cytokines tested in CM in alphabetical order.

4-1BB	DLL4	IGFBP-5	LIX	Pro-MMP-9
6Ckine	Dtk	IGFBP-6	LOX-1	Prostasin
ACE	E-Cadherin	IL-1 R4	L-Selectin	P-selectin
Activin A	EDAR	IL-10	Lungkine	RAGE
ADAMTS1	EGF	IL-12p40	Lymphotactin	RANTES
Adiponectin	Endocan	IL-12p70	MadCAM-1	Renin 1
ALK-1	Endoglin	IL-13	Marapsin	Resistin
ANG-3	Eotaxin	IL-15	MBL-2	SCF
ANGPTL3	Eotaxin-2	IL-17	MCP-1	SDF-1a
AR	Epigen	IL-17B	MCP-5	sFRP-3
Artemin	Epiregulin	IL-17B R	MCSF	Shh-N
Axl	E-selectin	IL-17E	MDC	SLAM
B7-1	Fas	IL-17F	Meteorin	TACI
BAFF R	Fas L	IL-1a	MFG-E8	TARC
bFGF	Fcg RIIB	IL-1b	MIG	TCA-3
BLC	Fetuin A	IL-1ra	MIP-1a	TCK-1
BTC	Flt-3L	IL-2	MIP-1b	TECK
C5a	Fractalkine	IL-2 Ra	MIP-1g	Testican 3
CCL28	Galectin-1	IL-20	MIP-2	TGFb1
CCL6	Galectin-3	IL-21	MIP-3a	TIM-1
CD27	Galectin-7	IL-22	MIP-3b	TNF RI
CD27L	Gas 1	IL-23	MMP-10	TNF RII
CD30	Gas 6	IL-28	MMP-2	TNFa
CD30L	G-CSF	IL-3	MMP-3	TPO
CD36	GITR	IL-3 Rb	Neprilysin	TRAIL
CD40	GITR L	IL-33	Nope	TRANCE
CD40L	GM-CSF	IL-4	NOV	TREM-1
CD48	gp130	IL-5	OPG	TremL1
CD6	Granzyme B	IL-6	OPN	TROY
Chemerin	Gremlin	IL-7	Osteoactivin	Tryptase ε
Chordin	H60	IL-7 Ra	OX40 Ligand	TSLP
Clusterin	HAI-1	IL-9	P-Cadherin	TWEAK
CRP	HGF	I-TAC	PDGF-AA	TWEAK R
CT-1	HGF R	JAM-A	Pentraxin 3	VCAM-1
CTLA4	ICAM-1	KC	Periostin	VEGF
CXCL16	IFNg	Kremen-1	Persephin	VEGF R1
Cystatin C	IFNg R1	Leptin	PF4	VEGF R2
DAN	IGF-1	Leptin R	PlGF-2	VEGF R3
Decorin	IGFBP-2	Limitin	Progranulin	VEGF-B
Dkk-1	IGFBP-3	Lipocalin-2	Prolactin	VEGF-D

The assay is a quantitative sandwich-based, glass-slide solid phase Enzyme-Linked ImmunoSorbent Assay (ELISA) that detects the fluorescence of the above 200 cytokines with a fluorescence laser scanner. Cytokine concentrations are determined by comparing the fluorescence intensity from an unknown sample to a standard curve.

In brief, the prepared glass slides with attached antibodies serve as the solid phase of the assay. Each glass slide is divided into 16 wells of identical cytokine antibody arrays with each array assaying for 20 cytokines. Each antibody, together with positive controls, is arrayed in quadruplicate per array.

Firstly, the glass slides are allowed to equilibrate to room temperature and air dried completely. Incomplete drying leads to “comet tails”, or thin smears of antibody spots. To assay for cytokines, the array surface is blocked then incubated with 8 known concentrations of each cytokine ranging from 0 to intensity max.

These positive controls (with 0 as a negative control) are spotted onto 8 wells of 5 glass slides to generate a standard curve for each slide, correlating intensity with concentration. Sample CM is then placed on the other 8 wells of the 5 glass slides for 1.5 hours at room temperature or overnight at 4°C. The array is then washed 5x for 5 minutes each with a wash buffer and incubated with a biotinylated detection antibody cocktail for 1.5 hours at room temperature. The array is then washed 5x for 5 minutes and incubated with a Cy3-conjugated streptavidin fluorophore for 1 hour at room temperature.

All incubation periods were performed with gentle rocking. The array is washed a final time (5x for 5 minutes) with a wash buffer and imaged with a gene microarray laser scanner. Densitometry analyses are performed to establish standard curves and final concentrations found in the CM.

3.5 Patch Clamping + Diazoxide

The patch clamp technique was used to determine resting membrane potential of cells under standard and hyperpolarizing (diazoxide) conditions.

3.5.1 Patch Clamp/Electrophysiological Recordings

Cells were isolated and plated following the neurosphere assay protocol detailed in 3.2.1 with the exception of petri dish size. Instead of 60mm petri dishes (Fisher Scientific, Canada), the lid of a 35mm petri dish was used (BD Falcon, Canada) Cells were incubated for 17 hours before measurement in standard conditions (SFM +EFH) or hyperpolarizing (SFM + EFH + 300μM Diazoxide) conditions.

For recordings, samples were transferred to a recording chamber mounted on a fixed-stage upright microscope (Axioskop 2 FS MOT; Carl Zeiss, Germany). NPCs were visualized using an IR-CCD camera (IR-1000, MTI, USA) with a 40x water immersion objective lens. Whole-cell patch-clamp recordings were obtained using Multiclamp 700A amplifiers (Axon instruments, Molecular Devices, USA) using standard borosilicate glass pipettes (thin-wall borosilicate tubes with filaments; World Precision Instruments, USA) of 9-10 MΩ resistance filled with intracellular solution containing: 110 mM K-gluconate; 10 mM KCl; 10 mM HEPES; 10 mM K2phosphocreatine; 4 mM ATP-Mg; 0.4 mM GTP, pH of 7.3 adjusted with KOH (290–300 mOsm). Subsequently, signals were digitized using a digitizer 1320X at 10 KHz.

3.5.2 Diazoxide

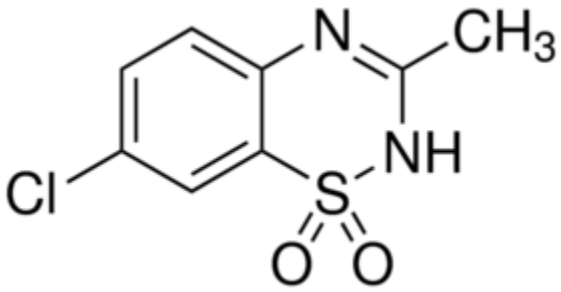

Figure 11: Chemical structure of diazoxide.

Diazoxide (Sigma-Aldrich, Germany) is a pan inward-rectifying potassium channel ($K_{ir}6.x$) activator (increases membrane permeability to potassium ions). By increasing intracellular concentrations of potassium, the cell is driven to a lower membrane potential, or hyperpolarized.

Diazoxide (Sigma-Aldrich, Germany) has been shown to hyperpolarize cells experimentally (Doyle & Egan 2003).

A stock solution of 25,000μM Diazoxide (Sigma-Aldrich, Germany) in anhydrous DMSO was made and kept at -20°C. Stock diazoxide was diluted into SFM + EFH to a concentration of 300μM and incubated at 37°C for one hour before neurosphere plating. Plated neurospheres were incubated for 17 – 21 hours with 300μM diazoxide in SFM + EFH before membrane potential measurements.

3.5.2.1 Dose Response Curve

To assess dosage effects of diazoxide on NPCs, the neurosphere assay was used. NPCs were plated at a density of 10 cells/μL in 24-well plates (ThermoFisher Scientific, Canada) in standard SFM + EFH conditions in addition to varying concentrations of diazoxide. Diazoxide concentrations tested were 0μM, 50μM, 100μM, 200μM, and 400μM.

NPCs were incubated at 37°C for 7 days and allowed to form neurospheres. Neurospheres were counted and binned according to size: 1) neurospheres with diameter larger than 80μm or 2) neurospheres with diameter between 50μm to 80μm. At 200μM diazoxide concentrations, neurosphere numbers began to significantly decrease from baseline 0μM diazoxide controls. Results are shown in Figure 15.

3.5.2.2 Diazoxide Galvanotaxis

Neurospheres were also plated on standard matrigel coated galvanotaxis plates as outlined in 3.2.2 Chamber Construction. NPCs were imaged for 3 hours after 17-21 hours of incubation in 300μM diazoxide. During imaging NPCs were also bathed in 300μM diazoxide + SFM + EFH. Migration metrics were assessed in the presence of diazoxide as outlined in 3.2.3 Time-Lapse Imaging and Galvanotaxis Setup and 3.2.4 Quantification of Cell Migration.

3.6 Statistical Analysis

All data were compiled using Microsoft Excel (Microsoft, Redmond, WA). Statistical analysis was carried out using GraphPad Prism 6 (GraphPad Software, La Jolla, CA). Quantified values are presented as group means ± Standard Error of the Mean (S.E.M.). Differences between group means were calculated using the Kruskal-Wallis nonparametric test followed by Dunn's correction for multiple pairwise comparisons. Kruskal-Wallis was selected as not all data sets sufficiently fit a normal distribution. Statistical significance was set at $p < 0.05$. Heatmap clustering and images were generated using RStudio (RStudio, Boston, MA) with additional gplots package downloaded from the Comprehensive R Archive Network (CRAN). Kyoto Encyclopedia of Genes and Genomes (KEGG) database was used to map known pathways and interactions.

4 Chapter 4
Results

4.1 Age Modulates Galvanotactic Migration

Using the galvanotactic platform, we assessed 7 migration metrics of neonate primary, neonate passaged, adult primary, and adult passaged NPCs. Briefly, the absolute (x, y) position of 15 cells per trial were tracked and converted to relative (x, y) positions with a singular (0, 0) origin point. As shown in Figure 12 and 13, a number of similarities and differences between adult and neonatal migration paths observed. Both populations migrated cathodally, as previously described (Babona-Pilipos et al. 2011) and share similar y-axis and x-axis spread suggesting a similar capacity for migration. More importantly, a similar x-axis spread shows a conserved response of NPCs across age and suggests a maintained mechanism for EF sensing through age. Interestingly, the path shape is more tortuous in neonatal age groups.

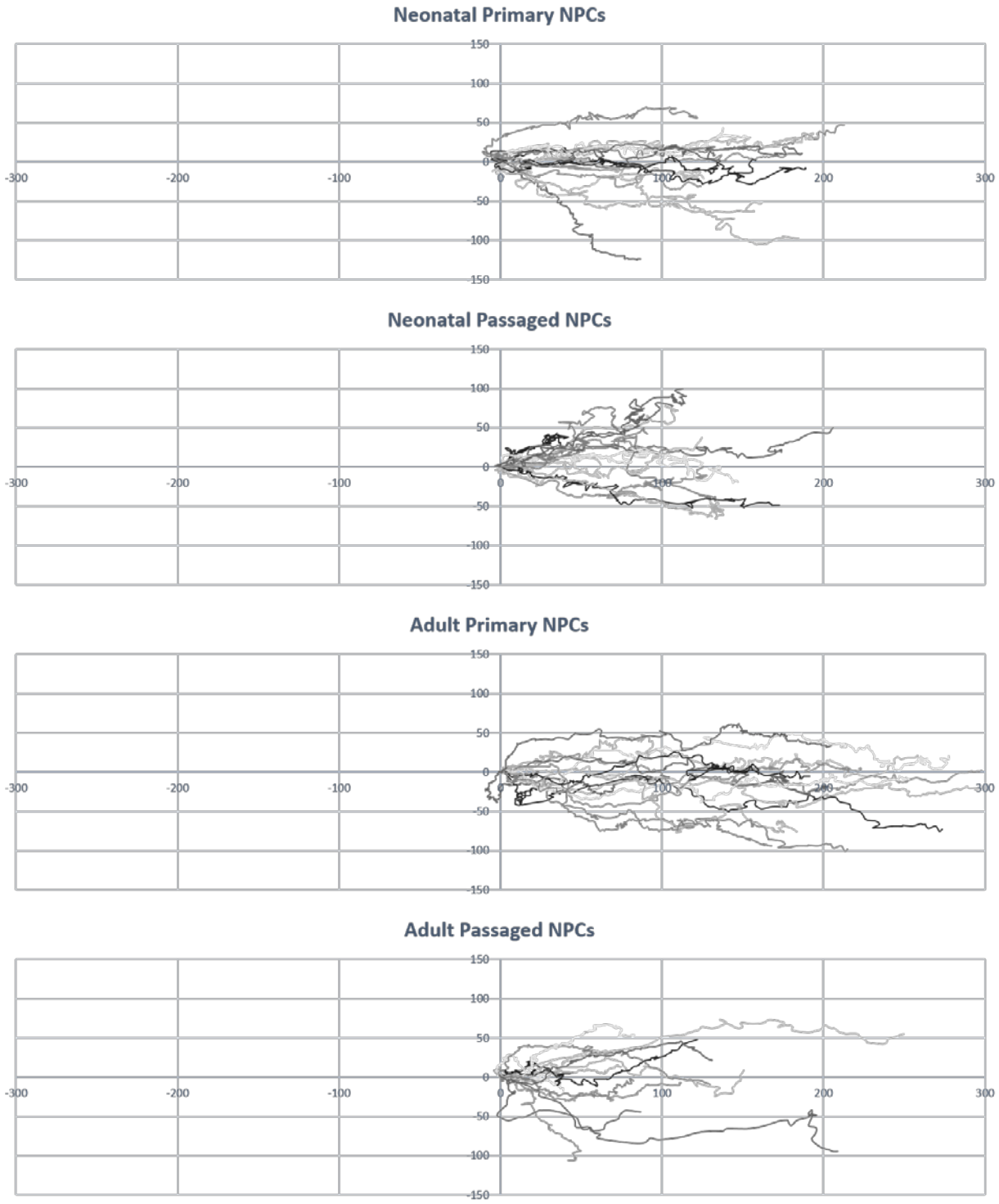

Figure 12: The paths each individual cell takes in the presence of an electric field corrected to a common origin point. Each individual line is representative of the migration of a single cell. Each graph shows data from one representative trial of Neonatal Primary NPCs, Adult Primary NPCs, Neonatal Passaged NPCs, and Adult Passaged NPCs. Shown primary trials are P0 and passaged trials are P2.

We quantified the migration paths using 7 metrics of migration: distance, displacement, speed, velocity, x-displacement, and directedness. Comparing between age groups (orange adult versus green neonatal bars), Figure 13 reveals that the distance, speed, and tortuosity of neonatal NPC migration is significantly greater than adult NPCs compared across both primary and passaged cultures. Although displacement of primary cells stays constant across age, the distance traveled by neonatal NPCs is consistently larger than the distance traveled by adult NPCs, suggesting that neonatal cells loop back along the x-axis to re-traverse previous areas. This is consistent with the finding that neonatal derived cells (across both primary and passaged cultures) have a more tortuous migratory pathway (Figure 13).

Interestingly, NPC migration speed changes significantly over age (in both primary and passaged cultures), whereas velocity stays constant in primary cultures with a smaller overall range than speed. Combined with their migration paths, this suggests that both neonatal and adult NPCs can migrate from point A to point B with similar effectiveness (same velocity) supporting a conserved response to EF stimulation over age. However, adult cells travel in a more direct, straight-line fashion than neonatal NPCs, suggesting a greater efficiency (slower speed, but similar end point) in reaching their final destination.

As shown in Figure 13, distance and speed are related and offer similar information, as does displacement and velocity.

Increased displacement, velocity, and x-displacement between passaged adult versus passaged neonate NPCs suggests that adult cells migrate in more of a straight line along the x-axis than neonatal cells do. Indeed, this is reflected in the increased speed and tortuosity of neonatal age groups (Figure 13).

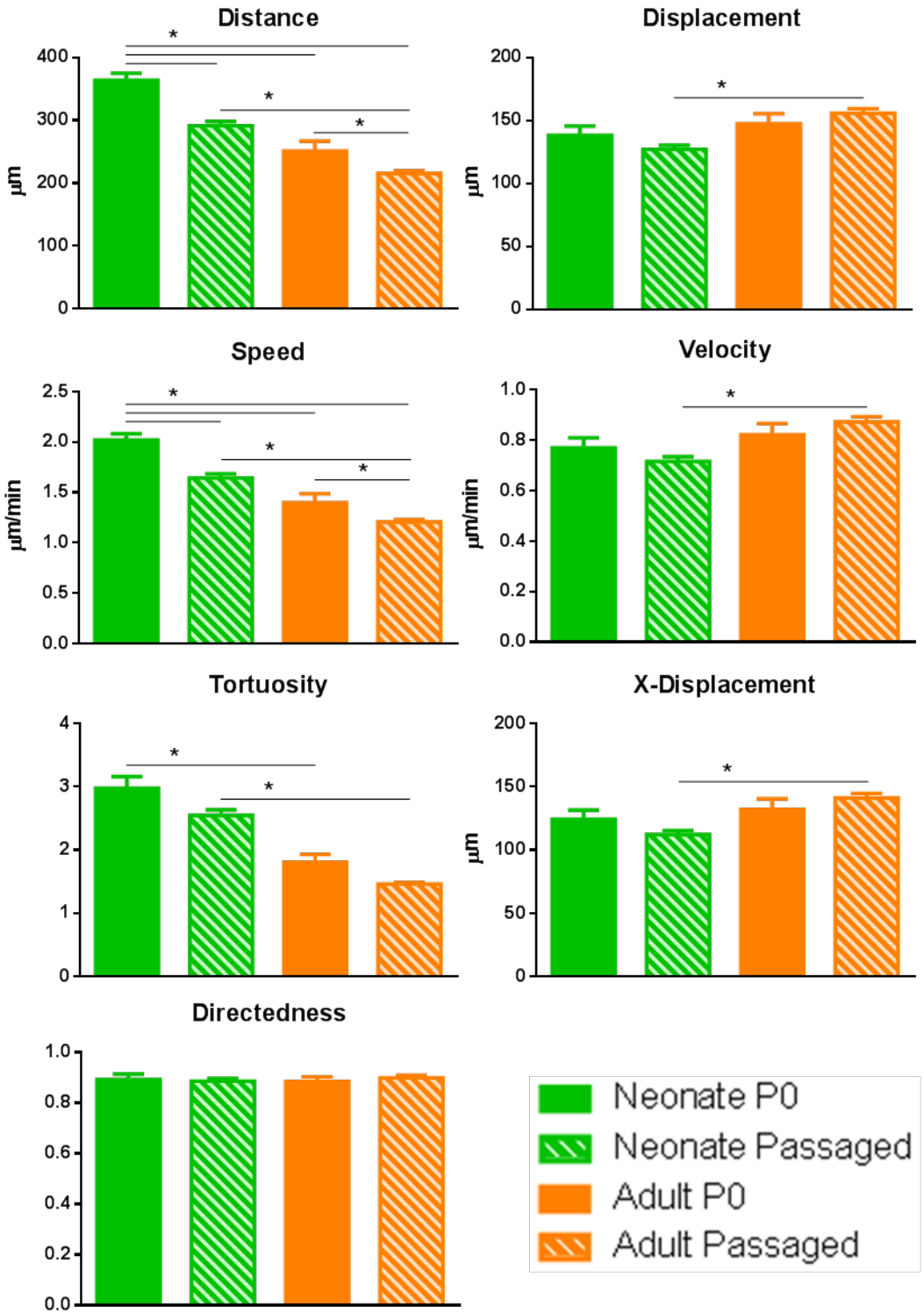

Figure 13: Quantified migration path metrics. Neonatal Primary (P0) NPCs migrate with an average distance of 363.58±11.38 µm; displacement of 138.20±7.32 µm; velocity of 0.77±0.04 µm/min; speed of 2.02±0.06 µm/min; tortuosity of 2.97±0.19; x-displacement of 124.20±7.34 µm; and directedness of 0.89±0.02. Neonatal Passaged (P1-4) NPCs migrate with an average distance of 291.10±7.20 µm; displacement of 127.00±3.28 µm; speed of 1.64±0.04 µm/min; velocity of 0.72±0.02 µm/min; tortuosity of 2.54±0.09; x-displacement of 112.20±3.20 µm; and directedness of 0.89±0.01. Adult Primary (P0) NPCs migrate with an average distance of 250.90±15.90 µm; displacement of 147.4±8.05 µm; speed of 1.39±0.09 µm/min; velocity of 0.82±0.05 µm/min; tortuosity of

1.81±0.12; x-displacement of 132.10±8.35 μm; and directedness of 0.88±0.02. Adult Passaged (P1-4) NPCs migrate with an average distance of 2015.4±4.33 μm; displacement of 148.4±3.74 μm; speed of 1.21±0.02 μm/min; velocity of 0.87±0.02 μm/min; tortuosity of 1.46±0.03; x-displacement of 141.00±3.72 μm; and directedness of 0.90±0.01. Graphs show mean of each group with S.E.M. Significance was set at $p < 0.05$. $n = 5$ for primary groups, $n = 20$ for passaged groups. Differences between group means was determined with Kruskal-Wallis non-parametric analysis and followed by Dunn's correction for multiple pairwise comparisons.

Any differences between speed and velocity are revealed in the tortuosity metric, a measure of how much a cell's path deviates from a straight line. The greater the difference between a cell's speed and velocity, the greater the cell's tortuosity.

X-displacement is a measure of how much the cell's motion is in the direction of the applied EF, in other words, how much distance is attributable as a cell response to the field. Interestingly, there is a small, but significant increase in x-displacement between adult passaged NPCs and neonate passaged NPCs. The observed difference across ages, in the absence of niche derived factors, suggests adult and neonatal NPCs may be intrinsically different. However, with differences appearing in the absence of niche, this suggests that there may also exist a conserved niche factor at play modulating the way cells sense and respond to an applied EF.

Lastly, directedness is a measure of what percent of a cell's migration is in the positive x-direction. Irrespective of age and presence/absence of the niche, NPCs respond to a dcEF of 250mV/mm with the same directedness. Nearly 90% of a cell's motion is consistently towards the cathode.

Due to the interplay between the migratory metrics, and based on the findings in Figure 13, further analysis will only consider three metrics: speed, tortuosity, and directedness. Removing distance, displacement, velocity, and x-displacement metrics will decrease repetition of data captured by speed, tortuosity, and directedness. Speed and tortuosity will indicate the qualities of a cell's migratory response to the electric field, whereas directedness will reflect the cell's ability the sense the electric field.

4.2 Membrane Potential

We next asked about how cells sense an electric field by examining the role of resting membrane potential (RMP) in transducing the electrical signal within the cell.

4.2.1 Membrane Potential Across Age

In a first series of experiments, we examined the RMP of NPCs across age. We performed patch clamp analysis to establish baseline measurements for neonate and adult primary and passaged cells. The RMPs of primary NPCs was -65mV, irrespective of age group (Neonate Primary RMP = -65.02±0.91 mV; Adult Primary RMP = -64.94±0.61 mV). Interestingly, passaged NPC RMPs were significantly depolarized compared to primary NPCs, with neonatal NPCs depolarizing about 15 mV (Neonate Passaged RMP = -51.70±2.18 mV) and adult NPCs depolarizing about 25 mV (Adult Passaged RMP = -40.01±3.84 mV). These altered RMPs between primary and passaged NPCs are similar to trends observed in their respective galvanotactic behaviour where passaged NPCs (irrespective of age) migrated with decreased speed and tortuosity relative to primary NPCs.

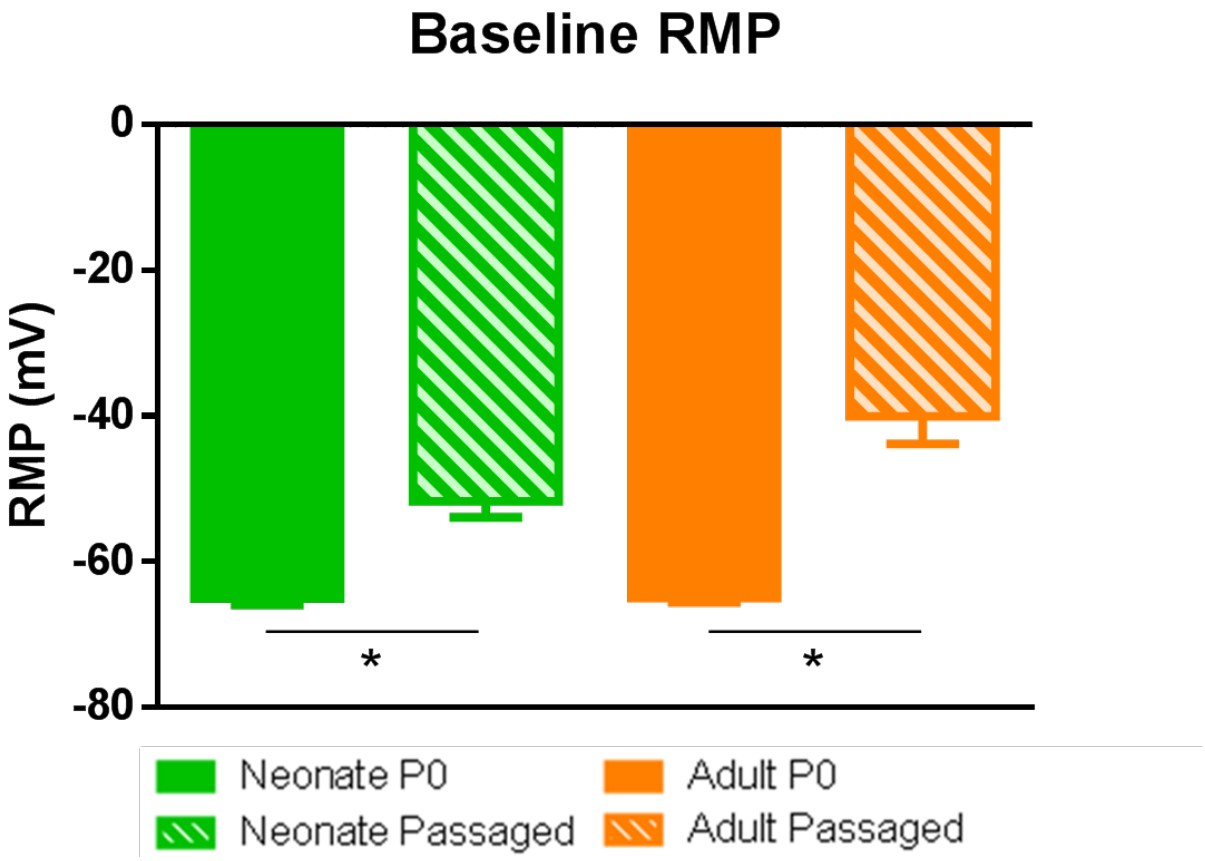

Figure 14: Neonate primary (P0) RMP = -65.02±0.91 mV; n = 13. Neonate passaged (P1-4) RMP = -51.70±2.18 mV; n = 27. Adult primary (P0) RMP = -64.94±0.61 mV; n = 25. Adult passaged (P1-4) RMP = -40.01±3.84 mV; n

= 15. Differences between group means was determined with Kruskal-Wallis non-parametric analysis and followed by Dunn's correction for multiple pairwise comparisons. Significance was set at $p < 0.05$.

4.2.2 Hyperpolarized Membrane Potential Inhibits NPC Proliferation

To assess the effects of membrane potential on galvanotaxis, we altered membrane potential using a pharmacological ion channel modulator. RMP is dependent on ion concentrations inside versus outside of the cell. The two main ions involved in establishing the RMP is sodium and potassium. The equilibrium potential of sodium is positive, thus, sodium channel activation will lead to a more depolarized membrane if the Na gradient was allowed to equilibrate. However, the equilibrium potential of potassium is negative. Thus, inward-rectifying potassium channel activation will lead to a more hyperpolarized membrane potential.

Previous studies have shown that depolarized RMP has been reported in multiple cancers such as cervical cancer, breast cancer, ovarian cancer, osteosarcoma, glioma, melanoma, small cell lung cancer, and myeloid leukemia to promote proliferation (Rao et al. 2015). Moreover, delayed-rectifying potassium channel inactivation via tetraethylammonium has been shown to decrease NPC proliferation (Yasuda et al. 2013). To determine whether RMP hyperpolarization via diazoxide activation of inward-rectifying potassium would exhibit similar effects on proliferation kinetics of NPCs, we performed a diazoxide dose response curve.

We performed a dose response curve of diazoxide concentrations ranging from 50 – 400 μM and assessed corresponding changes in the numbers of neurospheres. We observed a significant decrease in neurosphere at diazoxide concentrations greater than 200 μM (Figure 15) and selected to use 300 μM concentrations of diazoxide in the following RMP experiments. This loss of neurospheres was specific for >80um neurosphere colonies which have been shown to be stem cell derived and not due to the proliferation of progenitors in the primary cultures.

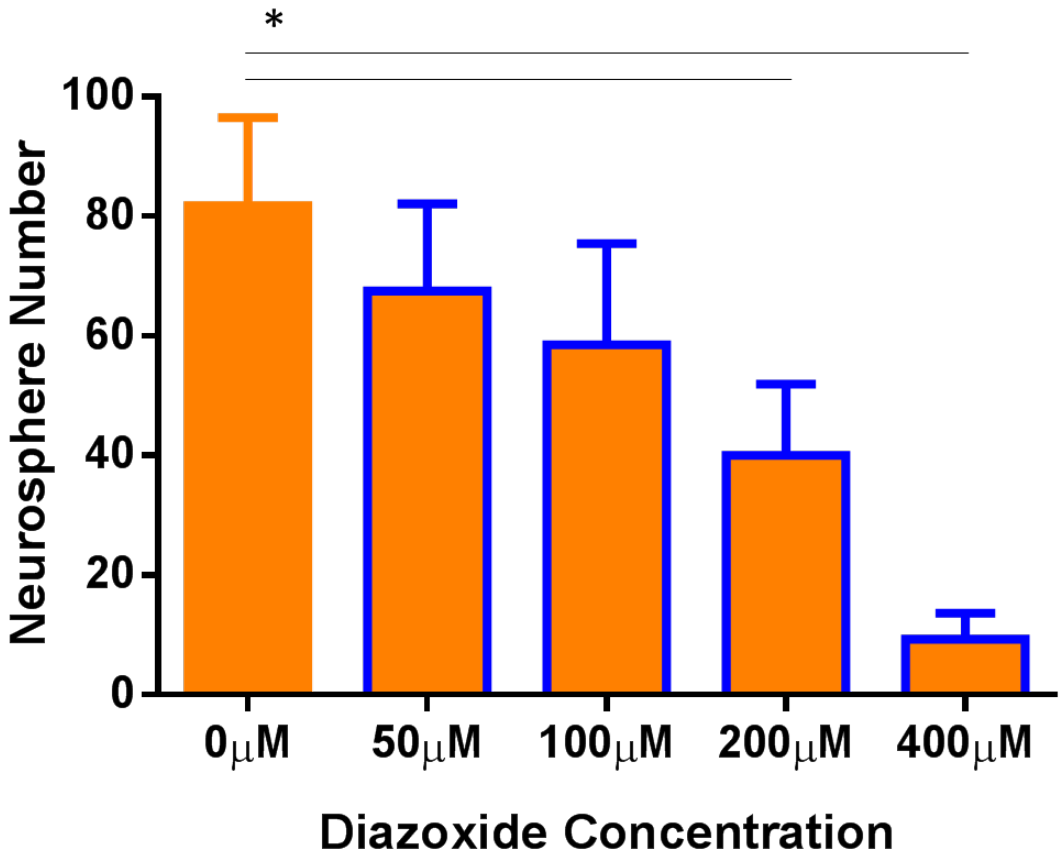

Figure 15: Adult NPCs (both primary and passaged) were plated at a density of 5000 cells/well in 24 well plates. Neurospheres above 80μm in diameter were counted. n = 3 per condition. Differences between group means was determined with Kruskal-Wallis non-parametric analysis and followed by Dunn's correction for multiple pairwise comparisons. Significance was set at $p < 0.05$.

To confirm if diazoxide was hyperpolarizing the RMP of NPCs, we performed patch clamp analysis of individual primary and passaged NPC from neonatal and adult mice. The concentration of diazoxide that inhibited neurosphere formation (300μM), hyperpolarized passaged NPCs (Figure 16) to the same RMP as primary NPCs. The inability to hyperpolarize membranes beyond -65 mV suggested a ceiling effect. Although no maximum hyperpolarization of NPCs has been reported, cells undergoing sustained hyperpolarization beyond 20 mV below baseline RMP have been shown to undergo cell death (Benítez-Rangel et al. 2011).

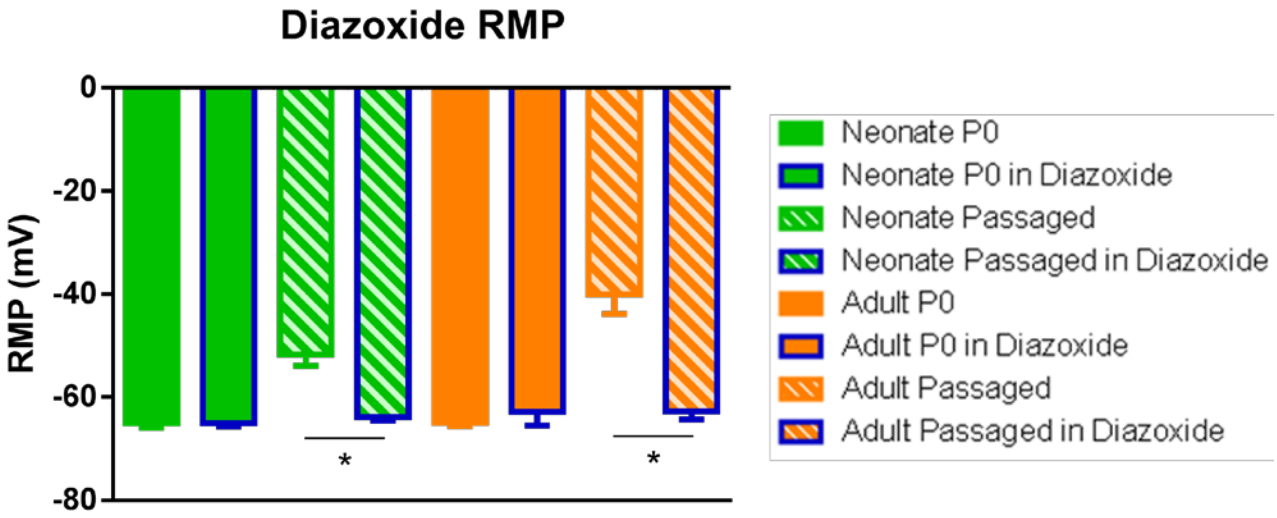

Figure 16: Neonate primary (P0) RMP = -65.02±0.91 mV; n = 13. Neonate passaged (P1-4) RMP = -51.70±2.18 mV; n = 27. Adult primary (P0) RMP = -64.94±0.61 mV; n = 25. Adult passaged (P1-4) RMP = -40.01±3.84 mV; n = 15. Neonate primary (P0) Diazoxide RMP = -65.02±0.70 mV; n = 6. Neonate passaged (P1-4) Diazoxide RMP = -63.86±0.70 mV; n = 18. Adult primary (P0) Diazoxide RMP = -62.81±2.72 mV; n = 18. Adult passaged (P1-4) Diazoxide RMP = -62.80±1.50 mV; n = 10. Differences between group means was determined with Kruskal-Wallis non-parametric analysis and followed by Dunn's correction for multiple pairwise comparisons.

To assay for potential of prolonged effects of diazoxide on NPC proliferation, NPCs were grown in the presence of either diazoxide or SFM for seven days. After which both groups were washed and passaged into both diazoxide and SFM conditions.

Neurospheres were plated at an average of 10 cells/μL. We observed a nearly 10-fold expansion of neurosphere numbers between primary and passaged NPCs in SFM, consistent with previous quantitative observations (unpublished data). Interestingly, passaging from either SFM or diazoxide into diazoxide, the expansion effect is diminished to approximate 4.5-fold but not completely abrogated. Consistently, in all trials, diazoxide NPCs formed 38-45% number of neurospheres compared to their SFM counterparts. Moreover, once diazoxide treated primary NPCs are washed and passaged into SFM conditions, the neurosphere expansion returns to a 10-fold increase. These findings suggest that RMP hyperpolarizationl acts to decrease NPC proliferation instead of causing cell death. However, to fully rule out cell death as a possibility further experiments such a live/dead cell assay will be required.

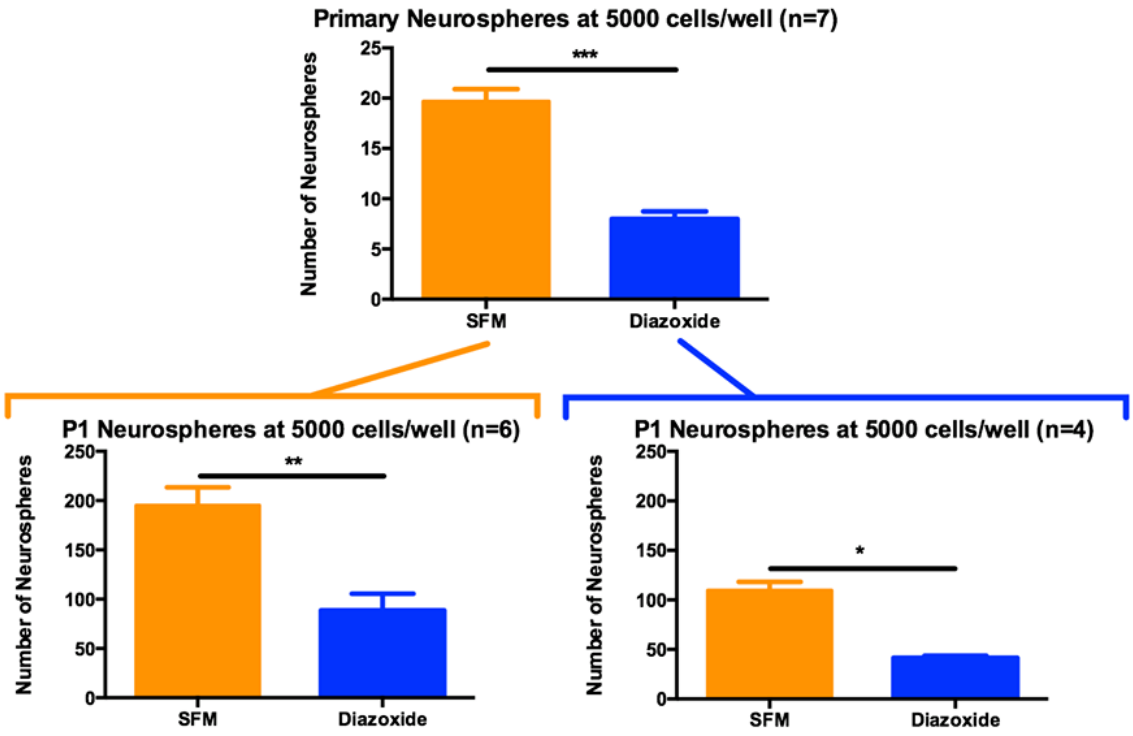

Figure 17: Neurosphere counts of SFM and 200μM Diazoxide groups throughout passaging. Only adult NPCs were assayed. Primary SFM Neurospheres = 19.68±1.22; Primary Diazoxide Neurospheres = 7.99±0.76; P1 SFM Neurospheres (From Primary SFM) = 195.10±18.29; P1 Diazoxide Neurospheres (From Primary SFM) = 88.64±16.92; P1 SFM Neurospheres (From Primary Diazoxide) = 109.07±8.46; P1 Diazoxide Neurospheres (From Primary Diazoxide) = 41.50±2.07.

Combined with data from Figure 14, NPCs are more depolarized in passaged cultures. This depolarization is also concomitant with a 10-fold expansion in neurosphere numbers. Passaging also removes niche factors present in primary cultures. RMP alone may not be sufficient to modulate NPC proliferation. A variety of possibilities could exist: a factor present in the niche may either modulate RMP to mediate proliferation effects or be modulated by RMP to carry out downstream effects, or be an interplay of both, or both niche factors and RMP affect a yet unknown third molecule. Further experiments are needed to tease apart these interactions.

4.2.3 Hyperpolarized Membrane Potential Rescues Migration

We hypothesized that RMP plays a role in the galvanotactic response of NPCs. We performed the galvanotactic assay in the presence of diazoxide and remarkably, we observed that diazoxide mediated RMP hyperpolarization enhanced NPC migration regardless of the presence or absence

of the niche, and independent of age (Figure 18). Speed and tortuosity were significantly increased compared to controls in the absence of diazoxide, and not significantly different from neonatal controls. Interestingly, RMP hyperpolarization reached a ceiling around --65mV. Similarly, RMP hyperpolarization could only increase NPC speed to a maximum of 2-2.5 μm/min and tortuosity of 3-3.5. The ceiling to migration speed and activity suggests an intrinsic maxima to how quickly a NPC might be capable of migrating.

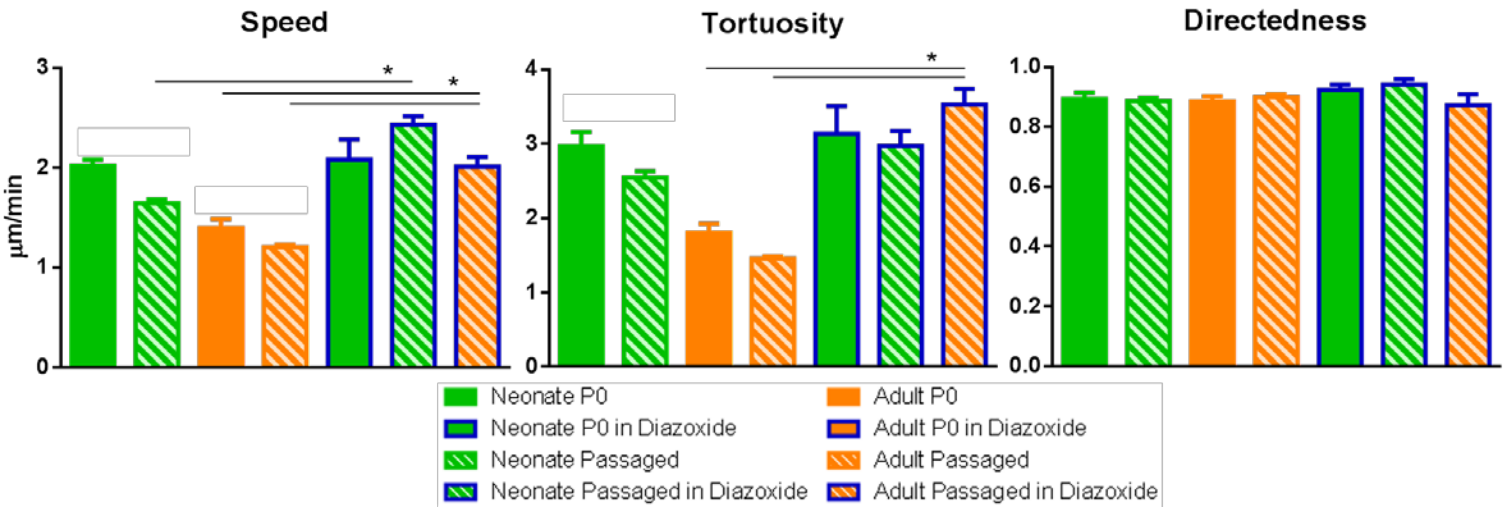

Figure 18: For ease of viewing, only significant differences between diazoxide treated groups and baseline controls are shown. Neonatal primary (P0) diazoxide NPCs migrate with a speed of 2.08±0.20 μm/min; tortuosity of 3.14±0.37; and directedness of 0.92±0.02. Neonatal passaged (P2-3) diazoxide NPCs migrate with a speed of 2.43±0.09 μm/min; tortuosity of 2.97±0.20; and directedness of 0.94±0.02. Adult passaged (P2-3) diazoxide NPCs migrate with a speed of 2.01±0.10 μm/min; tortuosity of 3.53±0.21; and directedness of 0.87±0.04. Graphs show mean of each group with S.E.M. Significance was set at $p < 0.05$. $n = 3$ for all present diazoxide groups. Differences between group means was determined with Kruskal-Wallis non-parametric analysis and followed by Dunn's correction for multiple pairwise comparisons.

These findings suggest that RMP may be a key regulator of galvanotactic migration and may be capable of overriding any potential inhibitory niche signals found in the adult.

4.3 Niche Derived Factors Can Regulate NPC Galvanotaxis

From section 4.1, we observed conserved trends between primary and passaged NPCs regardless of age, whereby passaged NPCs (in the absence of a niche) behaved significantly differently from their primary counterparts. From the rescue of NPC galvanotaxis shown in Figure 18 by

diazoxide, we determined that NPCs are capable of equivalent speed, tortuosity, and directedness of motility irrespective of age, indicating NPCs do not intrinsicially lose EF responsivity over time (chronological or replicative). We rationalized that the differences observed between primary and passaged culture conditions may reflect niche factor interactions present in their media. These interactions may regulate motility through RMP modulation or independently of RMP changes.

To investigate these potential interactions, we performed conditioned media experiments to examine the effects of secreted niche factors.

4.3.1 Conditioned Media Mixing

To analyze any effects the niche may contribute to modulating migration, we performed conditioned media (CM) mixing experiments. Using P2 NPC populations, we removed niche-derived factors from NPCs for 2 weeks then grew them in the presence of primary CM. We reasoned that if the neonatal niche contained factors that regulated galvanotaxis, we would observe an increase in the migration activity of passaged adult cells. Conversely, if neonatal factors did not increase the adult galvanotactic response to a neonatal phenotype, then (1) there may be no niche derived cues affecting galvanotaxis present; (2) adult NPCs are intrinsically less EF responsive or motile than adult NPCs; (3) adult cells no longer express receptors capable of responding to migration-promoting neonatal cues; or (4) an inhibitory factor capable of overriding neonatal cues could be present in the adult niche, in which case adult CM would inhibit the galvanotactic response of neonatal cells.

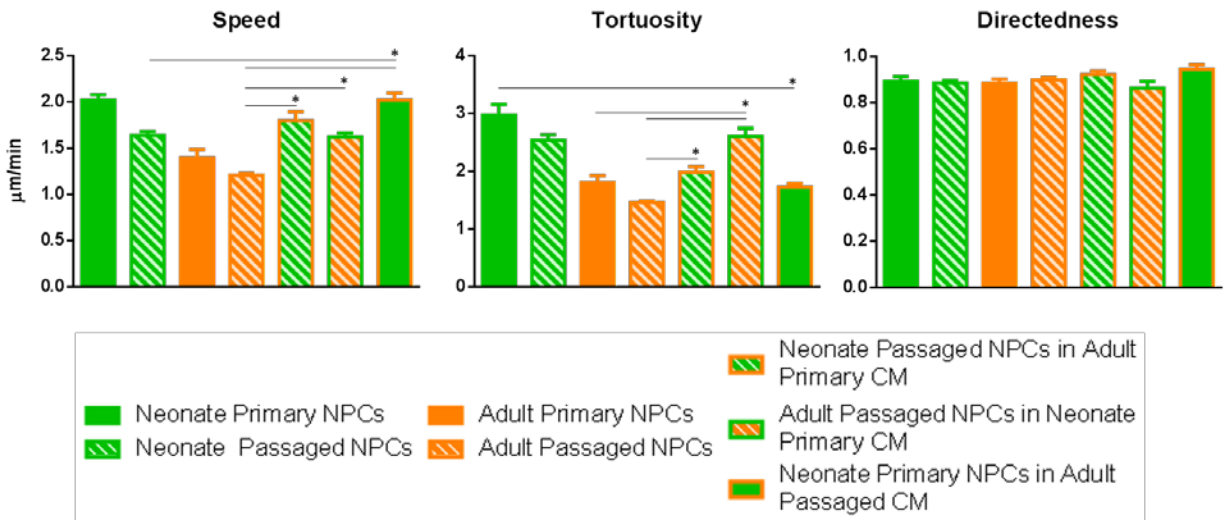

Figure 19: For ease of viewing, only significances between conditioned media and baseline metrics are shown. Graphs show mean of each group with S.E.M. Significance was set at $p < 0.05$. n = 5 for baseline primary neonate and adult cells. n = 20 for baseline passaged neonate and adult cells. n = 2 for all CM coculture groups. Neonate Passaged (P2) NPCs in Adult Primary (P0) CM Speed = 1.80±0.10 µm/min; Tortuosity = 1.98±0.10; Directedness = 0.92±0.02. Adult Passaged (P2) NPCs in Neonate Primary (P0) CM Speed = 1.63±0.04 µm/min; Tortuosity = 2.61±0.14; Directedness = 0.86±0.03. Neonate Primary (P0) NPCs in Adult Passaged (P2) CM Speed = 2.02±0.07 µm/min; Tortuosity = 1.73±0.06; Directedness = 0.94±0.02. Differences between group means was determined with Kruskal-Wallis non-parametric analysis and followed by Dunn's correction for multiple pairwise comparisons.

4.3.1.1 Passaged Adult NPCs in Primary Neonatal CM

Remarkably, when passaged adult cells are cultured in primary neonatal CM (Figure 19; orange hatched bars with green outline), we observed the speed and tortuosity of adult passaged NPCs was significantly increased from their baseline metrics (Figure 19; orange hatched bars) and not significantly different from neonatal cells (Figure 19; green bars). Of the possibilities stated above, the ability of adult NPCs to respond to neonatal cues rules out the possibilities that there are (1) no neonatal, galvanotaxis modulating factors present; (2) adult NPCs are intrinsically less EF responsive than neonatal NPCs; (3) adult NPCs are not capable of responding to neonatal cues; and (4) any inhibitory factors present in adult cultures are able to overcome neonatal activating factors. This suggests that NPCs retain their capacity for rapid migration through aging and are capable of responding to a migration promoting cue(s) present in the mobile phase of the neonatal niche.

4.3.1.2 Passaged Neonatal NPCs in Primary Adult CM

In the presence of primary adult CM, the speed of passaged neonatal NPCs did not change (Figure 19; hatched green bars with orange outline) compared to its baseline counterpart (Figure 19; green hatched bars). This lack of change not only strengthens the hypothesis that there exists an activating factor within the neonatal niche, but also suggests that those effects may be long-lasting. If there are inhibitory factors present within the adult niche, it is not enough to overcome the effects of any neonatal factors with regards to speed.

However, tortuosity of passaged neonatal NPCs significantly decreased in the presence of primary adult CM (Figure 19; hatched green bars with orange outline) to levels seen in adult NPCs (Figure 19; orange bars). This indicates that neonatal NPCs can be modulated by adult niche factors and are not intrinsically more EF sensitive. Decreased tortuosity indicates that NPCs are moving more in a straight line, more aligned with EF field direction and are thus more directed.

4.3.1.3 Primary Neonatal NPCs in Passaged Adult CM

We also examined the effects on primary neonatal NPCs by CM from passaged adult cultures (Figure 19; solid green bars with orange outline) as we observed the greatest difference in baseline migratory behaviour between these two cell populations. Remarkably, passaged adult CM significantly altered primary neonate NPC tortuosity without affecting speed, similar to the effects of primary adult CM.

This corroboratory finding suggests that speed and tortuosity may be distinct aspects of motility and can be differentially modulated. This finding also suggests that the factor may be present in primary and passaged cultures, indicating this factor may be secreted by adult NPCs and not neonatal NPCs to modulate only tortuosity of migration.

Overall, all findings suggest neonatal NPCs are not intrinsically different from adult NPCs with regard to their galvanotactic response to an applied EF. Behaviours of both populations may be modulated with secretable factors. These findings led us to further investigate the composition of conditioned media and potential underlying causes of NPC galvanotactic phenotype differences.

4.4 CM Analysis

Our data indicate that niche derived factors present in CM were able to regulate the galvanotactic response of NPC through age. To gain insight into potential factors, we used a quantitative, sandwich-based, glass-slide solid phase Enzyme-Linked ImmunoSorbent Assay (ELISA) which sampled CM for the presence of 200 cytokines, interleukins, growth factors, and receptors (RayBiotech, USA). Based on our observations, we hypothesized that a niche derived migration "activating" factor was present in primary neonatal CM and absent in primary adult CM.

We created heatmaps of protein expression between neonate and adult populations to compare and contrast the expression profile of secreted factors between ages. As shown in Figure 20 top right heatmap, we identified 23 hits expressed at 3x the concentration of the limit of detection of the assay (within the best confidence interval) in neonatal and adult populations (shown and identified in Table 2). Then analyzed time-related expression level changes and found overlap between secreted protein and differentially expressed protein functions to identify candidate molecules. A heatmap of absolute protein expression over age to determine relevant changes between age groups and graphed relative protein expression changes to identify expression profiles change over time (Figure 20 top left heatmap).

Table 2: 34 Secreted versus membrane-bound proteins of 23 factors expressed at levels 3x above the limit of detection, excluding secreted proteins EGF and bFGF.

Secreted	**Membrane-Bound**
Cystatin C	BLC
Eotaxin	EDAR
Fractalkine	Fas L
Galectin-3	Leptin R
IGF-1	P-Cadherin
IGFBP-5	TWEAK R
IL-23	VCAM-1
IL-4	
KC	
MCP-5	
MIP-1g	
MIP-2	
NOV	
PF4	
RANTES	
VEGF	

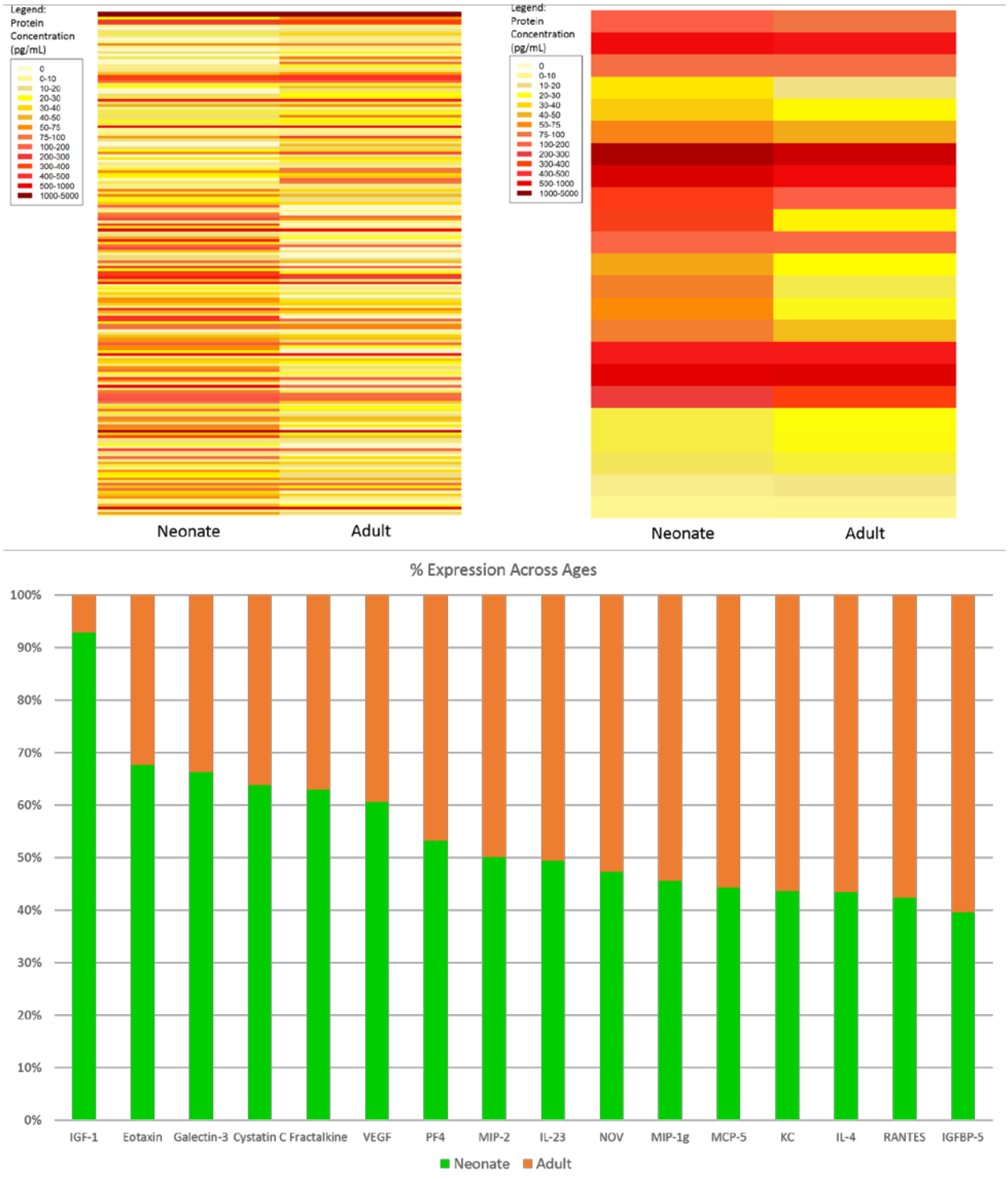

Figure 20: Heatmaps generated using R. Top left shows expression of all proteins assayed with non-zero concentration values. Top right shows expression levels of 23 putative hits excluding EGF and bFGF. Bottom shows relative expression of 16 hits of secreted factors, excluding EGF and bFGF, between neonatal and adult. n = 2.

Of the secreted proteins, IGF-1 was most highly expressed in neonates compared to adults. IGF-1 had been shown to increase proliferation in both hippocampal (Åberg et al. 2003) and SEZ (Bartlett et al. 1992) neural progenitor cells via MAPK and PI3K-Akt pathway signaling.

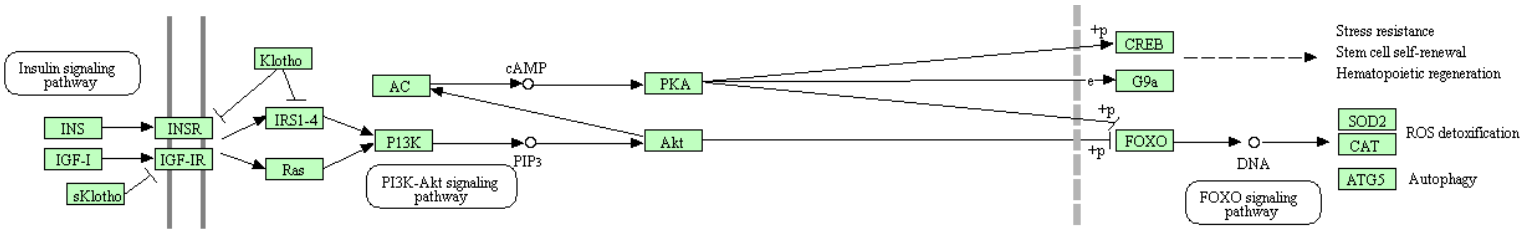

Figure 21: KEGG pathways database showing IGF1 interactions with Ras-PI3K-Akt pathways that have been shown to regulate cell proliferation and migration.

Given that IGF1 shows high relative expression in neonates, and interacts with known regulators of cell proliferation and migration, it is an attractive first target as a positive modulator of NPC migration. Future validation studies are also needed to confirm the effects of IGF1 on galvanotaxis.

5 Chapter 5 Discussion

Herein, we report findings of age differences between the galvanotactic migratory response of NPCs and factors modulating migration speed, tortuosity, and directedness. The following experiments do not analyze any neurospheres beyond a 4th passage. Nguyena et al. have shown hippocampal NPCs past a 12th passage display increased incidence of aneuploidy, growth factor-independent proliferation, and loosened restriction to a neural lineage (all suggestive of tumourigenic transformation; (Nguyena et al. 2013). Further groups have also shown stability in earlier passages and abnormalities in later passages such as increased susceptibility to viral infection (Pan et al. 2013) and genomic variability (Liu et al. 2014) neural stem cell lines. Our own lab has also shown morphological changes in murine SEZ-derived neurospheres with higher passage numbers (Morshead et al. 2002).

5.1 Age Changes in NPC Galvanotaxis

Adult populations show decreased migratory activity in comparison to neonatal populations across both primary and passaged group comparisons, with primary groups migrating with increased speed and tortuosity compared to passaged groups. Interestingly, regardless of age or passage number, directedness is unchanged from approximately 0.9 in all groups

Overall, we observed, in vitro, EF activated NPC migration at speeds between 1.2 – 2 μm/min, consistent with previous in vitro findings from our lab (Babona-Pilipos et al. 2011). In vivo, NPCs have been observed to migrate at 0.55 μm/min in response to ischemic stroke injury (Kojima et al. 2010). The decrease in speed may be due to cell differentiation in vivo or increased architectural complexity of the in vivo milieu.

Endogenous EF strengths in the mouse RMS have been reported to be on the magnitude of approximately 3 mV/mm (Cao et al. 2013). However, injury potentials experienced in vivo is currently hypothesized to be in the range of 40 – 200 mV/mm (Iwasa et al. 2017; Nuccitelli et al. 2008). In all experiments, the field strength used was 250 mV/mm. Although more similar in

magnitude to pathological potentials, this field strength showed optimal NPC migration response and no cell death over the course of 3 hour imaging.

At the same EF strength, both neonatal primary and passaged cells showed increased migration speed and tortuosity compared to their adult counterparts. This suggests two possibilities:

1. Neonatal cells are intrinsically more primed for motility. Expression of cell membrane receptors or channels may favour increased propensity for migration or EF sensitivity.

2. Extracellular factors from the neonatal niche have long lasting, migration promoting effects that are dampened with passaging (removal from niche).

Compared to previously determined tortuosity of CD1 adult mice (Babona-Pilipos et al. 2011), adult NPCs showed similar values around 1.2-1.8. However, neonatal mice showed approximately 2x increased tortuosity values of 2.5-3, indicating increased activity. This may potentially be due to the fact that post-natal day 8, neonatal mice are still undergoing oligodendrogenesis (Waly et al. 2014). As well, in development of the brain, NPCs normally migrate tangentially (along radial glial cells) to populate the layers of the brain (Malatesta & Gotz 2013). Neonatal NPCs could potentially be more “primed” to be more motile by prolonged exposure to migration permissive environments.

5.2 Resting Membrane Potential Modulates Galvanotaxis

We next questioned if RMP could modulate galvanotactic migration. We observed baseline potentials of approximately -65mV in primary NPCs. Passaged cells were depolarized by 15-25 mV. Interestingly, diazoxide hyperpolarized depolarized cells, but not past primary NPC RMP values of -65mV. This ceiling effect may be due to the types of channels expressed on murine NPCs. There is a channel and ion dependent maximum and minimum RMP that a cell may reach given stable ion concentrations. To determine if channel expression is indeed the cause of hyperpolarization ceiling, further experiments characterizing NPC channel expression, such as PCR, will be required. As well, the concentration of ions within the surrounding media could determine RMP changes; addition of 10% serum has been shown to transiently depolarize membranes in endothelial cells (Rothenberg et al. 1982).

RMP depolarization has been found in a number of cancers and hyperpolarization of membranes has been associated with a decline in proliferation and differentiation (Yang & Brackenbury 2013). RMP has been shown to be briefly hyperpolarized in keratinocytes and carcinomas with EGF (Pandiella et al. 1989). IGF-1 has also been shown to affect potassium (Wang et al. 2014) as well as calcium (Blair & Marshall 1997; Xing et al. 2006a) channels in hippocampal neurons, leading to hyperexcitability.

Interestingly, in adult primary NPCs, speed and tortuosity are slower than RMP hyperpolarization induced speed and tortuosity. Yet, the RMP for primary adult NPCs remained hyperpolarized at baseline. If RMP was indeed the sole regulator of galvanotaxis, we would not expect adult primary NPCs to exhibit decreased migration speed and tortuosity compared to neonate primary NPCs. Perhaps in the adult niche, there exists a negative modulator, or lack of a positive, modulator of galvanotaxis that feeds into/from RMP induced signaling. Or RMP may work in tandem with another signaling molecule/pathway to create nuanced responses to a cell's environment.

We used diazoxide, a potassium channel agonist, which resulted in a constitutively hyperpolarized cell membrane. This maintained hyperpolarization may not reflect a physiologically relevant state for the cell (Benítez-Rangel et al. 2011). However, this was sufficient to modify the galvanotactic response of the NPCs in the absence of niche-derived factors. It would be interesting to regulate RMP using other techniques such as temperature and/or pH (Buzatu 2009; Fitz et al. 1989) and to consider depolarizing the cell membrane with the use of pharmacological agents such as $BaCl_2$. Should RMP alone be sufficient to control NPC galvanotaxis, we would make the strong prediction that irrespective of other changes (age, pH, growth factor, or temperature) RMP depolarization would lead to decreased migration speed and tortuosity and perhaps even decreased directedness, whereas a hyperpolarized RMP would lead to increased migration speed and tortuosity, as well as increased directedness.

Interestingly, directedness has stayed constant throughout all baseline NPC measurements as well as with diazoxide treatment. Directedness is an important feature specific to (but not restricted to) EF induced migration. If RMP acts as an enhancer of EF signal, then would depolarization of the membrane lead to poorer migration outcomes?

In addition to cell proliferation, RMP depolarization has been shown to be associated with decreasing cell stiffness by destabilizing the f-actin cortex in vascular endothelial cells f-actin complexes (Callies et al. 2011). However, it is unknown if this holds true in NPCs. Should NPCs migrate with decreased speed and tortuosity, perhaps this actin cytoskeleton dysregulation may play a role. To test if RMP can modulate cytoskeletal elements, actin imaging may be performed.

5.3 Conditioned Media Mixing

We next worked to isolate a potential niche factor that could modulate RMPs. Using conditioned media (CM) mixing experiments, we have observed differences between baseline of passaged adult NPC migration with respect to neonate CM levels. However, this does not rule out the possibility that primary NPCs themselves secrete or express motility promoting factors.

Inherently, the neurosphere assay is not capable of parsing out NPCs from other niche cells that are part of the gross dissection. Potentially, loss of niche inputs may decrease NPC secretion/expression of a motility promoting factor. A follow-up experiment to confirm or reject this hypothesis would be to sort dissected cells either by flow cytometry fluorescence-based cell sorting or magnetic cell sorting to isolate an enriched population of NPCs, then coculturing purer populations of primary NPCs for 7 days before analyzing their migration. Or simply analyzing galvanotactic migration immediately after cell sorting. However, dissection and cell sorting is a traumatic process for individual cells. Measured metrics may not be reflective of stable growth conditions.

In CM experiments, neonatal CM was shown to containing activating factors. However, curiously, adult CM did not decrease the speed of migration for neonatal cells, but did decrease the tortuosity. When the speed stays the same but tortuosity decreases, this means cells are migrating in a more efficient fashion, travelling farther along the x-axis in the same amount of time. A more targeted migration profile emerges and may be a promising combination in modulating and optimizing migration of NPC transplant therapeutics.

CM analysis via antibody-sandwich ELISA and expression analysis revealed 23 potential modulators of NPC galvanotaxis. The strength of this method of detection lies in its sensitivity

and accuracy of protein detection. However, this form of analysis can only identify expression of a fixed number and identity of potential targets. In this assay, only 200 pre-defined proteins were analyzed. This assay would not capture expression of any proteins that are not represented in the array of 200 detectable proteins, thus this technique is not the most robust in identifying novel interactions. To better identify novel protein modulators, neonatal and adult CM may be compared using RNA sequencing, DNA microarray analysis, or 2D gel electrophoresis combined with mass spectrometry could be used to identify novel modulators.

5.4 Potential RMP Modifier: IGF1

From this analysis, IGF1 was identified as a potential modulator of galvanotaxis. Previous studies have shown that IGF1 is maximally expressed in the neonatal SEZ for 2 weeks after birth (Bartlett et al. 1992). IGF1 was shown to be necessary in maintaining NPC proliferation. In vitro, EGF and bFGF supplemented media did not induce proliferation in NPCs grown in the absence of insulin. When IGF1 was supplemented, neurosphere growth was restored (Arsenijevic et al. 2001). As well, IGF-1 was found to be necessary for proliferation of passaged NPCs in vitro (Erickson et al. 2008).

Interestingly, bFGF stimulation was shown to increase IGF1R expression on NPCs (Åberg et al. 2003). In a transplantation study, IGF1 was shown to have more gliogenic effects and IGF2 shown to promote NPC self-renewal, and migration through activation of the insulin receptor 1a (Ziegler et al. 2015).

The family of IGFs is an attractive target for neural stem cell modulation as IGFs have been shown to play an important role in development and cancer through activation of MAPK and PI3K-Akt pathways (Harris & Westwood 2012) which have been implicated in a multiplicity of cell behaviours including proliferation and migration. Recently, Kuo et al. have shown that IGF1R promoted germline stem cell symmetric division and migration by increasing expression of Oct4 and SDF1/CXCR4 (Kuo et al. 2018), which has been shown to be a chemotactic cue for NPC migration in response to injury (Yin et al. 2013).

Although IGFs show great promise in modulating complex cell behaviours, do they play a role in sensing EFs? Studies have shown that IGF-1 stimulates calcium influx in cerebellar granule neurons by indirectly acting on N and L type calcium channels (Blair & Marshall 1997). NPCs have been shown to express L and T type calcium channels (Babona-Pilipos et al. 2018), thus potentially may also be modulated by IGF1. Xing et al. have also implicated IGF1 in decreasing voltage-gated, calcium-independent potassium currents in a dose-dependent manner. As well, Xing et al. showed IGF1 could induce high-voltage activated calcium currents, but not sodium or low-voltage activated calcium currents (Xing et al. 2006b). From literature, IGFs present as a promising candidate to bridge EF sensing with intracellular machinery.

Ion channel regulation could be a pathway for IGF1 or any other CM factor to act on to affect RMP. EGF has also been shown to hyperpolarize cell membranes (Pandiella et al. 1989) and increase migration velocity (Babona-Pilipos et al. 2011). When EGF receptor was blocked, migration velocity decreased in NPCs. As well, blocking of L-type Ca^{2+} channels (a channel affected by IGF1) by nifedipine was shown to halt NPC migration after 1.5 hours of EF stimulation (Babona-Pilipos et al. 2018).

Beyond potassium and calcium, sodium also plays a large role in established RMP. ENaCs have been shown to play a role in keratinocyte directedness and are polarized to the leading edge during cell migration. Overexpression of ENaC could induce normally non-galvanotactic cells to migrate in the presence of an electric field (Yang et al. 2013). Modulators of RMP may be the key to galvanotactic control.

5.5 Cell Membrane Potential During Galvanotaxis

Measuring cell membrane potential during galvanotaxis may not be possible using patch clamp methods. Ungrounded circuits could influence RMP measurements and reliability of measurements will decrease. As well, free currents within the galvanotactic chamber may interfere with RMP measurements.

During patch clamp analysis, motility of the cell must be stopped to ensure patch clamp success. Also, migration of cells cannot be concurrently imaged, as the imaging is focused on the entry

point of the microelectrode. In order to assess NPC RMP during galvanotaxis, another methods of measurement is required.

The next step to address this question is to image voltage changes along the NPC membrane in the presence and absence of EFs ± Diazoxide. Voltage-sensitive dyes (or potentiometric dyes) could be used to visualize NPC migration and RMP fluctuations concurrently. As RMPs only exist in a living cells, any voltage-sensitive dye must be live-cell compatible. Possible ways to investigate this is in using membrane potential indicators such as DiBac live-cell voltage dyes.

As seen from previous migration data, hyperpolarization aided cell migration. If RMP hyperpolarizes during EF stimulus, it corroborates the theory that RMP aids in transducing EF signals.

Alternative possibilities include:

1. RMP is not a whole cell phenomenon, but rather, localized. Some domains may hyperpolarize, others may depolarize, thus creating an intracellular field and aiding in creating polarity within the cell.

2. RMP is a whole cell phenomenon. During EF stimulation, NPCs hyperpolarize as part of an activating signal for galvanotaxis. This could act as a positive guidance or migratory cue, and conversely, RMP depolarization acts as an inhibitory cue.

3. RMP is a whole cell phenomenon. During EF stimulation, NPCs depolarize when undergoing galvanotaxis. This rejects the hypothesis that hyperpolarized RMPs facilitate galvanotaxis. More data should be gathered to form a new hypothesis of mechanism.

4. RMP does not change. RMP fluctuation does not affect galvanotaxis. Previous correlations of hyperpolarized RMP with increased galvanotaxis may then be due to downstream effects of potassium efflux under influence of diazoxide.

The last step to fully elucidate a potential mechanism (signalling protein modulates RMP which changes cytoskeletal organization) is to establish the link between RMP and the cytoskeleton.

5.6 Sensing EFs: The Current View

EFs are ubiquitous from development to adulthood. Capable of long-lasting and/or short ranging spatiotemporal roles, EFs can influence a wide variety of cell phenotypes. Hence, bioelectricity has enormous impacts on cell behaviour and morphogenesis. Yet, important questions remain. How does a cell sense an EF? How does a cell then transduce an electric signal into a chemical or mechanical output? How does a cell make sense of this electrical information?

Potential explanations can be categorized into four logical possibilities. The first possibility would postulate that whole-cell membrane potential magnitude itself is responsible for information transfer. In other words, downstream effects are electrostatically guided. Regardless of what events take place intra- or extracellularly, as long as the membrane potential is modulated, there will be a change in cell behaviour due to electrostatic forces of attraction and repulsion of cellular components. The second possibility is that distinct domains of differing membrane potentials exist within the same cell, created by spatially separated ion transporters and channels. Only by having differential domains can a signal be differentiated from “noise”. The third possibility is that different frequencies of membrane potential fluctuations are responsible for information transfer. Similar to the second possibility, distinct membrane potential patterns store information, but rather than a spatial distinction, the cell would use a pattern of temporally distinct membrane potential variations to guide behaviour. Lastly, the fourth possibility postulates that downstream effects may not be determined by membrane potential, but rather, it is the membrane channels, ions, receptors, and charged molecules themselves that influence downstream effects. In this case, membrane potential may simply be a by-product of membrane channel activity.

Unlocking the answers to these questions will provide valuable insights into an evolutionarily ancient method of information transfer. As well, these answers will help inform regenerative therapies. In transplantation therapies, the introduction conductive polymers to act as biocompatible scaffolds has been shown to improve neural stem cell outcomes and functional recovery (Song & George 2017; N. Li et al. 2013; Tang et al. 2017). These conductive scaffolds have also been shown to modulate RMP (Jayaram et al. 2017). As well, applied EFs have been shown to improve wound closure time and increased recruitment of endogenous cells (Messerli

& Graham 2011; Hotary & Robinson 1990; Baer et al. 2015). Further research into how cells respond and sense EF will help refine and optimize existing therapeutic techniques.

6 Chapter 6 Conclusions

We have observed conserved age and passage differences in the galvanotactic response of cultured NPCs. Neonatal NPCs consistently showed greater migration speed and tortuosity than adult NPCs. As well, primary NPCs exhibited increased migration speed and tortuosity compared to passaged NPCs. To elucidate the underlying cause of this differential migration pattern over age and passage time, we next analyzed RMP of NPCs.

Interestingly, regardless of niche, passage, or age conditions, RMP hyperpolarization increased activation of both NPC migration speed and tortuosity, suggesting that cell migratory activity has increased. Alternatively, RMP hyperpolarization may have increased NPC sensitivity to external EFs.

RMP has been implicated in cell proliferation (Aprea & Calegari 2012) and ion flux is a necessary part of sustained, directed migration (Özkucur et al. 2011; Stock et al. 2013). As well, RMP modulation of both NPC proliferation kinetics and migration suggests that it acts as a pleiotropic signal capable of regulating multiple cell behaviours. EFs have also been shown to exhibit pleiotropic effects to increase migration speed as well as proliferation. The similarity in effects suggests that RMP is a promising candidate modulator of galvanotactic behaviour in two possible ways. RMP may act as an intrinsic, master patterning signal independent of external control, or RMP may act downstream of a factor capable of altering ion flux within the cell.

We next investigated what was present within the milieu of NPCs within the neurosphere assay. Did NPCs themselves interact with each other or secrete migration promoting, or RMP modulating factors? Or as we predict, does that migration promoting factor originate from the niche? Specifically, the neonatal niche?

We analyzed niche and cell-cell interactions through conditioned media and cell-cell mixing experiments. We saw no cell-cell effects on NPC migration. However in conditioned media mixing experiments, we were able to upregulate passaged adult NPC speed and tortuosity by adding neonatal primary conditioned media.

To isolate the factor responsible this upregulation, we analyzed the components of our conditioned media via an antibody-sandwich ELISA. Out of 200 analyzed proteins, we identified 34 highly expressed proteins within the conditioned media. Of the top 10 differentially expressed proteins, we identified IGF1 as a potential modulator of NPC galvanotaxis, however further experiments are required to validate this hypothesis.

As adult NPC galvanotaxis is capable of increasing in speed and tortuosity by addition of neonatal CM in a similar fashion to chemically induced RMP hyperpolarization, we propose that there exists an endogenous signaling factor highly expressed in neonatal NPCs capable of modulating the RMP of NPCs to control migration kinetics.

Consistent with our observations, IGF1 is highly expressed in primary neonatal NPC cultures. Neonatal cells exhibit increased migration speed and tortuosity, compared to adult passaged NPCs, as well as increased proliferation upon passaging. IGF1 has been implicated in pathways affecting NPC proliferation and migration in other cell types. As well, IGF1 has been shown to affect potassium and calcium ion current flux in neurons. The IGF protein family and cognate receptors may prove to be a promising potential bridge between EF and intracellular behaviour. Exciting future investigations may uncover an answer to the biggest question in bioelectricity as well as open new possibilities for powerful NPC regenerative therapies!

7 Chapter 7
Future Directions

Galvanotaxis is a promising field with many open questions. Particularly in NPCs, there is still much to learn about the mechanisms underlying this unique bioelectric phenomenon. The biggest question in bioelectricity still remains. If elucidated, it could potentially lead to profound ramifications in basic understanding of biology and in therapeutic applications. Three main questions stem from the work of this thesis:

1. Do age related changes follow a linear progression of decline? Does galvanotaxis change further over time? Or is homeostatic quiescence maintained in old age? These questions may be investigated by characterizing NPC galvanotaxis in older age groups (22 months) as well as analysis of CM factors in older age groups. The baseline assessment of cellular capacities and milieu may offer insights into progression of aging mechanisms and also offer insights into optimization of donor/recipient age effects in transplantation therapies.

2. What is the precise mechanism used by cells to sense EF? Does pharmaceutically depolarized RMP lead to decreased galvanotactic speed and tortuosity? Is IGF1 a controlling factor in modulating NPC RMP? These investigations seek to further elucidate galvanotactic mechanisms. Teasing apart roles of cellular mechanisms of migration from galvanotaxis presents a unique difficulty as galvanotaxis depends on the machinery of migration. The key to understanding galvanotactic mechanisms lie in investigating upstream modulator of common migration machinery.

3. How does galvanotaxis affect future therapeutic applications? Does RMP or EF stimulation affect NPC proliferation? If RMP does indeed exhibit pleiotropic effects, is galvanotaxis a viable therapeutic in vivo? These questions seek to identify and characterize the role galvanotaxis and EF stimulation play in vivo. As well, these questions seek to assess the suitability of EF stimulation in vivo and what conditions are necessary to optimize EF therapeutics.

7.1 Characterization of Galvanotaxis in Old Age

The next step in analyzing age effects on galvanotaxis is to analyze galvanotactic migration in old mice of 22 months of age. The lifespan of a mouse is approximately 24-26 months (Martin-Montalvo et al. 2013) hence 18-22 months of age is considered “old age”.

A recent report by Apostolopoulou et al. showed RNA expression over time showed significant similarities between 22 month and neonatal populations (Apostolopoulou et al. 2017), consistent with our findings of old primary NPCs recapitulating neonatal mice phenotypes.

If older cohort mice indeed behave similarly to neonatal cohorts, this would suggest there may be a factor present that is non-linearly decreasing with time, highly present in neonatal populations then decreased in adults and re-expressed at 22 months. The next step to investigate this similarity between phenotypes would be to look for a factor that is highly expressed in neonatal and old conditioned media that also shows low expression in adult groups.

7.2 Conditioned Media Analyses

Incorporating the older cohort of 18-22 months, factor analysis of old CM will be conducted. As well, currently underway are investigations into physiological concentrations of IGF-1 supplementation in galvanotaxis as well as introduction of IGF-1 blockers in culture. NPC migration as well as proliferation kinetics will be observed under both conditions.

As well, it is currently unknown what genes may be upregulated/downregulated during and by galvanotaxis. Our current assay only tests for a predetermined set of proteins. Experiments to identify novel interactions include techniques such as cDNA microarrays and RNA sequencing. 2-D gel electrophoresis coupled with mass spectrometry could also help identify novel protein interations.

CM of all neonatal, adult, and old primary plus passaged cell groups should be analyzed for differences and correlated back to galvanotactic migration metrics to identify more potential activators as well as inhibitors.

As galvanotaxis is a rapid phenomenon, there lies great technical difficulty in capturing such data while EF stimulation is occurring. Even after EF stimulation, it is unknown how long the effects last.

To overcome these unknowns, different sampling time points of the same group of NPCs should be assessed. Time points should consist of three major segments: before EF stimulation, during EF stimulation, and post-EF stimulation. In an example experiment, NPCs should be assessed for sequence expressions before EF stimulation to establish baseline controls. Controls may be sampled during free-floating NPC sphere growth times and after adherence to migratory substrates. Experimental sampling should occur at relevant timepoints of EF stimulation. 15 minutes has been shown to be the time frame needed for NPCs to fully respond to an EF (Babona-Pilipos et al. 2011). NPCs may be sampled again at 3 hours, when EF stimulation concludes. Protein translation occurs at 5 amino acids per second and the average size of a protein is ~350 amino acids in length (Milo et al. 2009). At a rate of approximately 1 protein synthesized per minute and unknown number of polyribosomes, transcripts, and need for transcription within a cell, rates of protein translation range from minutes to hours. As well, muscle cells have been shown to upregulate exercise related proteins for up to 36 hours after exercise (MacDougall et al. 1995). Follow-up sampling to test for long term protein upregulation should then occur at post-stimulation times of 1 day, 2 days, 3 days, 4 days, and 7 days.

To corroborate if identified CM factors mediate cell-sensing of an electric field, baseline resting membrane potential should next be established and the effects of target factors on RMP should be verified.

7.3 Resting Membrane Potential of Old NPCs

Resting membrane potential (RMP) of old NPCs should first be performed and assessed in the presence of diazoxide to test for similar effects and responses in older cell populations.

To fully understand the effect of RMP on galvanotaxis, the effects of depolarizing agents on RMP should also be investigated. As well, in the interest of comprehensiveness, a dose response curve of diazoxide in relation to RMP changes can be performed to connect RMP effects to NPC

proliferation. As described previously, RMP depolarization decreases cell stiffness by dissociating actin filaments (Callies et al. 2011). Galvanotactic migration should then be assessed under depolarizing conditions to test for associations.

As well, the effects of IGF-1 on RMP should be tested to assess if IGF-1 possesses RMP modulating as part of a pathway for NPC EF sensing.

7.4 Cell Membrane Potential Modulation of NPC Proliferation

As described above, RMP has also been implicated in control of cell proliferation. If RMP has pleiotropic effects, we want to further investigate effects of RMP modulation on NPC proliferation. If the effects of proliferation and migration are proportionally or inversely related, it may give clues as to how or if RMP acts as a master morphogenic regulator.

We next wanted to modulate RMP to test for NPC specific proliferation. Using diazoxide, we investigated the effects of membrane hyperpolarization and saw a decrease (Figure 17). Next experiments will look at prolonged diazoxide exposure without niche factors present.

We also used $BaCl_2$ to investigate effects of depolarization, however, those studies proved variable and inconclusive (Liu and Velayudan, unpublished data). It is yet unknown if depolarization failed to promote NPC proliferation or if $BaCl_2$ was unable to induce NPC depolarization. Further investigations with alternative modulators are necessary.

7.5 Future potential of in vivo Galvanotaxis

Current work in our lab is testing in vivo galvanotaxis efficacy. Parameters of stimulation time versus rest time, stimulation frequency, and electrode design are still being investigated. Future investigations of in vivo stimulation should include baseline field measures of healthy brains. Followed by measurement of injury potentials from electrode implantation as well as applied EF strengths in distant portions of the brain.

Cross age NPC transplantation studies between neonatal, adult, and old mice will elucidate donor/recipient effects. As well, effects of candidate galvanotaxis promoting or proliferation promoting factors should be tested to see if an effect on transplanted NPCs in the niche still persists. The experiments outlined above aligns well with principles of biphasic electrical stimulation as both are direct current EFs.

Current work in cell biology is using mathematical models to predict cell migration paradigms (Wadkin et al. 2018), as well as use conductive bioscaffolds to help promote migration (Song & George 2017). As outlined in section 1.8.2, the clinical applications of EF therapeutics are manifold. Specific to the guided migration of NPCs by EFs, transplanted NPCs could be stimulated to grow and migrate faster towards a lesion site, whether that lesion be neurodegenerative or traumatic in origin.

References

Abdallah, N.M.-B. et al., 2010. Early age-related changes in adult hippocampal neurogenesis in C57 mice. *Neurobiology of Aging*, 31(1), pp.151–161.

Åberg, M.A.I. et al., 2003. IGF-I has a direct proliferative effect in adult hippocampal progenitor cells. *Molecular and Cellular Neuroscience*, 24(1), pp.23–40.

Adams, D.S. & Levin, M., 2013. Endogenous voltage gradients as mediators of cell-cell communication: strategies for investigating bioelectrical signals during pattern formation. *Cell and Tissue Research*, 352(1), pp.95–122.

Agarwal, S.M. et al., 2013. Transcranial direct current stimulation in schizophrenia. *Clinical Psychopharmacology and Neuroscience*, 11(3), pp.118–125.

Akkermann, R., Beyer, F. & Küry, P., 2017. Heterogeneous populations of neural stem cells contribute to myelin repair. *Neural Regeneration Research*, 12(4), pp.509–517.

Allen, R.D., 1981. Motility. *The Journal of Cell Biology*, 91(3), pp.148–155.

Alsharidah, M. et al., 2013. Primary human muscle precursor cells obtained from young and old donors produce similar proliferative, differentiation and senescent profiles in culture. *Aging Cell*, 12(3), pp.333–344.

Altizer, A.M. et al., 2001. Endogenous electric current is associated with normal development of the vertebrate limb. *Developmental Dynamics*, 221(4), pp.391–401.

Altman, J., 1962. Are new neurons formed in the brains of adult mammals? *Science*, 135(3509), pp.1127–1128.

Altman, J., 1969. Autoradiographic and histological studies of postnatal neurogenesis. IV. Cell proliferation and migration in the anterior forebrain, with special reference to persisting neurogenesis in the olfactory bulb. *The Journal of Comparative Neurology*, 137(4), pp.433–457.

Altman, J., 1963. Autoradiographic investigation of cell proliferation in the brains of rats and

cats. *The Anatomical Record*, 145(4), pp.573–591.

Altman, J. & Das, G.D., 1965. Autoradiographic and histological evidence of postnatal hippocampal neurogenesis in rats. *Journal of Comparative Neurology*, 124(3), pp.319–335.

Altman, J. & Das, G.D., 1966. Autoradiographic and histological studies of postnatal neurogenesis. I. A longitudinal investigation of the kinetics, migration and transformation of cells incoorporating tritiated thymidine in neonate rats, with special reference to postnatal neurogenesi. *Journal of Comparative Neurology*, 126(3), pp.337–389.

Anthony, T.E. et al., 2004. Radial Glia Serve as Neuronal Progenitors in All Regions of the Central Nervous System. *Neuron*, 41, pp.881–890.

Anton, E.., Kreidberg, J.A. & Rakic, P., 1999. Distinct Functions of α3 and αV Integrin Receptors in Neuronal Migration and Laminar Organization of the Cerebral Cortex. *Neuron*, 22(2), pp.277–289.

Apostolopoulou, M. et al., 2017. Non-monotonic Changes in Progenitor Cell Behavior and Gene Expression during Aging of the Adult V-SVZ Neural Stem Cell Niche. *Stem Cell Reports*, 9(6), pp.1931–1947.

Aprea, J. & Calegari, F., 2012. Bioelectric state and cell cycle control of mammalian neural stem cells. *Stem Cells International*.

Arsenijevic, Y. et al., 2001. Insulin-like growth factor-I is necessary for neural stem cell proliferation and demonstrates distinct actions of epidermal growth factor and fibroblast growth factor-2. *The Journal of Neuroscience*, 21(18), pp.7194–7202.

Artemenko, Y. et al., 2016. Chemical and mechanical stimuli act on common signal transduction and cytoskeletal networks. *Proceedings of the National Academy of Sciences of the United States of America*, 113(47), pp.E7500–E7509.

Arulmoli, J. et al., 2015. Static stretch affects neural stem cell differentiation in an extracellular matrix-dependent manner. *Scientific Reports*, 5(1), p.8499.

Arvidsson, A. et al., 2002. Neuronal replacement from endogenous precursors in the adult brain

after stroke. *Nature Medicine*, 8(9), pp.963–970.

Babona-Pilipos, R. et al., 2011. Adult subependymal neural precursors, but not differentiated cells, undergo rapid cathodal migration in the presence of direct current electric fields. *PLoS ONE*, 6(8).

Babona-Pilipos, R. et al., 2018. Calcium influx differentially regulates migration velocity and directedness in response to electric field application. *Experimental Cell Research*, 368(2), pp.202–214.

Babona-Pilipos, R., Popovic, M.R. & Morshead, C.M., 2012. A galvanotaxis assay for analysis of neural precursor cell migration kinetics in an externally applied direct current electric field. *Journal of Visualized Experiments*, (68), pp.1–8.

Baer, M.L., Henderson, S.C. & Colello, R.J., 2015. Elucidating the Role of Injury-Induced Electric Fields (EFs) in Regulating the Astrocytic Response to Injury in the Mammalian Central Nervous System W. Hu, ed. *PLoS ONE*, 10(11), p.e0142740.

Bagó, J.R., Sheets, K.T. & Hingtgen, S.D., 2016. Neural stem cell therapy for cancer. *Methods*, 99, pp.37–43.

Baker, S.A., Baker, K.A. & Hagg, T., 2004. Dopaminergic nigrostriatal projections regulate neural precursor proliferation in the adult mouse subventricular zone. *European Journal of Neuroscience*, 20(2), pp.575–579.

Barkho, B.Z. et al., 2008. Endogenous Matrix Metalloproteinase (MMP)-3 and MMP-9 Promote the Differentiation and Migration of Adult Neural Progenitor Cells in Response to Chemokines. *Stem Cells*, 26(12), pp.3139–3149.

Bartlett, W.P., Li, X.S. & Williams, M., 1992. Expression of IGF-1 mRNA in the murine subventricular zone during postnatal development. *Brain Research*, 12(4), pp.285–291.

Bátiz, L.F. et al., 2016. Exosomes as Novel Regulators of Adult Neurogenic Niches. *Frontiers in Cellular Neuroscience*, 9, p.501.

Bayer, S.A., Yackel, J.W. & Puri, P.S., 1982. Neurons in the rat dentate gyrus granular layer

substantially increase during juvenile and adult life. *Science*, 216(4548), pp.890–892.

Beane, W.S. et al., 2013. Bioelectric signaling regulates head and organ size during planarian regeneration. *Development*, 140(2), pp.313–322.

Bear, J.E. & Haugh, J.M., 2014. Directed migration of mesenchymal cells: where signaling and the cytoskeleton meet. *Current Opinion in Cell Biology*, 30, pp.74–82.

Belvindrah, R. et al., 2007. Beta1 Integrins Control the Formation of Cell Chains in the Adult Rostral Migratory Stream. *Journal of Neuroscience*, 27(10), pp.2704–2717.

Belvindrah, R. et al., 2009. Postnatal Neurogenesis: From Neuroblast Migrationto Neuronal Integration. *Reviews in the Neurosciences*, 20(5–6), pp.331–346.

Benítez-Rangel, E. et al., 2011. Ion channel inhibitors block caspase activation by mechanisms other than restoring intracellular potassium concentration. *Cell Death & Disease*, 2(1), p.e113.

Van Den Berge, S.A. et al., 2011. The proliferative capacity of the subventricular zone is maintained in the parkinsonian brain. *Brain*, 134(11), pp.3249–3263.

Del Bigio, M.R., 2010. Ependymal cells: Biology and pathology. *Acta Neuropathologica*, 119(1), pp.55–73.

Binggeli, R. & Weinstein, R.C., 1986. Membrane potentials and sodium channels: Hypotheses for growth regulation and cancer formation based on changes in sodium channels and gap junctions. *Journal of Theoretical Biology*, 123(4), pp.377–401.

Blackiston, D.J., McLaughlin, K.A. & Levin, M., 2009. Bioelectric controls of cell proliferation: Ion channels, membrane voltage and the cell cycle. *Cell Cycle*, 8(21), pp.3527–3536.

Blair, L.A.. & Marshall, J., 1997. IGF-1 Modulates N and L Calcium Channels in a PI 3-Kinase-Dependent Manner. *Neuron*, 19(2), pp.421–429.

Bondolfi, L. et al., 2004. Impact of age and caloric restriction on neurogenesis in the dentate gyrus of C57BL/6 mice. *Neurobiology of Aging*, 25(3), pp.333–340.

Borgens, R.B., Callahan, L. & Rouleau, M.F., 1987. Anatomy of axolotl flank integument during limb bud development with special reference to a transcutaneous current predicting limb formation. *Journal of Experimental Zoology*, 244(2), pp.203–214.

Bortone, D. & Polleux, F., 2009. KCC2 Expression Promotes the Termination of Cortical Interneuron Migration in a Voltage-Sensitive Calcium-Dependent Manner. *Neuron*, 62(1), pp.53–71.

Bovetti, S., Hsieh, Y.-C., et al., 2007. Blood vessels form a scaffold for neuroblast migration in the adult olfactory bulb. *Journal of Neuroscience*, 27(22), pp.5976–5980.

Bovetti, S., Bovolin, P., et al., 2007. Subventricular zone-derived neuroblast migration to the olfactory bulb is modulated by matrix remodelling. *European Journal of Neuroscience*, 25(7), pp.2021–2033.

Breunig, J.J., Haydar, T.F. & Rakic, P., 2011. Neural Stem Cells: Historical Perspective and Future Prospects. *Neuron*, 70(4), pp.614–625.

Brousse, B. et al., 2015. Region and dynamic specificities of adult neural stem cells and oligodendrocyte precursors in myelin regeneration in the mouse brain. *Biology Open*, 4(8), pp.980–92.

Brunoni, A.R. et al., 2016. Transcranial direct current stimulation for acute major depressive episodes: Meta-analysis of individual patient data. *British Journal of Psychiatry*, 208(6), pp.522–531.

Buzatu, S., 2009. The temperature-induced changes in membrane potential. *Rivista di biologia*, 102(2), pp.199–217.

Callies, C. et al., 2011. Membrane potential depolarization decreases the stiffness of vascular endothelial cells. *Journal of Cell Science*, 124(11), pp.1936–1942.

Cao, L. et al., 2013. Endogenous electric currents might guide rostral migration of neuroblasts. *EMBO reports*, 14(2), pp.184–190.

Cao, L. et al., 2015. Physiological Electrical Signals Promote Chain Migration of Neuroblasts by

Up-Regulating P2Y1 Purinergic Receptors and Enhancing Cell Adhesion. *Stem Cell Reviews and Reports*, 11(1), pp.75–86.

Capilla-Gonzalez, V. et al., 2014. Age-related changes in astrocytic and ependymal cells of the subventricular zone. *Glia*, 62(5), pp.790–803.

Capilla-Gonzalez, V. et al., 2015. Regulation of subventricular zone-derived cells migration in the adult brain. *Advances in Experimental Medicine and Biology*, 853, pp.1–21.

Carboni, C. et al., 2018. An initial study on the effect of functional electrical stimulation in erectile dysfunction: a randomized controlled trial. *International Journal of Impotence Research*, 30(3), pp.97–101.

Cardozo, D., 2016. An intuitive approach to understanding the resting membrane potential. *Advances in Physiology Education*, 40, pp.543–547.

Cargnello, M. & Roux, P.P., 2011. Activation and Function of the MAPKs and Their Substrates, the MAPK-Activated Protein Kinases. *Microbiology and Molecular Biology Reviews*, 75(1), pp.50–83.

Carnicero, E. et al., 2013. Embryonic cerebrospinal fluid activates neurogenesis of neural precursors within the subventricular zone of the adult mouse brain. *Cells Tissues Organs*, 198(5), pp.398–404.

Carpentier, P.A. & Palmer, T.D., 2009. Immune Influence on Adult Neural Stem Cell Regulation and Function. *Neuron*, 64(1), pp.79–92.

Castrioto, A. et al., 2011. Ten-Year Outcome of Subthalamic Stimulation in Parkinson Disease. *Archives of Neurology*, 68(12), pp.1550–1556.

Cervera, J., Meseguer, S. & Mafe, S., 2016. The interplay between genetic and bioelectrical signaling permits a spatial regionalisation of membrane potentials in model multicellular ensembles. *Scientific Reports*, 6(1), p.35201.

Chaker, Z., Codega, P. & Doetsch, F., 2016. A mosaic world: puzzles revealed by adult neural stem cell heterogeneity. *Wiley Interdisciplinary Reviews: Developmental Biology*, 5(6),

pp.640–658.

Chao, P.G. et al., 2007. Effects of Applied DC Electric Field on Ligament Fibroblast Migration and Wound Healing. *Connective Tissue Research*, 48(4), pp.188–197.

Chao, P.H. et al., 2000. Chondrocyte translocation response to direct current electric fields. *Journal of Biomechanical Engineering*, 122(3), pp.261–267.

Checchin, D. et al., 2006. Potential Role of Microglia in Retinal Blood Vessel Formation. *Investigative Opthalmology & Visual Science*, 47(8), pp.3595–3602.

Chen, Y.A. et al., 2018. The Proliferation Capacity of Cultured Neural Stem Cells Promoted by CSF Collected from SAH Patients Correlates to Clinical Outcome. *Scientific Reports*, 8(1), p.1109.

Chernet, B.T. & Levin, M., 2013. Transmembrane voltage potential is an essential cellular parameter for the detection and control of tumor development in a Xenopus model. *Disease Models & Mechanisms*, 6(3), pp.595–607.

Chiang, M., Robinson, K.R. & Vanable, J.W., 1992. Electrical fields in the vicinity of epithelial wounds in the isolated bovine eye. *Experimental Eye Research*, 54(6), pp.999–1003.

Clausell, M., Fang, Z. & Chen, W., 2014. In Vivo Study of Transepithelial Potential Difference (TEPD) in Proximal Convoluted Tubules of Rat Kidney by Synchronization Modulation Electric Field. *The Journal of Membrane Biology*, 247(7), pp.601–609.

Codega, P. et al., 2014. Prospective Identification and Purification of Quiescent Adult Neural Stem Cells from Their In Vivo Niche. *Neuron*, 82(3), pp.545–559.

Coles-Takabe, B.L.K. et al., 2008. Don't Look: Growing Clonal Versus Nonclonal Neural Stem Cell Colonies. *Stem Cells*, 26(11), pp.2938–2944.

Cone, C.D., 1971. Unified theory on the basic mechanism of normal mitotic control and oncogenesis. *Journal of Theoretical Biology*, 30(1), pp.151–181.

Cone, C.D.J. & Cone, C.M., 1976. Induction of mitosis in mature neurons in central nervous

system by sustained depolarization. *Science*, 192(4235), pp.155–158.

Conover, J.C. & Notti, R.Q., 2008. The neural stem cell niche. *Cell and Tissue Research*, 331(1), pp.211–224.

Conover, J.C. & Shook, B.A., 2011. Aging of the subventricular zone neural stem cell niche. *Aging and Disease*, 2(1), pp.49–63.

Cooper, M.S. & Keller, R.E., 1984. Perpendicular orientation and directional migration of amphibian neural crest cells in dc electrical fields. *Proceedings of the National Academy of Sciences of the United States of America*, 81(1), pp.160–164.

Crevenna, A.H. et al., 2013. Electrostatics control actin filament nucleation and elongation kinetics. *Journal of Biological Chemistry*, 288(17), pp.12102–12113.

Dai, J. et al., 2013. Migration of neural stem cells to ischemic brain regions in ischemic stroke in rats. *Neuroscience Letters*, 552, pp.124–128.

Dandekar, M.P. et al., 2018. Deep brain stimulation for treatment-resistant depression: an integrative review of preclinical and clinical findings and translational implications. *Molecular Psychiatry*, 23(5), pp.1094–1112.

Datta, A. et al., 2009. Gyri-precise head model of transcranial direct current stimulation: Improved spatial focality using a ring electrode versus conventional rectangular pad. *Brain Stimulation*, 2(4), pp.201–207.

Delgado, A.C. et al., 2014. Endothelial NT-3 Delivered by Vasculature and CSF Promotes Quiescence of Subependymal Neural Stem Cells through Nitric Oxide Induction. *Neuron*, 83(3), pp.572–585.

Djamgoz MBA et al., 2001. Directional movement of rat prostate cancer cells in direct-current electric field: involvement of voltagegated Na+ channel activity. *Journal of Cell Science*, 114(14), pp.2697–2705.

Doetsch, F., 2003. A niche for adult neural stem cells. *Current Opinion in Genetics and Development*, 13(5), pp.543–550.

Doetsch, F. & Alvarez-Buylla, A., 1996. Network of tangential pathways for neuronal migration in adult mammalian brain. *Proceedings of the National Academy of Sciences of the United States of America*, 93(25), pp.14895–14900.

Doetsch, F., García-Verdugo, J.M. & Alvarez-Buylla, A., 1997. Cellular composition and three-dimensional organization of the subventricular germinal zone in the adult mammalian brain. *The Journal of Neuroscience*, 17(13), pp.5046–5061.

Douet, V. et al., 2013. Fractone-heparan sulphates mediate FGF-2 stimulation of cell proliferation in the adult subventricular zone. *Cell Proliferation*, 46(2), pp.137–145.

Douet, V., Arikawa-Hirasawa, E. & Mercier, F., 2012. Fractone-heparan sulfates mediate BMP-7 inhibition of cell proliferation in the adult subventricular zone. *Neuroscience Letters*, 528(2), pp.120–125.

Doyle, M.E. & Egan, J.M., 2003. Pharmacological Agents That Directly Modulate Insulin Secretion. *Pharmacological Reviews*, 55(1), pp.105–131.

Dudek, F., Yasumura, T. & Rash, J.E., 1998. "Non-synaptic" mechanisms in seizures and epileptogenesis. *Cell Biology International*, 22(11–12), pp.793–805.

Dumont, C.M. et al., 2017. Factors Released from Endothelial Cells Exposed to Flow Impact Adhesion, Proliferation, and Fate Choice in the Adult Neural Stem Cell Lineage. *Stem Cells and Development*, 26(16), p.scd.2016.0350.

Elias, L.A.B., Wang, D.D. & Kriegstein, A.R., 2007. Gap junction adhesion is necessary for radial migration in the neocortex. *Nature*, 448(7156), pp.901–907.

Enwere, E. et al., 2004. Aging Results in Reduced Epidermal Growth Factor Receptor Signaling, Diminished Olfactory Neurogenesis, and Deficits in Fine Olfactory Discrimination. *Journal of Neuroscience*, 24(38), pp.8354–8365.

Erickson, R.I. et al., 2008. Roles of insulin and transferrin in neural progenitor survival and proliferation. *Journal of Neuroscience Research*, 86(8), pp.1884–1894.

Ermolaeva, M. et al., 2018. Cellular and epigenetic drivers of stem cell aging. *Nature Reviews*

Molecular Cell Biology, accepted, p.1.

Faissner, A., Roll, L. & Theocharidis, U., 2017. Tenascin-C in the matrisome of neural stem and progenitor cells. *Molecular and Cellular Neuroscience*, 81, pp.22–31.

Farboud, B. et al., 2000. DC Electric Fields Induce Rapid Directional Migration in Cultured Human Corneal Epithelial Cells. *Experimental Eye Research*, 70(5), pp.667–673.

Feng, J.-F. et al., 2012. Guided Migration of Neural Stem Cells Derived from Human Embryonic Stem Cells by an Electric Field. *Stem Cells*, 30(2), pp.349–355.

Ferrier, J. et al., 1986. Osteoclasts and osteoblasts migrate in opposite directions in response to a constant electrical field. *Journal of Cellular Physiology*, 129(3), pp.283–288.

Fischer, J. et al., 2011. Prospective isolation of adult neural stem cells from the mouse subependymal zone. *Nature Protocols*, 6(12), pp.1981–1989.

Fitz, J.G., Trouillot, T.E. & Scharschmidt, B.F., 1989. Effect of pH on membrane potential and K+ conductance in cultured rat hepatocytes. *American Journal of Physiology*, 257(6), pp.G961–G968.

Flores, I. et al., 2008. The longest telomeres: a general signature of adult stem cell compartments. *Genes & Development*, 22(5), pp.654–667.

Foulds, I.S. & Barker, A.T., 1983. Human skin battery potentials and their possible role in wound healing. *British Journal of Dermatology*, 109(5), pp.515–522.

Fourgeaud, L. et al., 2016. TAM receptors regulate multiple features of microglial physiology. *Nature*, 532(7598), pp.240–244.

Franco, S.J. et al., 2011. Reelin regulates cadherin function via Dab1/Rap1 to control neuronal migration and lamination in the neocortex. *Neuron*, 69(3), pp.482–497.

Fröhlich, F. & McCormick, D.A., 2010. Endogenous Electric Fields May Guide Neocortical Network Activity. *Neuron*, 67(1), pp.129–143.

Fuentealba, L.C., Obernier, K. & Alvarez-Buylla, A., 2012. Adult neural stem cells bridge their

niche. *Cell Stem Cell*, 10(6), pp.698–708.

Fujikake, K. et al., 2018. Detachment of Chain-Forming Neuroblasts by Fyn-Mediated Control of cell–cell Adhesion in the Postnatal Brain. *The Journal of Neuroscience*, 38(19), pp.4598–4609.

Fujioka, T. et al., 2017. β1 integrin signaling promotes neuronal migration along vascular scaffolds in the post-stroke brain. *EBioMedicine*, 16, pp.195–203.

Funk, R.H., 2013. Ion Gradients in Tissue and Organ Biology. *Biological Systems*, 2(1), p.1000105.

Funk, R.H.W., 2015. Endogenous electric fields as guiding cue for cell migration. *Frontiers in Physiology*, 6(MAY), p.143.

Funk, R.H.W., Monsees, T. & Özkucur, N., 2009. Electromagnetic effects – From cell biology to medicine. *Progress in Histochemistry and Cytochemistry*, 43(4), pp.177–264.

Furutachi, S. et al., 2013. p57 controls adult neural stem cell quiescence and modulates the pace of lifelong neurogenesis. *The EMBO Journal*, 32(7), pp.970–981.

Fuxe, K. et al., 1996. Computer-assisted mapping of basic fibroblast growth factor immunoreactive nerve cell populations in the rat brain. *Journal of Chemical Neuroanatomy*, 11(1), pp.13–35.

Gall, C. et al., 2016. Alternating current stimulation for vision restoration after optic nerve damage: A randomized clinical trial M. M. DeAngelis, ed. *PLoS ONE*, 11(6), p.e0156134.

Gao, R. chi et al., 2011. Different roles of membrane potentials in electrotaxis and chemotaxis of Dictyostelium cells. *Eukaryotic Cell*, 10(9), pp.1251–1256.

Gates, M.A. et al., 1995. Cell and molecular analysis of the developing and adult mouse subventricular zone of the cerebral hemispheres. *Journal of Comparative Neurology*, 361(2), pp.249–266.

Gincberg, G. et al., 2012. Neural stem cells: Therapeutic potential for neurodegenerative

diseases. *British Medical Bulletin*, 104(1), pp.7–19.

Gomez-Gaviro, M. V. et al., 2012. Betacellulin promotes cell proliferation in the neural stem cell niche and stimulates neurogenesis. *Proceedings of the National Academy of Sciences of the United States of America*, 109(4), pp.1317–1322.

Gonfloni, S., 2013. Targeting DNA damage response: Threshold, chromatin landscape and beyond. *Pharmacology & Therapeutics*, 138(1), pp.46–52.

Graus-Porta, D. et al., 2001. Beta1-class integrins regulate the development of laminae and folia in the cerebral and cerebellar cortex. *Neuron*, 31(3), pp.367–379.

Greene, N.D.E. & Copp, A.J., 2009. Development of the vertebrate central nervous system: Formation of the neural tube. *Prenatal Diagnosis*, 29(4), pp.303–311.

Groiss, S.J. et al., 2009. Deep brain stimulation in Parkinson-s disease. *Therapeutic Advances in Neurological Disorders*, 2(6), pp.379–391.

Guo, X. et al., 2015. The Galvanotactic Migration of Keratinocytes is Enhanced by Hypoxic Preconditioning. *Scientific Reports*, 5(1), p.10289.

Haan, N. & Song, B., 2014. Therapeutic Application of Electric Fields in the Injured Nervous System. *Advances in Wound Care*, 3(2), pp.156–165.

Hack, I. et al., 2007. Divergent roles of ApoER2 and Vldlr in the migration of cortical neurons. *Development*, 134(21), pp.3883–3891.

Handa, Y., Yagi, R. & Hoshimiya, N., 1998. Application of functional electrical stimulation to the paralyzed extremities. *Neurologia medico-chirurgica*, 38(11), pp.784–788.

Harris, L.K. & Westwood, M., 2012. Biology and significance of signalling pathways activated by IGF-II. *Growth Factors*, 30(1), pp.1–12.

Haubensak, W. et al., 2004. Neurons arise in the basal neuroepithelium of the early mammalian telencephalon: A major site of neurogenesis. *Proceedings of the National Academy of Sciences of the United States of America*, 101(9), pp.3196–3201.

Hayashi, T. et al., 1998. Inductions of hepatocyte growth factor and its activator in rat brain with permanent middle cerebral artery occlusion. *Brain Research*, 799(2), pp.311–316.

Hedlund, E. et al., 2016. Dopamine Receptor Antagonists Enhance Proliferation and Neurogenesis of Midbrain Lmx1a-expressing Progenitors. *Scientific Reports*, 6(1), p.26448.

Higginbotham, H. et al., 2006. GSK3β and PKCζ function in centrosome localization and process stabilization during Slit-mediated neuronal repolarization. *Molecular and Cellular Neuroscience*, 32(1–2), pp.118–132.

Hinds, J.W., 1968. Autoradiographic study of histogenesis in the mouse olfactory bulb. II. Cell proliferation and migration. *Journal of Comparative Neurology*, 134(3), pp.305–322.

Hirota, Y. et al., 2018. ApoER2 Controls Not Only Neuronal Migration in the Intermediate Zone But Also Termination of Migration in the Developing Cerebral Cortex. *Cerebral Cortex*, 28(1), pp.223–235.

Hirota, Y. & Nakajima, K., 2017. Control of Neuronal Migration and Aggregation by Reelin Signaling in the Developing Cerebral Cortex. *Frontiers in Cell and Developmental Biology*, 5, p.40.

Hitoshi, S. et al., 2007. Antidepressant drugs reverse the loss of adult neural stem cells following chronic stress. *Journal of Neuroscience Research*, 85(16), pp.3574–3585.

Hodkin, E.F. et al., 2018. Automated FES for upper limb rehabilitation following stroke and spinal cord injury. *IEEE Transactions on Neural Systems and Rehabilitation Engineering*, 26(5), pp.1067–1074.

Höglinger, G.U. et al., 2004. Dopamine depletion impairs precursor cell proliferation in Parkinson disease. *Nature Neuroscience*, 7(7), pp.726–735.

Horner, P.J. & Gage, F.H., 2000. Regenerating the damaged central nervous system. *Nature*, 407(6807), pp.963–970.

Hotary, K.B. & Robinson, K.R., 1990. Endogenous electrical currents and the resultant voltage gradients in the chick embryo. *Developmental Biology*, 140(1), pp.149–160.

Hu, H., 1999. Chemorepulsion of neuronal migration by Slit2 in the developing mammalian forebrain. *Neuron*, 23(4), pp.703–711.

Hu, H. et al., 1996. The role of polysialic acid in migration of olfactory bulb interneuron precursors in the subventricular zone. *Neuron*, 16(4), pp.735–743.

Hu, W. & Stead, M., 2014. Deep brain stimulation for dystonia. *Translational Neurodegeneration*, 3(1), p.2.

Hu, X.L. et al., 2017. Persistent Expression of VCAM1 in Radial Glial Cells Is Required for the Embryonic Origin of Postnatal Neural Stem Cells. *Neuron*, 95(2), pp.309–325.

Imitola, J. et al., 2004. Directed migration of neural stem cells to sites of CNS injury by the stromal cell-derived factor 1alpha/CXC chemokine receptor 4 pathway. *Proceedings of the National Academy of Sciences of the United States of America*, 101(52), pp.18117–18122.

Iwasa, S.N., Babona-Pilipos, R. & Morshead, C.M., 2017. Environmental Factors That Influence Stem Cell Migration: An "Electric Field." *Stem Cells International*, 2017, pp.1–9.

Iwasa, S.N., Popovic, M.R. & Morshead, C.M., 2018. Skin-derived precursor cells undergo substrate-dependent galvanotaxis that can be modified by neighbouring cells. *Stem Cell Research*.

Iyama, T. & Wilson, D.M., 2013. DNA repair mechanisms in dividing and non-dividing cells. *DNA Repair*, 12(8), pp.620–636.

J. Beebe, S., 2013. Bioelectrics in Basic Science and Medicine: Impact of Electric Fields on Cellular Structures and Functions. *Journal of Nanomedicine & Nanotechnology*, 4(2), pp.1–9.

Jaffe, L.F. & Nuccitelli, R., 1974. An ultrasensitive vibrating probe for measuring steady extracellular currents. *Journal of Cell Biology*, 63(2), pp.614–628.

Jayaram, D.T. et al., 2017. Controlling the Resting Membrane Potential of Cells with Conducting Polymer Microwires. *Small*, 13(27), p.1700789.

Jezierska-Wozniak, Katarzyna,Seweryn Lipiński, Łukasz Grabarczyk, Monika Barczewska, Aleksandra Habich, Joanna Wojtkiewicz, W.M., 2017. Migration of human mesenchymal stem cells stimulated with pulsed electric field and the dynamics of the cell surface glycosylation. *Advances in Clinical and Experimental Medicine*.

Jiao, Q. et al., 2017. Cell-Cell Connection Enhances Proliferation and Neuronal Differentiation of Rat Embryonic Neural Stem/Progenitor Cells. *Frontiers in Cellular Neuroscience*, 11, p.200.

Jin, K. et al., 2002. Vascular endothelial growth factor (VEGF) stimulates neurogenesis in vitro and in vivo. *Proceedings of the National Academy of Sciences of the United States of America*, 99(18), pp.11946–11950.

Jinnou, H. et al., 2018. Radial Glial Fibers Promote Neuronal Migration and Functional Recovery after Neonatal Brain Injury. *Cell Stem Cell*, 22(1), pp.128–137.

Kaneko, N. et al., 2010. New Neurons Clear the Path of Astrocytic Processes for Their Rapid Migration in the Adult Brain. *Neuron*, 67(2), pp.213–223.

Kaneko, N., Sawada, M. & Sawamoto, K., 2017. Mechanisms of neuronal migration in the adult brain. *Journal of Neurochemistry*, 141(6), pp.835–847.

Kang, N., Weingart, A. & Cauraugh, J.H., 2018. Transcranial direct current stimulation and suppression of contralesional primary motor cortex post-stroke: a systematic review and meta-analysis. *Brain Injury*, 32(9), pp.1063–1070.

Katsimpardi, L. et al., 2014. Vascular and neurogenic rejuvenation of the aging mouse brain by young systemic factors. *Science*, 344(6184), pp.630–634.

Kawauchi, T., 2012. Cell adhesion and its endocytic regulation in cell migration during neural development and cancer metastasis. *International Journal of Molecular Sciences*, 13(4), pp.4564–4590.

Kazanis, I. et al., 2010. Quiescence and Activation of Stem and Precursor Cell Populations in the Subependymal Zone of the Mammalian Brain Are Associated with Distinct Cellular and Extracellular Matrix Signals. *Journal of Neuroscience*, 30(29), pp.9771–9781.

Kelleher, R.J. et al., 2004. Translational Control by MAPK Signaling in Long-Term Synaptic Plasticity and Memory. *Cell*, 116(3), pp.467–479.

Kempermann, G. et al., 2018. Cell Stem Cell Human Adult Neurogenesis: Evidence and Remaining Questions. *Cell Stem Cell*.

Kerever, A. et al., 2014. Perlecan is required for FGF-2 signaling in the neural stem cell niche. *Stem Cell Research*, 12(2), pp.492–505.

Keung, A.J. et al., 2011. Rho GTPases mediate the mechanosensitive lineage commitment of neural stem cells. *Stem Cells*, 29(11), pp.1886–1897.

Kierdorf, K. et al., 2013. Microglia emerge from erythromyeloid precursors via Pu.1-and Irf8-dependent pathways. *Nature Neuroscience*, 16(3), pp.273–280.

Kippin, T.E., Kapur, S. & van der Kooy, D., 2005. Dopamine Specifically Inhibits Forebrain Neural Stem Cell Proliferation, Suggesting a Novel Effect of Antipsychotic Drugs. *Journal of Neuroscience*, 25(24), pp.5815–5823.

Kippin, T.E., Martens, D.J. & van der Kooy, D., 2005. p21 loss compromises the relative quiescence of forebrain stem cell proliferation leading to exhaustion of their proliferation capacity. *Genes & Development*, 19(6), pp.756–767.

Knowles, M., Gatzy, J. & Boucher, R., 1981. Increased Bioelectric Potential Difference across Respiratory Epithelia in Cystic Fibrosis. *New England Journal of Medicine*, 305(25), pp.1489–1495.

Kojima, T. et al., 2010. Subventricular zone-derived neural progenitor cells migrate along a blood vessel scaffold toward the post-stroke striatum. *Stem Cells*, 28(3), pp.545–554.

Kokovay, E. et al., 2010. Adult SVZ lineage cells home to and leave the vascular niche via differential responses to SDF1/CXCR4 signaling. *Cell Stem Cell*, 7(2), pp.163–173.

Kokovay, E. et al., 2012. VCAM1 is essential to maintain the structure of the SVZ niche and acts as an environmental sensor to regulate SVZ lineage progression. *Cell Stem Cell*, 11(2), pp.220–230.

Kriegstein, A. & Alvarez-Buylla, A., 2009. The Glial Nature of Embryonic and Adult Neural Stem Cells. *Annual Review of Neuroscience*, 32(1), pp.149–184.

Kuhn, H.G., Dickinson-Anson, H. & Gage, F.H., 1996. Neurogenesis in the dentate gyrus of the adult rat: age-related decrease of neuronal progenitor proliferation. *The Journal of Neuroscience*, 16(6), pp.2027–2033.

Kuo, Y.-C. et al., 2018. IGF-1R Promotes Symmetric Self-Renewal and Migration of Alkaline Phosphatase + Germ Stem Cells through HIF-2α-OCT4/CXCR4 Loop under Hypoxia. *Stem Cell Reports*, 10(2), pp.524–537.

Labeed, F.H. et al., 2011. Biophysical Characteristics Reveal Neural Stem Cell Differentiation Potential H. Ulrich, ed. *PLoS ONE*, 6(9), p.e25458.

Lee, C. et al., 2012. The molecular profiles of neural stem cell niche in the adult subventricular zone. *PLoS One*, 7(11), p.e50501.

Lee, H.-W. et al., 1998. Essential role of mouse telomerase in highly proliferative organs. *Nature*, 392(6676), pp.569–574.

Lehtinen, M.K. et al., 2011. The Cerebrospinal Fluid Provides a Proliferative Niche for Neural Progenitor Cells. *Neuron*, 69(5), pp.893–905.

Leipzig, N.D. & Shoichet, M.S., 2009. The effect of substrate stiffness on adult neural stem cell behavior. *Biomaterials*, 30(36), pp.6867–6878.

Lempka, S.F. et al., 2017. Randomized clinical trial of deep brain stimulation for poststroke pain. *Annals of Neurology*, 81(5), pp.653–663.

Levin, M., 2014. Endogenous bioelectrical networks store non-genetic patterning information during development and regeneration. *Journal of Physiology*, 592(11), pp.2295–2305.

Levin, M., 2007. Large-scale biophysics: ion flows and regeneration. *Trends in Cell Biology*, 17(6), pp.261–270.

Levin, M. & Martyniuk, C.J., 2018. The bioelectric code: An ancient computational medium for

dynamic control of growth and form. *Biosystems*, 164, pp.76–93.

Li, N. et al., 2013. Three-dimensional graphene foam as a biocompatible and conductive scaffold for neural stem cells. *Scientific Reports*, 3(1), p.1604.

Li, Q. & Barres, B.A., 2018. Microglia and macrophages in brain homeostasis and disease. *Nature Reviews Immunology*, 18(4), pp.225–242.

Li, S. et al., 2013. Endothelial VEGF Sculpts Cortical Cytoarchitecture. *Journal of Neuroscience*, 33(37), pp.14809–14815.

Li, X. & Kolega, J., 2002. Effects of Direct Current Electric Fields on Cell Migration and Actin Filament Distribution in Bovine Vascular Endothelial Cells. *Journal of Vascular Research*, 39(5), pp.391–404.

Liddelow, S.A., 2011. Fluids and barriers of the CNS: A historical viewpoint. *Fluids and Barriers of the CNS*, 8(2).

Lim, D.A. et al., 2000. Noggin antagonizes BMP signaling to create a niche for adult neurogenesis. *Neuron*, 28(3), pp.713–726.

Lin, F. et al., 2008. Lymphocyte Electrotaxis In Vitro and In Vivo. *The Journal of Immunology*, 181(4), pp.2465–2471.

Litan, A. & Langhans, S.A., 2015. Cancer as a channelopathy: ion channels and pumps in tumor development and progression. *Frontiers in Cellular Neuroscience*, 9, p.86.

Liu, P. et al., 2014. Passage number is a major contributor to genomic structural variations in mouse iPSCs. *Stem Cells*, 32(10), pp.2657–2667.

Lledo, P.M., Merkle, F.T. & Alvarez-Buylla, A., 2008. Origin and function of olfactory bulb interneuron diversity. *Trends in Neurosciences*, 31(8), pp.392–400.

Llorens-Bobadilla, E. et al., 2015. Single-Cell Transcriptomics Reveals a Population of Dormant Neural Stem Cells that Become Activated upon Brain Injury. *Cell Stem Cell*, 17(3), pp.329–340.

Lois, C. & Alvarez-Buylla, A., 1994. Long-Distance Neuronal Migration in the Adult Mammalian Brain. *Science*, 264(5162), pp.1145–1148.

Lugert, S. et al., 2010. Quiescent and active hippocampal neural stem cells with distinct morphologies respond selectively to physiological and pathological stimuli and aging. *Cell Stem Cell*, 6(5), pp.445–456.

Luo, J. et al., 2006. The aging neurogenic subventricular zone. *Aging Cell*, 5(2), pp.139–152.

Luskin, M.B., 1993. Restricted proliferation and migration of postnatally generated neurons derived from the forebrain subventricular zone. *Neuron*, 11(1), pp.173–189.

MacDougall, J.D. et al., 1995. The Time Course for Elevated Muscle Protein Synthesis Following Heavy Resistance Exercise. *Canadian Journal of Applied Physiology*, 20(4), pp.480–486.

Malatesta, P., Appolloni, I. & Calzolari, F., 2008. Radial glia and neural stem cells. *Cell and Tissue Research*, 331(1), pp.165–178.

Malatesta, P. & Gotz, M., 2013. Radial glia - from boring cables to stem cell stars. *Development*, 140(3), pp.483–486.

Marin-Padilla, M., 1985. Early vascularization of the embryonic cerebral cortex: Golgi and electron microscopic studies. *Journal of Comparative Neurology*, 241(2), pp.237–249.

Marino, A.A. & Becker, R.O., 1970. Piezoelectric Effect and Growth Control in Bone. *Nature*, 228(5270), pp.473–474.

Marsh, G. & Beams, H.W., 1946. In vitro control of growing chick nerve fibers by applied electrical currents. *Journal of Cellular Physiology*, 27, pp.139–157.

Martens, D.J., Seaberg, R.M. & Van der Kooy, D., 2002. In vivo infusions of exogenous growth factors into the fourth ventricle of the adult mouse brain increase the proliferation of neural progenitors around the fourth ventricle and the central canal of the spinal cord. *European Journal of Neuroscience*, 16(6), pp.1045–1057.

Martin-Montalvo, A. et al., 2013. Metformin improves healthspan and lifespan in mice. *Nature Communications*, 4, p.2192.

Martin, C. et al., 2011. Intracellular pH gradients in migrating cells. *AJP: Cell Physiology*, 300(3), pp.C490–C495.

Martinez-Banaclocha, M., 2018. Ephaptic Coupling of Cortical Neurons: Possible Contribution of Astroglial Magnetic Fields? *Neuroscience*, 370, pp.37–45.

Maskell, D.L. et al., 2003. Chronological and replicative lifespan of polyploid Saccharomyces cerevisiae (syn. S. pastorianus). *FEMS Yeast Research*, 3(2), pp.201–209.

Maziarz, A. et al., 2016. How electromagnetic fields can influence adult stem cells: positive and negative impacts. *Stem Cell Research & Therapy*, 7(1), p.54.

McCaig, C.D. & Zhao, M., 1997. Physiological electrical fields modify cell behaviour. *BioEssays*, 19(9), pp.819–826.

McGinnis, M.E. & Vanable, J.W., 1986. Wound epithelium resistance controls stump currents. *Developmental Biology*, 116(1), pp.174–183.

McKasson, M.J., Huang, L. & Robinson, K.R., 2008. Chick embryonic Schwann cells migrate anodally in small electrical fields. *Experimental Neurology*, 211(2), pp.585–587.

Meletis, K. et al., 2008. Spinal cord injury reveals multilineage differentiation of ependymal cells A. Abeliovich, ed. *PLoS Biology*, 6(7), pp.1494–1507.

Meng, X. et al., 2011. PI3K mediated electrotaxis of embryonic and adult neural progenitor cells in the presence of growth factors. *Experimental Neurology*, 227(1), pp.210–217.

Mercier, F. & Douet, V., 2014. Bone morphogenetic protein-4 inhibits adult neurogenesis and is regulated by fractone-associated heparan sulfates in the subventricular zone. *Journal of Chemical Neuroanatomy*, 57–58, pp.54–61.

Mercier, F., Kitasako, J.T. & Hatton, G.I., 2002. Anatomy of the brain neurogenic zones revisited: Fractones and the fibroblast/macrophage network. *Journal of Comparative*

Neurology, 451(2), pp.170–188.

Merkle, F.T. et al., 2004. Radial glia give rise to adult neural stem cells in the subventricular zone. *Proceedings of the National Academy of Sciences of the United States of America*, 101(50), pp.17528–17532.

Messerli, M.A. & Graham, D.M., 2011. Extracellular electrical fields direct wound healing and regeneration. *Biological Bulletin*, 221(1), pp.79–92.

Metcalf, M.E.M. & Borgens, R.B., 1994. Weak applied voltages interfere with amphibian morphogenesis and pattern. *Journal of Experimental Zoology*, 268(4), pp.323–338.

Milo, R. et al., 2009. BioNumbers The database of key numbers in molecular and cell biology. *Nucleic Acids Research*, 38(SUPPL.1), pp.D750-3.

Mirsadeghi, S. et al., 2017. Development of membrane ion channels during neural differentiation from human embryonic stem cells. *Biochemical and Biophysical Research Communications*, 491(1), pp.166–172.

Mirzadeh, Z. et al., 2008. Neural Stem Cells Confer Unique Pinwheel Architecture to the Ventricular Surface in Neurogenic Regions of the Adult Brain. *Cell Stem Cell*, 3(3), pp.265–278.

Mirzadeh, Z. et al., 2010. The Subventricular Zone En-face: Wholemount Staining and Ependymal Flow. *Journal of Visualized Experiments*, (39).

Miyoshi, G. & Fishell, G., 2011. GABAergic interneuron lineages selectively sort into specific cortical layers during early postnatal development. *Cerebral Cortex*, 21(4), pp.845–852.

Monje, M.L., Toda, H. & Palmer, T.D., 2003. Inflammatory Blockade Restores Adult Hippocampal Neurogenesis. *Science*, 302(5651), pp.1760–1765.

Mori, T., Buffo, A. & Götz, M., 2005. The Novel Roles of Glial Cells Revisited: The Contribution of Radial Glia and Astrocytes to Neurogenesis. *Current Topics in Developmental Biology*, 69, pp.67–99.

Morrison, S.J. & Spradling, A.C., 2008. Stem cells and niches: mechanisms that promote stem cell maintenance throughout life. *Cell*, 132(4), pp.598–611.

Morshead, C.M. et al., 2002. Hematopoietic competence is a rare property of neural stem cells that may depend on genetic and epigenetic alterations. *Nature medicine*, 8(3), pp.268–273.

Morshead, C.M. et al., 1994. Neural stem cells in the adult mammalian forebrain: A relatively quiescent subpopulation of subependymal cells. *Neuron*, 13(5), pp.1071–1082.

Morshead, C.M. & van der Kooy, D., 1992. Postmitotic death is the fate of constitutively proliferating cells in the subependymal layer of the adult mouse brain. *The Journal of Neuroscience*, 12(1), pp.249–256.

Murase, S. & Horwitz, A.F., 2002. Deleted in colorectal carcinoma and differentially expressed integrins mediate the directional migration of neural precursors in the rostral migratory stream. *The Journal of Neuroscience*, 22(9), pp.3568–3579.

Nacher, J., Crespo, C. & McEwen, B.S., 2002. Doublecortin expression in the adult rat telencephalon. *European Journal of Neuroscience*, 14(4), pp.629–644.

Nadarajah, B. & Parnavelas, J.G., 2002. Modes of Neuronal Migration in the Developing Cerebral Cortex. *Nature Reviews Neuroscience*, 3, pp.423–432.

Nakajima, K.I. et al., 2015. KCNJ15/Kir4.2 couples with polyamines to sense weak extracellular electric fields in galvanotaxis. *Nature Communications*, 6(1), p.8532.

Neri, M. et al., 2010. Robust generation of oligodendrocyte progenitors from human neural stem cells and engraftment in experimental demyelination models in mice C. Kleinschnitz, ed. *PLoS ONE*, 5(4), p.e10145.

Ng, K.L. et al., 2005. Neuroscience: Dependence of olfactory bulb neurogenesis on prokineticin 2 signaling. *Science*, 308(5730), pp.1923–1927.

Nguyena, D. et al., 2013. Prolonged cultivation of hippocampal neural precursor cells shifts their differentiation potential and selects for aneuploid cells. *Biological Chemistry*, 394(12), pp.1623–1636.

Nimmerjahn, A., Kirchhoff, F. & Helmchen, F., 2005. Neuroscience: Resting microglial cells are highly dynamic surveillants of brain parenchyma in vivo. *Science*, 308(5726), pp.1314–1318.

Nishimura, K.Y., Isseroff, R.R. & Nuccitelli, R., 1996. Human keratinocytes migrate to the negative pole in direct current electric fields comparable to those measured in mammalian wounds. *Journal of Cell Science*, 109 (Pt 1), pp.199–207.

Noctor, S.C. et al., 2004. Cortical neurons arise in symmetric and asymmetric division zones and migrate through specific phases. *Nature Neuroscience*, 7(2), pp.136–144.

Nourse, J.L. et al., 2014. Membrane biophysics define neuron and astrocyte progenitors in the neural lineage. *Stem Cells*, 32(3), pp.706–716.

Nuccitelli, R., 2003. Endogenous electric fields in embryos during development, regeneration and wound healing. *Radiation protection dosimetry*, 106(4), pp.375–383.

Nuccitelli, R. et al., 2008. Imaging the electric field associated with mouse and human skin wounds. *Wound Repair and Regeneration*, 16(3), pp.432–441.

Nuccitelli, R. et al., 2011. The electric field near human skin wounds declines with age and provides a noninvasive indicator of wound healing. *Wound Repair and Regeneration*, 19(5), pp.645–655.

O'Keeffe, G.C. et al., 2009. Dopamine-induced proliferation of adult neural precursor cells in the mammalian subventricular zone is mediated through EGF. *Proceedings of the National Academy of Sciences of the United States of America*, 106(21), pp.8754–8759.

O'Sullivan, R.J. & Karlseder, J., 2010. Telomeres: Protecting chromosomes against genome instability. *Nature Reviews Molecular Cell Biology*, 11(3), pp.171–181.

Okano, H. & Sawamoto, K., 2008. Neural stem cells involvement in adult neurogenesis and repair. *Philosophical Transactions of the Royal Society B: Biological Sciences*, 363(15), pp.2111–2122.

Orida, N. & Feldman, J.D., 1982. Directional protrusive pseudopodial activity and motility in

macrophages induced by extracellular electric fields. *Cell Motility*, 2(3), pp.243–255.

Orlando, R.C. et al., 1989. Colonic and esophageal transepithelial potential difference in cystic fibrosis. *Gastroenterology*, 96(4), pp.1041–1048.

Oumesmar, B.N. et al., 1995. Expression of the Highly Polysialylated Neural Cell Adhesion Molecule During Postnatal Myelination and Following Chemically Induced Demyelination of the Adult Mouse Spinal Cord. *European Journal of Neuroscience*, 7(3), pp.480–491.

Oviedo, N.J. et al., 2010. Long-range neural and gap junction protein-mediated cues control polarity during planarian regeneration. *Developmental Biology*, 339(1), pp.188–199.

Özkucur, N. et al., 2009. Local calcium elevation and cell elongation initiate guided motility in electrically stimulated osteoblast-like cells. *PLoS ONE*, 4(7), p.e6131.

Özkucur, N. et al., 2011. Persistent directional cell migration requires ion transport proteins as direction sensors and membrane potential differences in order to maintain directedness. *BMC Cell Biology*, 12(1), p.4.

Pai, V.P. et al., 2015. Endogenous gradients of resting potential instructively pattern embryonic neural tissue via Notch signaling and regulation of proliferation. *The Journal of Neuroscience*, 35(10), pp.4366–4385.

Palmer, T.D., Takahashi, J. & Gage, F.H., 1997. The adult rat hippocampus contains primordial neural stem cells. *Molecular and Cellular Neuroscience*, 8(6), pp.389–404.

Pan, X. et al., 2013. Later Passages of Neural Progenitor Cells from Neonatal Brain Are More Permissive for Human Cytomegalovirus Infection. *Journal of Virology*, 87(20), pp.10968–10979.

Pandiella, A. et al., 1989. The effect of epidermal growth factor on membrane potential. Rapid hyperpolarization followed by persistent fluctuations. *The Journal of Biological Chemistry*, 264(22), pp.12914–12921.

Paratcha, G., Ibáñez, C.F. & Ledda, F., 2006. GDNF is a chemoattractant factor for neuronal precursor cells in the rostral migratory stream. *Molecular and Cellular Neuroscience*, 31(3),

pp.505–514.

Pardo, L.A. & Stühmer, W., 2014. The roles of K+ channels in cancer. *Nature Reviews Cancer*, 14(1), pp.39–48.

Peretto, P. et al., 2005. Chain formation and glial tube assembly in the shift from neonatal to adult subventricular zone of the rodent forebrain. *The Journal of Comparative Neurology*, 487(4), pp.407–427.

Peretto, P. et al., 1996. Glial tubes in the rostral migratory stream of the adult rat. *Brain Research Bulletin*, 42(1), pp.9–21.

Petri, A.-K. et al., 2017. Biological effects of exposure to static electric fields in humans and vertebrates: a systematic review. *Environmental Health*, 16(1), p.41.

Petrik, D. et al., 2018. Epithelial Sodium Channel Regulates Adult Neural Stem Cell Proliferation in a Flow-Dependent Manner. *Cell Stem Cell*, 22(6), pp.865–878.

Piccin, D. & Morshead, C.M., 2011. Wnt signaling regulates symmetry of division of neural stem cells in the adult brain and in response to injury. *Stem Cells*, 29(3), pp.528–538.

Piccin, D., Tufford, A. & Morshead, C.M., 2014. Neural stem and progenitor cells in the aged subependyma are activated by the young niche. *Neurobiology of Aging*, 35(7), pp.1669–1679.

Pinto, L. et al., 2008. Prospective isolation of functionally distinct radial glial subtypes—Lineage and transcriptome analysis. *Molecular and Cellular Neuroscience*, 38(1), pp.15–42.

Pokorný, J., Hašek, J. & Jelínek, F., 2005. Endogenous Electric Field and Organization of Living Matter. *Electromagnetic Biology and Medicine*, 24(3), pp.185–197.

Pokorný, J., Pokorný, J. & Kobilková, J., 2013. Postulates on electromagnetic activity in biological systems and cancer. *Integrative Biology*, 5(12), pp.1439–1446.

Pollen, A.A. et al., 2015. Molecular Identity of Human Outer Radial Glia during Cortical Development. *Cell*, 163(1), pp.55–67.

Ponti, A. et al., 2004. Two Distinct Actin Networks Drive the Protrusion of Migrating Cells. *Science*, 303(5691), pp.1782–1786.

Van Praag, H., Kempermann, G. & Gage, F.H., 1999. Running increases cell proliferation and neurogenesis in the adult mouse dentate gyrus. *Nature Neuroscience*, 2(3), pp.266–270.

Prothmann, C. et al., 2001. Primary cultures as a model for studying ependymal functions: Glycogen metabolism in ependymal cells. *Brain Research*, 920(1–2), pp.74–83.

Purdy, M.T. et al., 2015. Accelerating Neurite Outgrowth Through Electric Field Manipulation. In *World Congress on Medical Physics and Biomedical Engineering*. Toronto: Springer, Cham, pp. 1169–1172.

Qiu, C. et al., 2015. Can Neural Activity Propagate by Endogenous Electrical Field? *The Journal of Neuroscience*, 35(48), pp.15800–15811.

Qiu, J. et al., 2004. Regenerative Response in Ischemic Brain Restricted by p21 cip1/waf1. *The Journal of Experimental Medicine*, 199(7), pp.937–945.

Quiñones-Hinojosa, A. et al., 2006. Cellular composition and cytoarchitecture of the adult human subventricular zone: A niche of neural stem cells. *Journal of Comparative Neurology*, 494(3), pp.415–434.

Racila, D. & Bickenbach, J.R., 2009. Are epidermal stem cells unique with respect to aging? *Aging*, 1(8), pp.746–750.

Rakic, P., 2006. No more cortical neurons for you. *Science*, 313(5789), pp.928–929.

Ramírez-Castillejo, C. et al., 2006. Pigment epithelium-derived factor is a niche signal for neural stem cell renewal. *Nature Neuroscience*, 9(3), pp.331–339.

Ransohoff, R.M., 2016. A polarizing question: Do M1 and M2 microglia exist. *Nature Neuroscience*, 19(8), pp.987–991.

Rao, V.R. et al., 2015. Voltage-gated ion channels in cancer cell proliferation. *Cancers*, 7(2), pp.849–875.

Reid, B. et al., 2011. Specific ion fluxes generate cornea wound electric currents. *Communicative & Integrative Biology*, 4(4), pp.462–465.

Reynolds, B.A. & Weiss, S., 1992. Generation of neurons and astrocytes from isolated cells of the adult mammalian central nervous system. *Science*, 255(5052), pp.1707–1710.

Rice, D.S. & Curran, T., 2001. Role of the Reelin Signaling Pathway in Central Nervous System Development. *Annual Review of Neuroscience*, 24(1), pp.1005–1039.

Riquelme, P.A., Drapeau, E. & Doetsch, F., 2008. Brain micro-ecologies: neural stem cell niches in the adult mammalian brain. *Philosophical Transactions of the Royal Society B: Biological Sciences*, 363(1489), pp.123–137.

Robinson, K.R., 1985. The responses of cells to electrical fields: A review. *Journal of Cell Biology*, 101(6), pp.2023–2027.

Rolfe, A. & Sun, D., 2015. *Stem Cell Therapy in Brain Trauma: Implications for Repair and Regeneration of Injured Brain in Experimental TBI Models* F. H. Kobeissy, ed., Boca Raton, Florida: CRC Press, Taylor & Francis Group.

Romero-Grimaldi, C., Moreno-López, B. & Estrada, C., 2008. Age-dependent effect of nitric oxide on subventricular zone and olfactory bulb neural precursor proliferation. *Journal of Comparative Neurology*, 506(2), pp.339–346.

Rothenberg, P., Reuss, L. & Glasertt, L., 1982. Serum and epidermal growth factor transiently depolarize quiescent BSC-1 epithelial cells. *Proceedings of the National Academy of Sciences of the United States of America*, 79, pp.7783–7787.

Ruddy, R.M. & Morshead, C.M., 2018. Home sweet home: the neural stem cell niche throughout development and after injury. *Cell and Tissue Research*, 371(1), pp.125–141.

Ruf, S.P., Fallgatter, A.J. & Plewnia, C., 2017. Augmentation of working memory training by transcranial direct current stimulation (tDCS). *Scientific Reports*, 7(1), p.876.

Sabourin, J.-C. et al., 2009. A Mesenchymal-Like ZEB1 + Niche Harbors Dorsal Radial Glial Fibrillary Acidic Protein-Positive Stem Cells in the Spinal Cord. *Stem Cells*, 27(11),

pp.2722–2733.

Saha, B. et al., 2013. Cortical lesion stimulates adult subventricular zone neural progenitor cell proliferation and migration to the site of injury. *Stem Cell Research*, 11(3), pp.965–977.

Saltukoglu, D. et al., 2015. Spontaneous and electric field-controlled front-rear polarization of human keratinocytes. *Molecular Biology of the Cell*, 26(24), pp.4373–4386.

Sasai, Y. & De Robertis, E.M., 1997. Ectodermal patterning in vertebrate embryos. *Developmental Biology*, 182(1), pp.5–20.

Sawamoto, K. et al., 2006. New neurons follow the flow of cerebrospinal fluid in the adult brain. *Science*, 311(5761), pp.629–632.

Schaar, B.T. & McConnell, S.K., 2005. Cytoskeletal coordination during neuronal migration. *Proceedings of the National Academy of Sciences of the United States of America*, 102(38), pp.13652–13657.

Schafer, J.A., Troutman, S.L. & Andreoli, T.E., 1974. Volume reabsorption, transepithelial potential differences, and ionic permeability properties in mammalian superficial proximal straight tubules. *The Journal of General Physiology*, 64(5), pp.582–607.

Schmidt, C.E. et al., 1993. Integrin-cytoskeletal interactions in migrating fibroblasts are dynamic, asymmetric, and regulated. *Journal of Cell Biology*, 123(4), pp.977–991.

Schoenwolf, G.C. & Larsen, W.J. (William J., 2015. *Larsen's human embryology*,

Schwab, A. et al., 2012. Role of Ion Channels and Transporters in Cell Migration. *Physiological Reviews*, 92(4), pp.1865–1913.

Seleit, A. et al., 2017. Neural stem cells induce the formation of their physical niche during organogenesis. *eLife*, 6.

Shan, X. et al., 2018. Distinct Requirements for Extracellular and Intracellular MMP12 in the Development of the Adult V-SVZ Neural Stem Cell Niche. *Stem Cell Reports*, 10(3), pp.984–999.

Shen, Q. et al., 2008. Adult SVZ Stem Cells Lie in a Vascular Niche: A Quantitative Analysis of Niche Cell-Cell Interactions. *Cell Stem Cell*, 3(3), pp.289–300.

Shi, R. & Borgens, R.B., 1995. Three-dimensional gradients of voltage during development of the nervous system as invisible coordinates for the establishment of embryonic pattern. *Developmental Dynamics*, 202(2), pp.101–114.

Shi, Z. et al., 2017. Single-cell transcriptomics reveals gene signatures and alterations associated with aging in distinct neural stem/progenitor cell subpopulations. *Protein & Cell*, 9(4), pp.351–364.

Shigemoto-Mogami, Y. et al., 2014. Microglia Enhance Neurogenesis and Oligodendrogenesis in the Early Postnatal Subventricular Zone. *Journal of Neuroscience*, 34(6), pp.2231–2243.

Shihabuddin, L.S., Ray, J. & Gage, F.H., 1997. FGF-2 Is Suffcient to Isolate Progenitors Found in the Adult Mammalian Spinal Cord. *Experimental Neurology*, 148(2), pp.577–586.

Shingo, T. et al., 2003. Pregnancy-stimulated neurogenesis in the adult female forebrain mediated by prolactin. *Science*, 299(5603), pp.117–120.

Shrestha, B. et al., 2014. Repair of injured spinal cord using biomaterial scaffolds and stem cells. *Stem Cell Research & Therapy*, 5(4), p.91.

Sierra, A. et al., 2013. Janus-faced microglia: beneficial and detrimental consequences of microglial phagocytosis. *Frontiers in Cellular Neuroscience*, 7, p.6.

Sierra, A. et al., 2010. Microglia shape adult hippocampal neurogenesis through apoptosis-coupled phagocytosis. *Cell Stem Cell*, 7(4), pp.483–495.

Signer, R.A.J. & Morrison, S.J., 2013. Mechanisms that Regulate Stem Cell Aging and Life Span. *Cell Stem Cell*, 12(2), pp.152–165.

Smart, I., 1961. The subependymal layer of the mouse brain and its cell production as shown by radioautography after thymidine-H3injection. *Journal of Comparative Neurology*, 116(3), pp.325–347.

Smart, I.H., 1972. Proliferative characteristics of the ependymal layer during the early development of the spinal cord in the mouse. *Journal of Anatomy*, 111(Pt 3), pp.365–380.

Snapyan, M. et al., 2009. Vasculature Guides Migrating Neuronal Precursors in the Adult Mammalian Forebrain via Brain-Derived Neurotrophic Factor Signaling. *Journal of Neuroscience*, 29(13), pp.4172–4188.

Snyder, J.S. et al., 2011. Adult hippocampal neurogenesis buffers stress responses and depressive behaviour. *Nature*, 476(7361), pp.458–462.

Solano Fonseca, R. et al., 2016. Neurogenic Niche Microglia Undergo Positional Remodeling and Progressive Activation Contributing to Age-Associated Reductions in Neurogenesis. *Stem Cells and Development*, 25(7), pp.542–555.

Song, B. et al., 2004. Nerve regeneration and wound healing are stimulated and directed by an endogenous electrical field in vivo. *Journal of Cell Science*, 117(20), pp.4681–4690.

Song, J. et al., 2012. Neuronal circuitry mechanism regulating adult quiescent neural stem-cell fate decision. *Nature*, 489(7414), pp.150–154.

Song, S. & George, P.M., 2017. Conductive polymer scaffolds to improve neural recovery. *Neural Regeneration Research*, 12(12), pp.1976–1978.

Soong, H.K. et al., 1990. Movements of cultured corneal epithelial cells and stromal fibroblasts in electric fields. *Investigative Ophthalmology and Visual Science*, 31(11), pp.2278–2282.

Spassky, N. et al., 2005. Adult Ependymal Cells Are Postmitotic and Are Derived from Radial Glial Cells during Embryogenesis. *Journal of Neuroscience*, 25(1), pp.10–18.

Sperka, T. et al., 2012. Puma and p21 represent cooperating checkpoints limiting self-renewal and chromosomal instability of somatic stem cells in response to telomere dysfunction. *Nature Cell Biology*, 14(1), pp.73–79.

Steindler, D.A. et al., 1996. The subependymal zone: “brain marrow.” *Progress in Brain Research*, 108, pp.349–363.

Stiles, J. & Jernigan, T.L., 2010. The basics of brain development. *Neuropsychology Review*, 20(4), pp.327–348.

Stillwell, E.F., Cone, C.M. & Cone, C.D.J., 1973. Stimulation of DNA synthesis in CNS neurones by sustained depolarisation. *Nature New Biology*, 246(152), pp.110–1.

Stock, C. et al., 2013. Roles of Ion Transport in Control of Cell Motility. In *Comprehensive Physiology*. Hoboken, NJ, USA: John Wiley & Sons, Inc., pp. 59–119.

Strong, L.H., 1964. The early embryonic pattern of internal vascularization of the mammalian cerebral cortex. *Journal of Comparative Neurology*, 123(1), pp.121–138.

Sulik, G.L. et al., 1992. Effects of steady electric fields on human retinal pigment epithelial cell orientation and migration in culture. *Acta Ophthalmologica*, 70(1), pp.115–22.

Sun, Y.-H. et al., 2016. An Experimental Model for Simultaneous Study of Migration of Cell Fragments, Single Cells, and Cell Sheets. *Methods in Molecular Biology*, 1407, pp.251–272.

Sundelacruz, S., Levin, M. & Kaplan, D.L., 2009. Role of membrane potential in the regulation of cell proliferation and differentiation. *Stem Cell Reviews and Reports*, 5(3), pp.231–246.

Svitkina, T.M. et al., 1997. Analysis of the actin-myosin II system in fish epidermal keratocytes: Mechanism of cell body translocation. *Journal of Cell Biology*, 139(2), pp.397–415.

Szatkowski, M. et al., 2000. Electrophysiological recordings from the rat prostate gland in vitro: Identified single-cell and transepithelial (lumen) potentials. *BJU International*, 86(9), pp.1068–1075.

Tang, Y., Yu, P. & Cheng, L., 2017. Current progress in the derivation and therapeutic application of neural stem cells. *Cell Death and Disease*, 8(10), p.e3108.

Tata, M., Ruhrberg, C. & Fantin, A., 2015. Vascularisation of the central nervous system. *Mechanisms of Development*, 138, pp.26–36.

Tate, C.C. et al., 2009. Laminin and fibronectin scaffolds enhance neural stem cell

transplantation into the injured brain. *Journal of Tissue Engineering and Regenerative Medicine*, 3(3), pp.208–217.

Tavazoie, M. et al., 2008. A Specialized Vascular Niche for Adult Neural Stem Cells. *Cell Stem Cell*, 3(3), pp.279–288.

Taverna, E., Götz, M. & Huttner, W.B., 2014. The Cell Biology of Neurogenesis: Toward an Understanding of the Development and Evolution of the Neocortex. *Annual Review of Cell and Developmental Biology*, 30(1), pp.465–502.

Timpl, R. et al., 1979. Laminin--a glycoprotein from basement membranes. *The Journal of Biological Chemistry*, 254(19), pp.9933–9937.

Tong, C.K. et al., 2014. Axonal control of the adult neural stem cell niche. *Cell Stem Cell*, 14(4), pp.500–511.

Trepat, X., Chen, Z. & Jacobson, K., 2012. Cell migration. *Comprehensive Physiology*, 2(4), pp.2369–2392.

Trollinger, D.R., Rivkah Isseroff, R. & Nuccitelli, R., 2002. Calcium channel blockers inhibit galvanotaxis in human keratinocytes. *Journal of Cellular Physiology*, 193(1), pp.1–9.

Tropepe, V. et al., 1997. Transforming growth factor-alpha null and senescent mice show decreased neural progenitor cell proliferation in the forebrain subependyma. *The Journal of Neuroscience*, 17(20), pp.7850–7859.

Urrego, D. et al., 2014. Potassium channels in cell cycle and cell proliferation. *Philosophical Transactions of the Royal Society B: Biological Sciences*, 369(1638), p.20130094.

Verkhovsky, A.B. et al., 2003. Orientational Order of the Lamellipodial Actin Network as Demonstrated in Living Motile Cells. *Molecular Biology of the Cell*, 14(11), pp.4667–4675.

Verkhratsky, A., Krishtal, O.A. & Petersen, O.H., 2006. From Galvani to patch clamp: The development of electrophysiology. *Pflugers Archiv European Journal of Physiology*, 453(3), pp.233–247.

Verleysdonk, S. et al., 2005. Glycogen metabolism in rat ependymal primary cultures: Regulation by serotonin. *Brain Research*, 1060(1–2), pp.89–99.

Villeda, S.A. et al., 2011. The ageing systemic milieu negatively regulates neurogenesis and cognitive function. *Nature*, 477(7362), pp.90–94.

Wada, T. et al., 2006. Vascular Endothelial Growth Factor Directly Inhibits Primitive Neural Stem Cell Survival But Promotes Definitive Neural Stem Cell Survival. *Journal of Neuroscience*, 26(25), pp.6803–6812.

Wadkin, L.E. et al., 2018. Correlated random walks of human embryonic stem cell in-vitro. *Cell Behavior*.

Walker, D.G. & Lue, L.F., 2015. Immune phenotypes of microglia in human neurodegenerative disease: Challenges to detecting microglial polarization in human brains. *Alzheimer's Research and Therapy*, 7(1), p.56.

Waly, B. El et al., 2014. Oligodendrogenesis in the normal and pathological central nervous system. *Frontiers in Neuroscience*.

Wang, E. et al., 2003. Bi-directional migration of lens epithelial cells in a physiological electrical field. *Experimental Eye Research*, 76(1), pp.29–37.

Wang, H. et al., 2014. Insulin-Like Growth Factor-1 Receptor-Mediated Inhibition of A-type K+ Current Induces Sensory Neuronal Hyperexcitability Through the Phosphatidylinositol 3-Kinase and Extracellular Signal-Regulated Kinase 1/2 Pathways, Independently of Akt. *Endocrinology*, 155(1), pp.168–179.

Wang, J., Wen, J.-B. & Li, X.-L., 2018. No effect of transcranial direct current stimulation of the dorsolateral prefrontal cortex on short-term memory. *CNS Neuroscience and Therapeutics*, 24(1), pp.58–63.

Wang, S. & Basson, M.D., 2011. Akt directly regulates focal adhesion kinase through association and serine phosphorylation: implication for pressure-induced colon cancer metastasis. *AJP: Cell Physiology*, 300(3), pp.C657–C670.

Wang, T.W. et al., 2011. Hepatocyte growth factor acts as a mitogen and chemoattractant for postnatal subventricular zone-olfactory bulb neurogenesis. *Molecular and Cellular Neuroscience*, 48(1), pp.38–50.

Wang, X., Gao, X., et al., 2016. Traumatic Brain Injury Severity Affects Neurogenesis in Adult Mouse Hippocampus. *Journal of Neurotrauma*, 33(8), pp.721–733.

Wang, X., Seekaew, P., et al., 2016. Traumatic Brain Injury Stimulates Neural Stem Cell Proliferation via Mammalian Target of Rapamycin Signaling Pathway Activation. *eNeuro*, 3(5), p.ENEURO.0162-16.2016.

Wang, Y.-Z. et al., 2011. Concise Review: Quiescent and Active States of Endogenous Adult Neural Stem Cells: Identification and Characterization. *Stem Cells*, 29(6), pp.907–912.

Webb, D.J. et al., 2004. FAK–Src signalling through paxillin, ERK and MLCK regulates adhesion disassembly. *Nature Cell Biology*, 6(2), pp.154–161.

Weiss, S. et al., 1996. Multipotent CNS stem cells are present in the adult mammalian spinal cord and ventricular neuroaxis. *The Journal of Neuroscience*, 16(23), pp.7599–7609.

Weiss, S.A. & Faber, D.S., 2010. Field effects in the CNS play functional roles. *Frontiers in Neural Circuits*, 4, p.15.

Whitman, M.C. et al., 2009. Blood vessels form a migratory scaffold in the rostral migratory stream. *Journal of Comparative Neurology*, 516(2), pp.94–104.

Williams, A. et al., 2010. Deep brain stimulation plus best medical therapy versus best medical therapy alone for advanced Parkinson's disease (PD SURG trial): a randomised, open-label trial. *The Lancet Neurology*, 9(6), pp.581–591.

Wright, S.H., 2004. Generation of resting membrane potential. *Advances in Physiology Education*, 28, pp.139–142.

Xing, C. et al., 2006a. Effects of insulin-like growth factor 1 on voltage-gated ion channels in cultured rat hippocampal neurons. *Brain Research*, 1072(1), pp.30–35.

Xing, C. et al., 2006b. Effects of insulin-like growth factor 1 on voltage-gated ion channels in cultured rat hippocampal neurons. *Brain Research*, 1072(1), pp.30–35.

Xu, C., Loh, H.H. & Law, P.Y., 2016. Effects of addictive drugs on adult neural stem/progenitor cells. *Cellular and Molecular Life Sciences*, 73(2), pp.327–348.

Xu, D. & Ponce, F., 2017. Deep Brain Stimulation for Alzheimer's Disease. *Current Alzheimer Research*, 14(4), pp.356–361.

Xue, G. & Hemmings, B.A., 2013. PKB/akt-dependent regulation of cell motility. *Journal of the National Cancer Institute*, 105(6), pp.393–404.

Yamamoto, S. ichi et al., 2001. Proliferation of parenchymal neural progenitors in response to injury in the adult rat spinal cord. *Experimental Neurology*, 172(1), pp.115–127.

Yamashita, T. et al., 2006. Subventricular Zone-Derived Neuroblasts Migrate and Differentiate into Mature Neurons in the Post-Stroke Adult Striatum. *Journal of Neuroscience*, 26(24), pp.6627–6636.

Yang, H.-Y. et al., 2013. The epithelial sodium channel mediates the directionality of galvanotaxis in human keratinocytes. *Journal of Cell Science*, 126(9), pp.1942–1951.

Yang, M. & Brackenbury, W.J., 2013. Membrane potential and cancer progression. *Frontiers in Physiology*, 4, p.185.

Yasuda, T., Cuny, H. & Adams, D.J., 2013. Kv3.1 channels stimulate adult neural precursor cell proliferation and neuronal differentiation. *The Journal of physiology*, 591(10), pp.2579–2591.

Yin, W. et al., 2013. The migration of neural progenitor cell mediated by SDF-1 is NF-κB/HIF-1α dependent upon hypoxia. *CNS Neuroscience and Therapeutics*, 19(3), pp.145–153.

Yuzwa, S.A. et al., 2017. Developmental Emergence of Adult Neural Stem Cells as Revealed by Single-Cell Transcriptional Profiling. *Cell Reports*, 21(13), pp.3970–3986.

Yuzwa, S.A. et al., 2016. Proneurogenic Ligands Defined by Modeling Developing Cortex

Growth Factor Communication Networks. *Neuron*, 91(5), pp.988–1004.

Zamir, E. et al., 2000. Dynamics and segregation of cell–matrix adhesions in cultured fibroblasts. *Nature Cell Biology*, 2(4), pp.191–196.

Zhang, K. et al., 2010. Long-term results of thalamic deep brain stimulation for essential tremor. *Journal of Neurosurgery*, 112(6), pp.1271–1276.

Zhang, R.L. et al., 2014. Stroke increases neural stem cells and angiogenesis in the neurogenic niche of the adult mouse. *PLoS ONE*, 9(12), p.e113972.

Zhao, M. et al., 1996. Directed migration of corneal epithelial sheets in physiological electric fields. *Investigative Ophthalmology and Visual Science*, 37(13), pp.2548–2558.

Zhao, M. et al., 1999. Electric Field-directed Cell Motility Involves Up-regulated Expression and Asymmetric Redistribution of the Epidermal Growth Factor Receptors and Is Enhanced by Fibronectin and Laminin W. J. Nelson, ed. *Molecular Biology of the Cell*, 10(4), pp.1259–1276.

Zhao, M., 2009. Electrical fields in wound healing—An overriding signal that directs cell migration. *Seminars in Cell & Developmental Biology*, 20(6), pp.674–682.

Zhao, M. et al., 2004. Electrical stimulation directly induces pre-angiogenic responses in vascular endothelial cells by signaling through VEGF receptors. *Journal of Cell Science*, 117(3), pp.397–405.

Zhao, M. et al., 1997. Human corneal epithelial cells reorient and migrate cathodally in a small applied electric field. *Current Eye Research*, 16(10), pp.973–984.

Zhao, M. et al., 2002. Membrane lipids, EGF receptors, and intracellular signals colocalize and are polarized in epithelial cells moving directionally in a physiological electric field. *The FASEB Journal*, 16(8), pp.857–859.

Zhou, Y. et al., 2015. Membrane potential modulates plasma membrane phospholipid dynamics and K-Ras signaling. *Science*, 349(6250), pp.873–876.

Ziegler, A.N., Levison, S.W. & Wood, T.L., 2015. Insulin and IGF receptor signalling in neural-stem-cell homeostasis. *Nature Reviews Endocrinology*, 11(3), pp.161–170.

Appendix

Contributions

This section details the contributions of technicians, trainees, collaborators, faculty mentors and funding sources that have made this thesis possible.

Lab technician Venkateswaran Subramaniam made serum free media used in experiments.

Lab technician Ricky Siu ordered animals and maintained mice colonies used in experiments.

Post-doctoral fellow Jessica Livingston-Thomas and Nadia Sachewsky ordered animals used in experiments.

Master's student Daniel Derkach and lab technician Ricky Siu provided some C57BL/6 post-natal day 8 pups used in experiments.

Dr. Penney Gilbert's lab provided one 22 month old C57BL/6 mouse in experiments.

Post-doctoral fellow Erica Scott provided base R code used in heatmap comparing conditioned media differences.

PhD candidate Mohsen Afshar consulted in conditioned media analysis interpretation.

Undergraduate student Iflah Shahid aided in further developing heatmap R code and IGF-1 validation experiments as well as aided in tracking neural stem cell galvanotactic migration.

Undergraduate student Prashanth Surjeet aided in establishing neural precursor cell dose-response curves to Diazoxide and Barium Chloride as well as assessing neural precursor cell proliferative responses in both conditions.

Undergraduate student James Anupol analyzed effects on neural precursor cell proliferation in the presence and absence of 300μM Diazoxide.

Principal Investigator Dr. Cindi Morshead, PhD candidates Stephanie Iwasa and Rehnuma Islam provided thesis manuscript feedback.

Collaborator post-doctoral fellow Homeira Moradi performed neural precursor cell whole-cell voltage patch clamp.

Mentors Dr. Cindi Morshead, Dr. Milos Popovic, Dr. Molly Shoichet, and Dr. Penney Gilbert consulted on project viability and experimental design.

This research was supported by funding from NSERC CGS-M, IMS Entrance Scholarship, SCN Travel Award, and OIRM.

Copyright Acknowledgements